"Petrography and Geochemistry
of the McArthur Township Area, Ontario"

by

MEHRAN TABATABAI

A thesis submitted to the Department of Geological Sciences
in partial fulfilment of the requirements
for the degree of
Master of Science

Brock University
St. Catharines, Ontario
October, 1978

ABSTRACT

The McArthur Township area in the Archean Abitibi Belt of northeast
Ontario contains northwesterly trending volcanic rocks which are located
on a limb of a large syncline. The axial trace of the syncline passes
through the adjacent Douglas Township. The Archean volcanic rocks and
associated sedimentary rocks are intruded and deformed by two large plutons
and a few smaller hypabyssal intrusions.

A petrographic and geochemical study of the Precambrian rocks exposed
in the study area was undertaken in order to investigate the metamorphic
grade and geochemical characteristics of the rocks. All the samples were
studied with the microscope and analysis of 20 major and trace elements
were determined on a selection of the less altered specimens by x-ray
fluorescence.

Three different periods of igneous activity have occurred in the
study area. The first two periods were dominated by volcanic extrusive
rocks accompanied by gabbroic sills. The third cycle is the diapiric
intrusion of the granitic plutons and subsequent metamorphism of the
older rocks to the low to medium grade. Two periods of sedimentation are
also recognized in the study area which occurred after the first and second
cycle of volcanism.

Chemically, the lavas are subdivided into three main associations:
(1) The komatiitic association is characterized by high MgO, high Ni,
low TiO_2 and a low $FeO*/(FeO* + MgO)$ ratio. They occupy the base of each
volcanic cycle and some of the flows exhibit spinifex textures.
(2) The tholeiitic association displays distinct iron and titanium en-
richment trends in the intermediate members.

(3) The calc-alkaline association contains low FeO* and TiO_2 and high

Ni contents relative to modern calc-alkaline types. They are formed at

the end of each cycle of volcanism and overlie the tholeiitic flows. All

three associations of the first volcanic cycle are exposed in the study

area, while the second cycle is represented by a komatiitic sequence.

The volcanic rocks were possibly formed by multiple partial melting

of the Archean mantle to produce parental magmas under various P - T

conditions.

C O N T E N T S

PETROCHEMISTRY OF THE ROCKS

General

Chemistry Of Extrusives

LIST OF FIGURES

LIST OF PLATES

LIST OF TABLES

INTRODUCTION

GENERAL

Archean greenstone belts, containing thick sequences of extrusive and associated hypabyssal intrusive rocks, predominantly basaltic in composition, but ranging from ultramafic to rhyolitic types, have been subjected to considerable major element geochemical study in the past decade. However, trace element distributions and detailed investigation of stratigraphic variations in major elements, including the redistribution of many elements as a result of metamorphic alterations, have received little attention.

To investigate the detailed elemental distribution and to determine the stratigraphic trends in the lava pile, an area in the vicinity of McArthur Township was selected. The study area is underlain dominantly by volcanic rocks which are diapirically intruded by two large granitic plutons.

LOCATION

The area of study is located in the northwestern section of Timiskaming District within western parts of the Abitibi greenstone belt (Fig. 1). It includes McArthur Township, the west side of Fripp Township and the north and northwest parts of Bartlett and Musgrove Townships (Fig. 2 and 3). The area is delineated by longitudes 81° 12' 16" to 81° 26' 06" and latitudes 48° 10' 17" to 48° 16' 30". The study area is located approximately 30 km south of Timmins and has a total area of 213 sq. km. An all-weather road from Timmins provides access to major parts of the area; other parts may be reached by four-wheel drive vehicles.

1
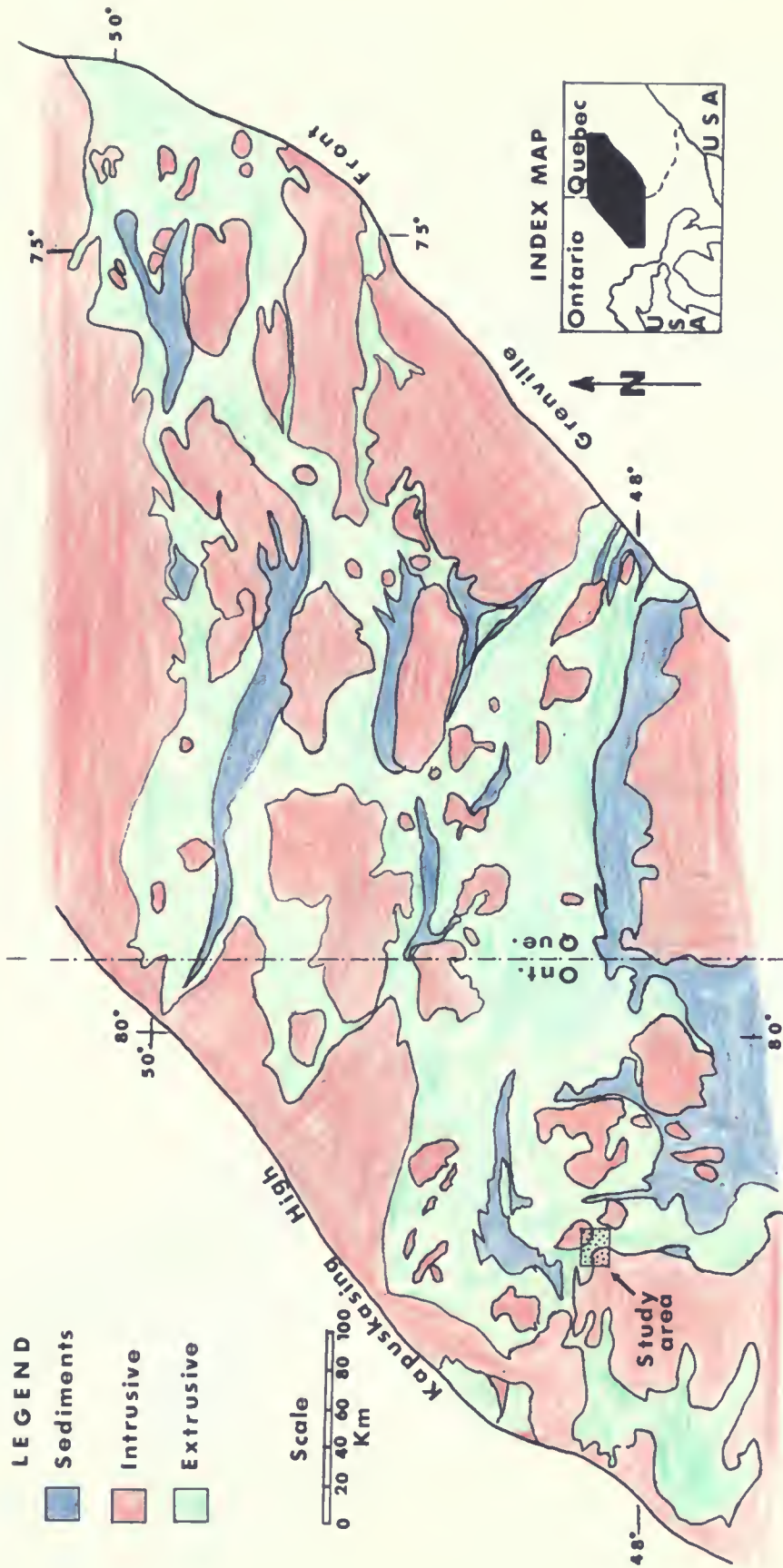
Figure 1   Sketch map of the Abitibi greenstone belt showing the location of the study area.

3
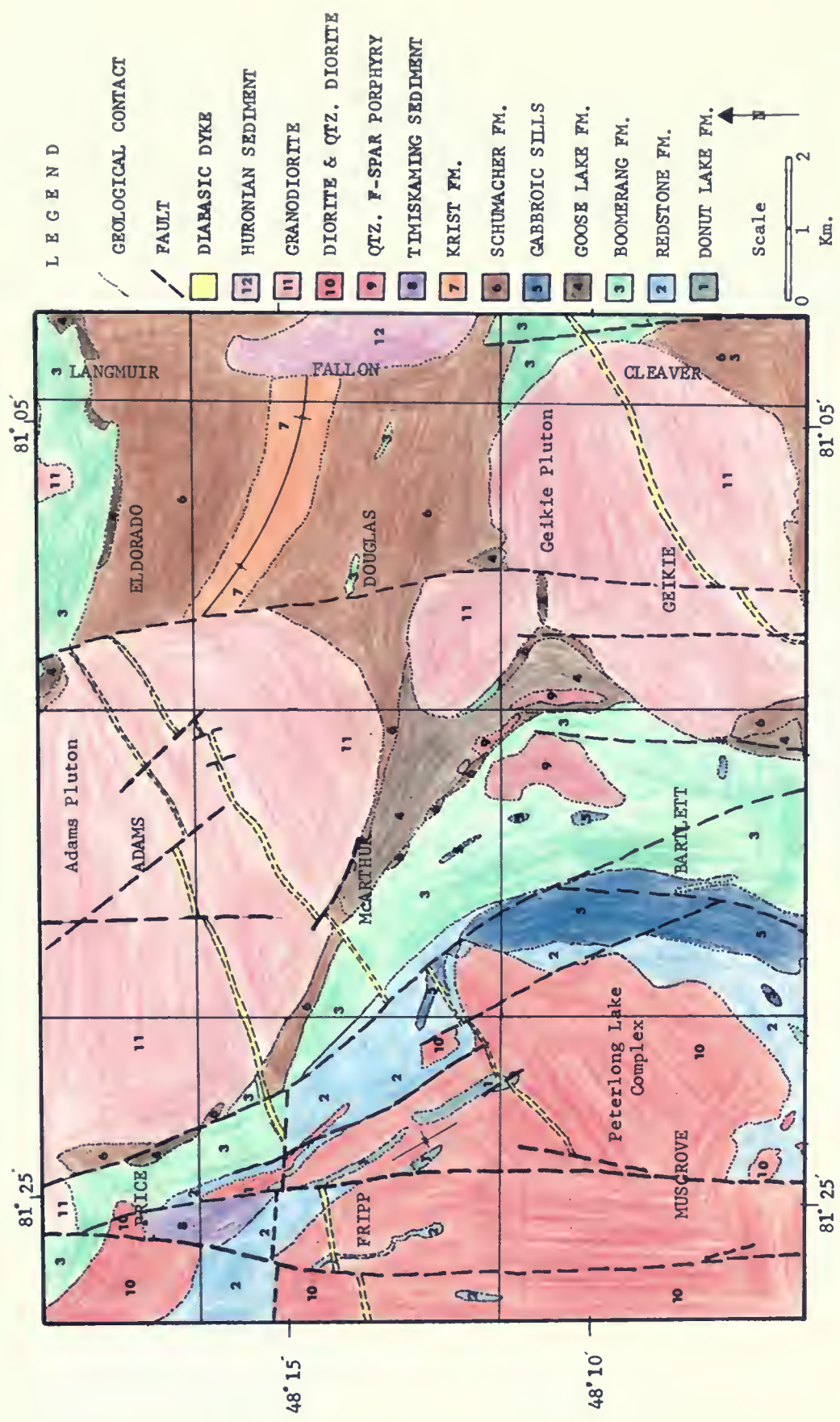
Figure 2   Generalized geologic map of the surrounding area.(Modified after Pyke,1974,1978).

4

Figure 3   Geological map of the study area showing the sample locations.

PREVIOUS WORK

The first published information on the geology and resources of McArthur Township was accomplished by Hopkins (1912). Later in 1924, Hopkins provided a sketch map of the geology of McArthur Township. In 1926 E. L. Bruce prepared a geological map of the McArthur, Bartlett, Douglas and Geikie Townships. The most recent mapping of the area was done by Pyke (1971, 1972, 1973, 1974, 1978) at a scale of one inch to one quarter mile. He divided the volcanic rocks present in the area into two groups, "lower" and "upper", of which each consists of three different units. The lower unit is ultramafic in composition, the middle and upper ones are mafic and intermediate to felsic respectively. These lavas were erupted during two cycles of volcanism with a period of erosion and sedimentation afterward. During the Kenoran Orogeny the rocks were folded and deformed by intrusion of granitic plutons. According to Pyke (1978) the last five volcanic units dip northeastward, toward the center of a synclinal axis.

Goodwin (1977) studied the chemical composition of the representative samples from the area. He has called the lavas erupted during the first cycle of volcanism the "Redstone River Group" and those erupted during the second cycle of volcanism the "Bowman Subgroup" which is the lowermost unit of the "Blake River Group". The Redstone River Group furthermore is divided into a lower tholeiitic unit and an upper calc-alkalic unit. The Bowman Subgroup features Magnesium-tholeiites including peridotitic lava flows and includes dacitic pyroclastic rocks in the upper levels.

PRESENT STUDY

The need for further study of the lavas in the McArthur Township area arose after Pyke (1978) mapped the area and on the basis of his structural

information and petrography suggested two main cycles of volcanism; in addition to a period of sedimentation, intrusion, and tectonic activity. The purpose in this report is to present the results of a petrographic and geochemical investigation of these rocks, including the spinifex-textured komatiitic types. Here an attempt is made to assess the strati-graphic and structural interpretations of Pyke (1978). In addition the relative degree of regional metamorphism across the belt are considered.

In the present study the six formation names proposed by Pyke (1975) for the distinctive stratigraphic units in the Timmins area are adopted, since they are structurally located on the other flank of existing syncline in the area. The terms Keewatin and Timmiskaming are used in a lithological rather than in a time classification sense.

REGIONAL GEOLOGY

The Abitibi greenstone belt is one of the most intensely prospected parts of Canadian Shield. This is the result of the many rich economic deposits found within the area. The Abitibi belt, like other greenstone belts in Canada, South Africa and Australia, is characterized a thick sequence of volcanic and sedimentary rocks, with associated plutons (Fig. 1).

Volcanism in the belt was cyclic; each cycle starting with ultramafic or mafic rocks and terminating with felsic rocks. The number of recognized cycles varies from place to place. Five cycles of volcanism are recognized in the upper Blake River Group of the Noranda area (Spence and De Rosen-Spence, 1975); and two in the Timmins area (Dunbar, 1948; Ferguson, et al., 1968, Pyke, 1975). The lavas were erupted on the surface of a metamorphosed sialic crust (Jolly, 1978) and are dated by zircon techniques (Krogh and Davis, 1971) as 2.75 - 2.95 billion years old.

Deposition of the sediments was sporadic before, during and after volcanism (Dimroth et al., 1973). Post volcanic,deep water greywackes are the dominant sedimentary rock type. Iron formation of probable sedimentary origin is consistently associated with a variety of volcanic rocks and sediments. Goodwin (1973) recognized three facies within iron formation defining the original shelf-basin relationships. The shallow water oxide facies grade transitionally through the carbonate facies to the deeper water sulfide facies toward the center of the belt.

Many diapiric plutons are also present in the area; most are the result of the Kenoran Orogeny, which took place between 2.7 and 2.4 b.y. before the present. The plutons have intruded the lavas along the antiformal structures. The major folds are generally isoclinal, doubly plunging, upright with east-west trending axes. Steep faults cut across the major folds and generally trend either northeast or northwest.

Three periods of metamorphism were recognized by Jolly (1975, 1978); (a) pre-volcanic regional metamorphism of the sialic basement to amphibolite and granulite facies associated with several deformations and intrusions; (b) regional metamorphism of the lavas and some sediments to prehnite-pumpellyite grade due to burial and an increase in geothermal gradient; (c) thermal metamorphism of the rocks adjacent to the Kenoran intrusions to amphibolite and greenchist facies.

GENERAL GEOLOGY

Geological Setting of the McArthur Township Area: The bedrock in the study area is of Precambrian age. Unconsolidated Pleistocene and recent deposits cover much of the area. The oldest lithologic unit of Keewatin metavolcanic rocks shows two main cycles of volcanism, each consisting

of a lower unit of ultramafic metavolcanics (rich in MgO), an overlying unit of mafic metavolcanics and an upper unit of intermediate to felsic metavolcanics. These rocks, particularly the younger ones, are intruded by numerous gabbroic sills.

The general stratigraphic sequence (Pyke, 1978), progresses in a northwesterly direction from the southwestern part of the area which comprises the following six units:

(1) A high-Mg ultramafic unit, the Donut Lake Formation, is the oldest series of volcanic flows. The lavas are spinifex-textured but not pillowed.

(2) Massive to pillowed mafic volcanic rocks of the Redstone Formation overlie the Donut Lake Formation. A number of gabbroic sills cut these flows.

(3) An agglomeratic, tuffaceous intermediate to felsic unit, the Boomerang Formation, comprises the upper part of the first volcanic cycle. Numerous layers of iron formation and gabbroic sills are included within this unit.

(4) A high-Mg ultramafic unit, the Goose Lake Formation, is the base of the second volcanic cycle. The presence of spinifex-textured flows is the main characteristic of this unit. Goose Lake Formation pinches out at the center of McArthur Township and is not present in Fripp Township.

(5) An unpillowed layered mafic metavolcanic unit, the Schumacher Formation, overlies the Goose Lake Formation; however, it is also present between the Boomerang and Goose Lake Formations as a result of faulting.

(6) An upper intermediate to felsic unit, the Krist Formation, is mainly composed of tuff and lapilli tuff with some breccia (Pyke, 1978). This unit does not appear in the study area, but is exposed in Douglas Township (Fig. 2).

Interlayered with the Redstone, Boomerang, Goose Lake and Schumacher Formations are many gabbroic sills which may represent feeders to some of the overlaying mafic metavolcanics (Pyke, 1978).

The volcanic rocks are intruded by two large granitic plutons, assumed to be of Kenoran age. The eastern side of a large batholith (Peterlong Lake Complex) appears in the west and southwest part of the area and a large stock of porphyritic granodiorite (Adams Pluton) underlies the north and northeast part of the study area. Four smaller intrusions are also present in the area. A northwesterly trending quartz diorite sill is present on the western side of McArthur Lake. The others, two small quartz feldspar porphyry and one trondhjemitic intrusion, probably of sub-volcanic derivation, invades the Boomerang Formation. Some sedimentary rocks, rich in quartz, feldspar and biotite are exposed at the northwest tip of Quartz Lake. Finally, several sets of Precambrian diabase dykes of various ages traverse the area. These dykes cut every type of rock, are repeatedly faulted, and are therefore assumed to be the youngest rocks in the area. Regional metamorphism of the volcanic and sedimentary rocks present in the area to greenschist and Amphibolite facies took place during Kenoran Orogeny.

Structural Geology: All units face toward the north-northeast in the south and southwestern parts of the area. Further north, tops indicate the sequence faces northeast, probably because of deformations related to the intrusion of the Adams Pluton. No obvious unconformity exists within the metavolcanic sequence. All the volcanic rocks, with the exception of the Donut Lake Formation dip between 50° to 87° toward the northeast. Tops in the Redstone and Boomerang Formations were determined by using pillow lavas and in the Goose Lake Formation by spinifex textures. Therefore the
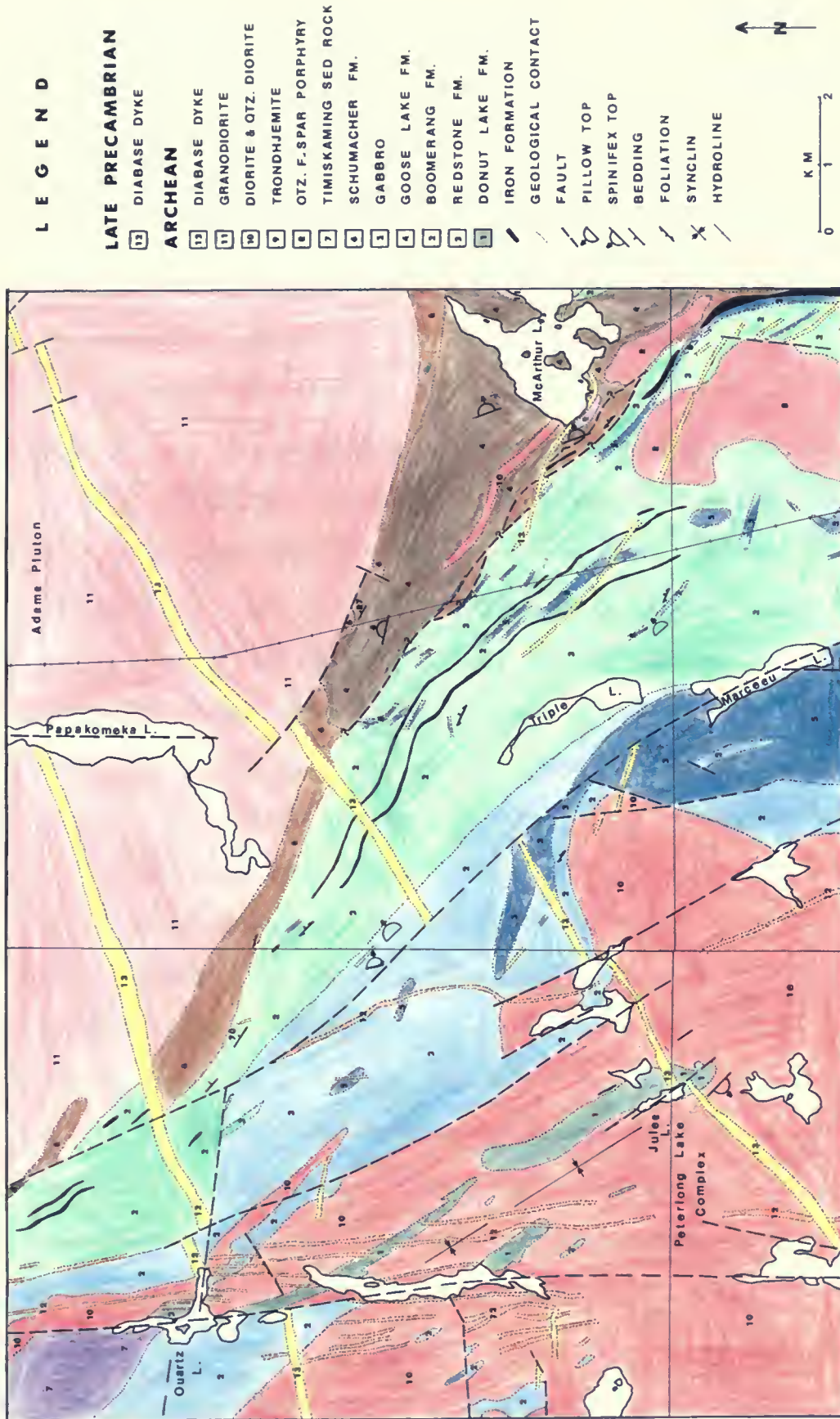
Figure 4   Geological map of the study area. (Modified after Pyke,1978).

L E G E N D

LATE PRECAMBRIAN
- 13   DIABASE DYKE

ARCHEAN
- 13   DIABASE DYKE
- 12   GRANODIORITE
- 12   DIORITE & QTZ. DIORITE
-   TRONDHJEMITE
-   QTZ. F.SPAR PORPHYRY
-   TIMISKAMING SED ROCK
- 6   SCHUMACHER FM.
-   GABBRO
- 4   GOOSE LAKE FM.
- 3   BOOMERANG FM.
- 2   REDSTONE FM.
- 1   DONUT LAKE FM.
-   IRON FORMATION

GEOLOGICAL CONTACT
FAULT
PILLOW TOP
SPINIFEX TOP
BEDDING
FOLIATION
SYNCLINE
HYDROLINE

K M
0   1   2

lavas represent the southwestern limb of a large northwestern trending synclinal structure, the axial trace of which appears within the Krist Formation in Douglas Township, northwest of the area studied (Fig. 2). Pyke (1978) determined that the Donut Lake Formation around Donut Lake (Fig. 4) faced southwestward, by using the spinifex textures. He concluded that the two incomplete bands of ultramafic rocks in Fripp Township are located on opposite limbs of a syncline as shown in Figure 4. A few of the outcrops, especially of mafic metavolcanic rocks are slightly to moderately foliated and show schistosity with an attitude more or less parallel to bedding. Pillow lavas in sample location 42 (Fig. 3) are elongated (about 50%) parallel to the contact of the Redstone Formation and the Peterlong Lake Complex. Major faulting occurred, during the Middle to Late Precambrian, in north to northwestern direction mainly with sinistral offset (Pyke, 1973). Offsets of diabase dykes in McArthur and Fripp Townships suggest strike-slip movement of up to 1.7 and 1.4 km respectively. The vertical movement of these faults is unknown.

As mentioned in an earlier section, the Schumacher Formation is exposed as lenticles between the Goose Lake and Boomerang Formations. If faulting is not present, the younger Schumacher Formation is located below the older Goose Lake Formation. The relationship would be the result of (a) a graben-like sinking of part of the lava pile caused by two normal faults, so that Schumacher Formation occupies a graben between the Boomerang and Goose Lake Formations (Fig. 5a); (b) thrusting of the Goose Lake Formation over the Schumacher and Boomerang Formations, so that the Schumacher Formation is now present as an imbricate wedge between the other two formations (Fig. 5b); or (c) multiple normal and reverse faulting within the area indicating more complex stratigraphic relationships of different units.
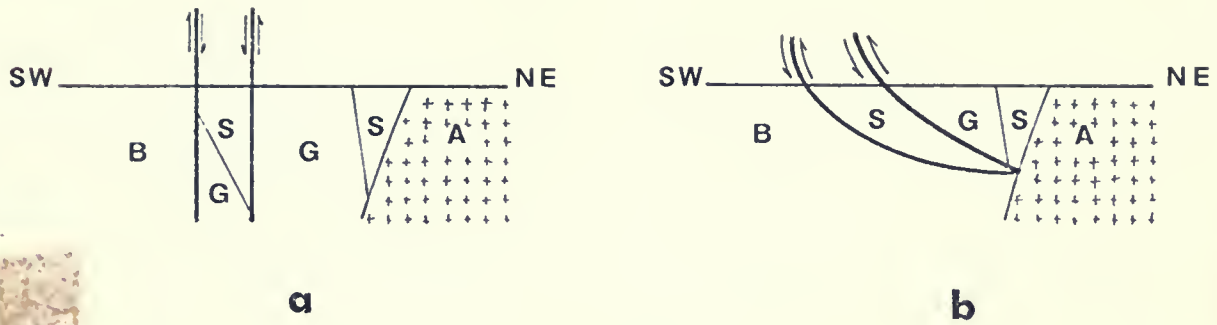
Figure 5: Cross-section (NE -SW) of McArthur Township, (not to scale), showing the possible fault relationships between Boomerang (B), Goose Lake (G) and Schumacher (S) Formations. A=Adams Pluton. (a) normal faulting, (b) thrusting.

PETROGRAPHY

DONUT LAKE FORMATION

General Relations: The Donut Lake Formation is the oldest volcanic unit exposed in the area. All the exposures are found within the Peterlong Lake Complex, a large batholith covering western parts of the study area. The lava flows are generally fine-grained and tend to weather dark grey, although they have a greenish-black color on fresh surfaces. Samples 14 and 15 which were taken adjacent to the batholith (Fig. 3) have a greenish color as a result of an extensive growth of tremolite crystals. A few of the samples display slight schistosity parallel to the boundaries of this unit.

Petrography: Fine-grained secondary minerals make up most of the lava. The rocks can be divided into two groups according to the type of amphibole they carry:

1) The rocks with tremolite as the most abundant mafic mineral, show extensive chloritization and are commonly associated with talc (Plate 1a). Samples taken from the vicinity of Donut Lake are severely altered and composed mainly of carbonates (magnesite), talc and chlorite, with minor amounts of magnetite (Plate 1b). Tremolite is colorless to faint green and displays a long prismatic habit. Crystals may be as long as 6 mm but are mostly fine-grained. Chlorite with a pale to dark green color, is very fine-grained and fills the spaces between the tremolite grains. Highly birefringent crystals of talc are commonly accompanied by tremolite crystals.

13

PLATE 1

Donut Lake Formation

(a) Photomicrograph of long needle-like growth of tremolite (in all
     directions, therefore the rhombic ones are perpendicular to the
     page). The interstitial minerals are talc (top left) and fine-
     grained chlorite (crossed nicols, X 125).
     Sample 15

(b) Photomicrograph of altered and degraded serpentinite, the dark spots
     are prisma of chlorite, the grey minerals are fine-grained magnesite
     and light grey parts are talc (crossed nicols, X 125).
     Sample 269

(c) Photomicrograph of equidimentional cummingtonite crystals with ser-
     pentine and talc bordering the grain boundaries (crossed nicols,
     X 125).
     Sample 17

(d) Photomicrograph of irregularly fractured olivine (right central) and
     clinopyroxene (light grey, bottom) and cummingtonite showing a well
     developed cleavage pattern (left). The fractures and grain boundaries
     of olivine are infilled with serpentine (crossed nicols, X 125).
     Sample 19

(e) Photomicrograph of small needles of chlorite growing into cumming-
     tonite crystals (crossed nicols, X 125).
     Sample 17

(f) Photomicrograph of chrome-spinel (verdelite) with opaque surroundings
     and translucent center, indicating the increase in iron content out-
     ward (plane light, X 31).
     Sample 19

PLATE 1

a
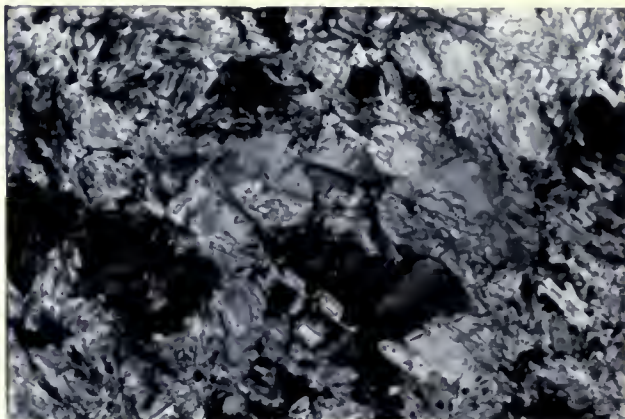
b
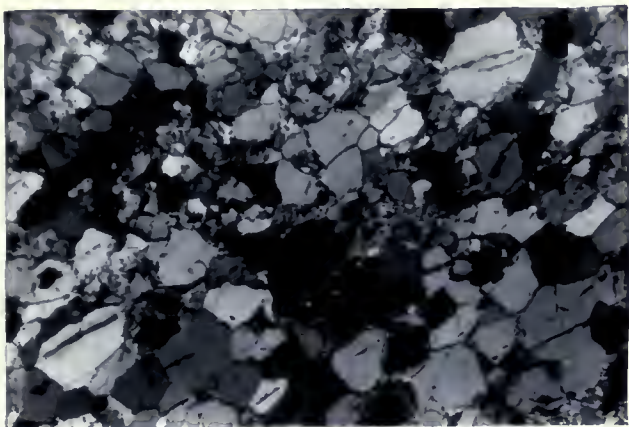
c
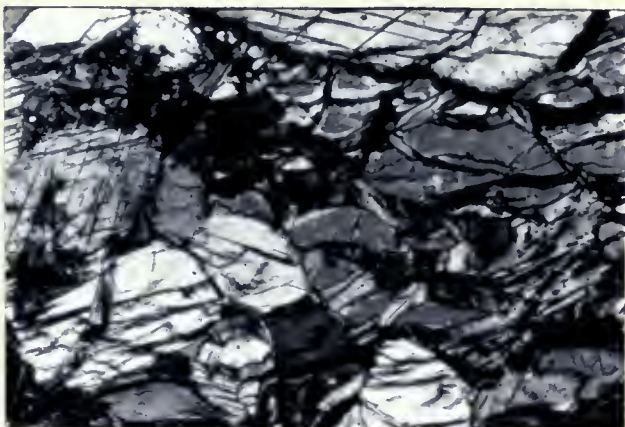
d
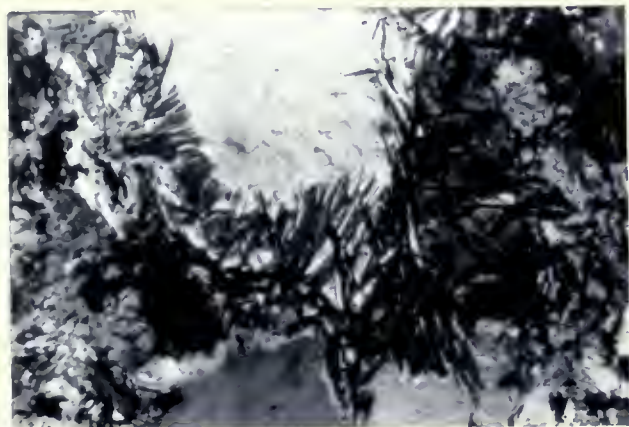
e
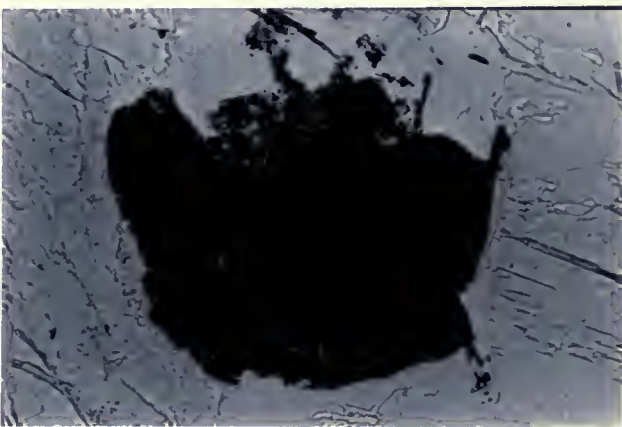
f

2) The second group contains cummingtonite along with rare hornblendes as the predominant mafic mineral. Such rocks exhibit widespread serpentinization. Cummingtonite is colorless to neutral in thin sections and subhedral and equidimentional in habit (Plate 1c). Some of these grains are serpentinized on the edges. Serpentine, making up an average of about 25% of a rock, occurs either in narrow veinlets (Plate 1d), which cut olivine, clinopyroxene and amphibole crystals, or as a groundmass constituent. A few fine-grained needle-like chlorite show initiation of their growth where they grow across cummingtonite grain boundaries resulting in a penetrative deformation (Plate 1e). The most abundant accessory mineral is magnetite, which is most commonly associated with serpentine. A few sections contain trace amounts of pyrite, sphene and some spinel crystals. Spinel probably belongs to the chromite series, in view of showing some diagnostic optical properties of iron rich chromite (Plate 1f). It is commonly translucent in the inner parts of grains, where it is normally yellow to redish-brown and opaque round its margins. This appears to be due to a trend from a more magnesian to a more ferroan type of chromite with growth of the crystal (Stanton, 1972). Chromite has been reported from Munro Township by Arndt et al. (1977). Anhedral crystals of clinopyroxene (diopside) and a few olivine crystals are identified in some of the thin sections (Plate 1d). These minerals are degraded and embayed on edges by serpentine and magnetite, forming mantles around the grains.

REDSTONE FORMATION

General Relations: The tholeiitic basalt and basaltic andesite of the Redstone Formation is best exposed in the southwestern part of the McArthur and the eastern portion of Fripp Townships (Fig. 4). The lavas are

PLATE 2

Elongated pillow lava observed in Redstone Formation
which is elongated parallel to the border of the
Peterlong Lake Complex.
Sample location 42   Grid Reference 751412

surrounded along the southwestern and northeastern sides by the Peterlong Lake Complex and Boomerang Formation, respectively. The presence of some medium-grained lava flows suggests thicker flow units in this formation. Most of the selected samples are from massive lavas. Deformed pillow lavas are exposed at site 42 (Fig. 3), (Plate 2). The pillows are elongated parallel to the contact of the eastern batholith and the Redstone Formation, suggesting that compressional forces were applied during intrusion of the batholith. Quartz veins are associated with many of the outcrops. The lavas commonly weather to various shades of grey to dark green color. A few medium to coarse-grained gabbroic phases are developed in these rocks.

Petrography: None of the original mineralogy, except for magnetite and apatite in a few samples, has been preserved in the rocks as a result of the metamorphic alterations. Sample locations 32, 35 and 36 are the zone of apatite accumulate. The flows are divided into two main groups according to the kind of amphibole present. The arbitrary distinction between actinolite and hornblende used here is based on the following three criteria: (a) actinolite is pleochroic pale green to green, whereas the hornblende has a dark green to brownish-green color on the Z direction; (b) actinolite commonly grows in needle-like habits in contrast to hornblende which has stubby ends; and (c) actinolite crystal has a higher birefringence than hornblende in thin sections of the same thickness.

In the first group most of the rocks exhibit long lath-shaped needles of actinolite which are pleochroic pale yellow to pale green (Plate 3a). Needles of actinolite commonly grow into calcium-plagioclase or secondary sodium-plagioclase. In some cases crystals are anhedral and display stubby habits with needle-like grain terminations. Chlorite commonly

PLATE 3

Redstone Formation

(a) Photomicrograph of fine needles of actinolite with a preferred orien-
     tation within the plagioclase groundmass. Granular quartz crystals
     occur in blebs within the matrix along with grains of zoisite (higher
     relief, right bleb) (crossed nicols, X 31).
     Sample 39

(b) Photomicrograph of fine-grained biotite flakes (grey, left central)
     and chlorite replacing biotite (dark grey flake, right central). The
     groundmass is fine-grained hornblende, plagioclase and quartz. The
     sample exhibit a slight banding (crossed nicols, X 125).
     Sample 189

(c) Photomicrograph of hornblende crystals and twinned crystals of
     andesine (left center) (crossed nicols, X 125).
     Sample 32

(d) Photomicrograph of fine-grained sphene surrounding magnetite crys-
     tals (plane light, X 31).
     Sample 189

PLATE 3

a

b
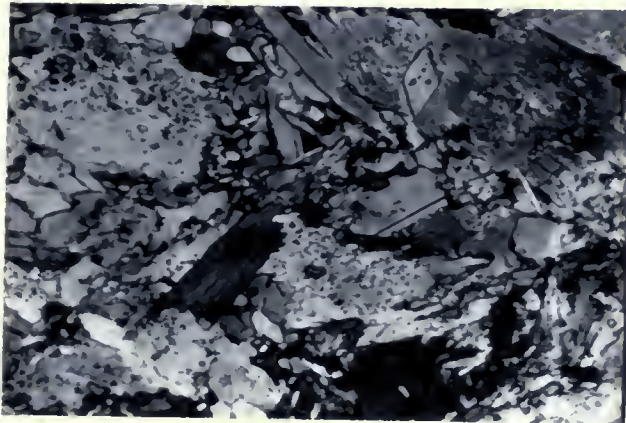
c
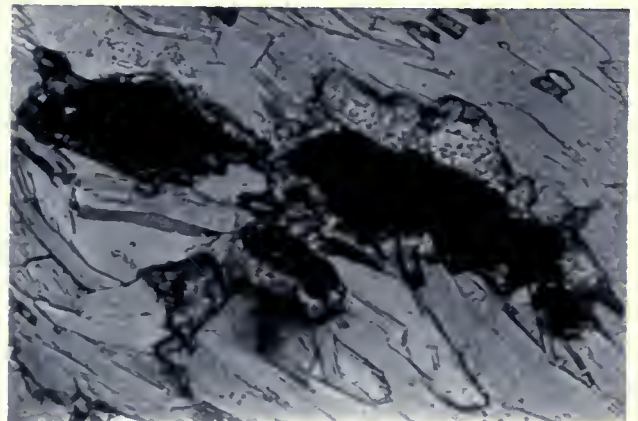
d

surrounds actinolite crystals. The pleochroism of chlorite ranges from pale green to green while its habit varies from single prismatic grains to prismatic aggregates. Calcium-feldspar is habitually replaced by anhedral crystals of albite with frequent twinning, minerals of the epidote group (zoisite, clinozoisite and rarely pisticite), sericite and carbonates. The rocks contain an average of 10% quartz by volume, which occurs in blebs, veins and groundmass and display a granular texture (Plate 3a). When a quartz veinlet cuts a mixed zoisite and quartz vein, it commonly becomes rich in carbonates. Prehnite rarely occurs in rock fractures.

The second group of rocks carries an abundance of highly pleochroic green to brownish-green anhedral hornblende crystals. Brown flackes of biotite exist in a number of sections but in most of them it has altered to chlorite (Plate 3b). In most cases Ca - plagioclase has altered to sodium-plagioclase, zoisite and sericite but rarely carbonates. Accompanying this alteration is the release of a minor amount of silica (Moorhouse, 1959) causing the appearance of fine-grained quartz. Relict andesine crystals are observed in the rocks taken adjacent to the Peterlong Lake Complex (Plate 3c). Pyrite is the most abundant accessory mineral in both of these groups. In most cases it is oxidized to hydrous iron oxides on the edges. Fine-grained sphene surrounds the magnetite and pyrite crystals (Plate 3d). A few grains of zircon are traced in one of the thin sections.

BOOMERANG FORMATION

General Relations: The Boomerang Formation is the only unit in the area to contain abundant andesite and dacite. It extends from southeast to northwest with the outcrops mainly along the hydroline in McArthur Township (see Fig. 4). Here the intermediate rocks are of a pyroclastic type, which were probably formed by volcanic explosions near an extrusive vent.

PLATE 4

(a)   An outcrop of an agglomrate showing the different litho-
       logies of the fragments.
       Sample 102   Grid Reference 805395

(b)   This picture shows the contact between gabbro (dark grey)
       and the Boomerang Formation (light grey)
       Sample 28 and 29   Grid Reference 788388

Stratified tuffs, tuff breccia and agglomerates are the main lith-
ologies (Plate 4a). In addition some massive rocks with fine grained
vesicules are present. These vesicules are normally filled with quartz
or plagioclase. The rocks weather to various shades of grey. The entire
collection of 41 samples displays a light grey to greenish-grey color on
the fresh surfaces. A few bands of iron formation and several gabbroic
sills cut these rocks (Plate 4b).

Petrography: Augite as a relict mineral of these rocks is distinguished
in the specimens taken from the vicinity of iron formation bands. Degradation
of pyroxene to uralite is well developed in a few of the thin sections.
The most abundant mineral recognized is secondary albite produced by the
low temperature decomposition of calcium-plagioclase. However, the presence
of relict calcium-plagioclase is not uncommon. Subhedral crystals of ande-
sine and oligoclase (An$_{20}$ - An$_{40}$) distinguished, using the Faque Methode.
Medium-sized plagioclase crystals, in a fine-grained groundmass, cause num-
bers of rocks to be porphyritic in thin sections (Plate 5a). Orthoclase
is not as common as plagioclase; however, this mineral is observed in small
quantities in a few of the rocks. Feldspar crystals are generally peppered
by fine-grained white mica, a phase that is even more widespread in rock
matrices. Minerals of the epidote group are not widespread but, when
present, occur interstitially to albitized plagioclase laths. The saus-
suritization of the plagioclase in most cases are accompanied by chloritiz-
ation. Quartz ordinarily appears with a granular texture, either in blebs
or in the groundmass of most of the rocks. It also exists as isolated
medium-grained anhedral crystals. Actinolite is developed as long and
tiny needles (Plate 5b) that cause many rocks to be banded in thin sections.

PLATE 5

Boomerang Formation

(a) Photomicrograph of medium-sized twinned and partly sericitized
     plagioclase phenocrysts set in a groundmass of fine-grained plagio-
     clase, quartz and saussurite (crossed nicols, X 125).
     Sample 115

(b) Photomicrograph of actinolite needles growing radially away from
     secondary albite toward a quartz and albite zone. The dark flakes
     in the centre are stipnomelane (plane light, X 31).
     Sample 109

(c) Photomicrograph of biotite (high birefringence) which is partly
     altered to chlorite (dark grey, right central), fine-grained plagio-
     clase makes the groundmass of the sample (crossed nicols, X 125).
     Sample 194

PLATE 5
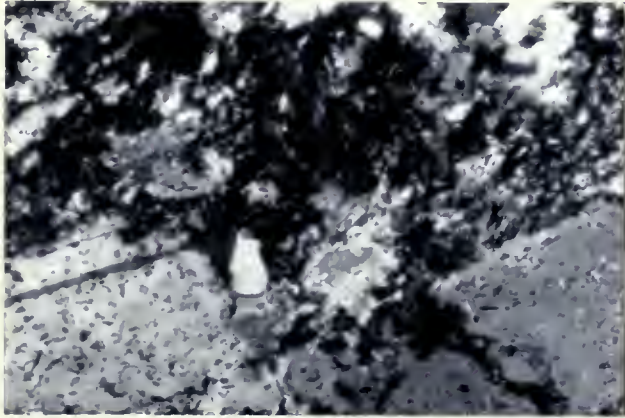
a
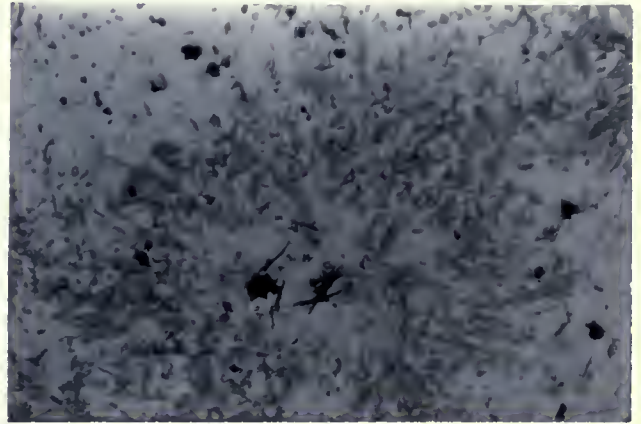
b
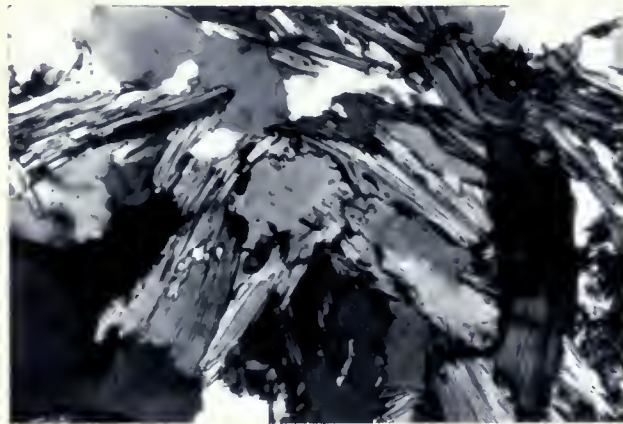
c

Chlorite is fine-grained and generally forms a mesh-like network embaying feldspar grains. Fine-grained, plate-like, pleochroic brown crystals of biotite were detected in many rocks carrying amphibole (Plate 5c). The amount of biotite tends to increase towards a northwestern direction. Dark brownish-orange stilpnomelane is a minor phase in rocks without chlorite (Plate 5b). Accessory minerals are sphene and euhedral crystals of pyrite which might have altered to hydrous iron oxides. Other iron oxides and ilmenite are scarce.

GOOSE LAKE FORMATION

General Relations: High magnesium ultramafic rocks of the Goose Lake Formation are present in several outcrops in the southwestern and central parts of McArthur Township. Samples were selected from outcrops both south and northwest of McArthur Lake and also from outcrops in central parts of McArthur Township, where a hydroline (Fig. 3) passes through this formation. Thirty-six rock samples and thirteen diamond drill cores were sampled. These specimens are very fine-grained and are dark greenish grey to black on the fresh surface. Each outcrop contains several flow units of various thicknesses. In a typical flow unit (Fig. 6A) the upper chilled margin (C1) is highly fractured and breaks the rock into several polyhedra, producing a structure that superficially resembles a breccia (Arndt et al., 1977). The spinifex-textured part of the flows (S) ranging in width from 10 to 400 cm is beneath the flow top (Plate 6a). Pyke et al. (1973) define spinifex as a texture in which large needles or blades of olivine, or clinopyroxene in some cases, are either randomly oriented or parallel to one another. This texture is generally viewed as having been developed by the rapid cooling of a crystal-poor ultramafic liquid in situ. Spinifex texture is an excellent factor for determining the top of the flow. There are three different ways to

PLATE 6

(a)   This picture shows a spinifex-textured part of a flow with
      olivine needles decreasing in size from left to right (bot-
      tom to top). The spinifex-free zone is shown at the bottom
      left corner of the picture.
      Sample locations 67, 68   Grid Reference 799416
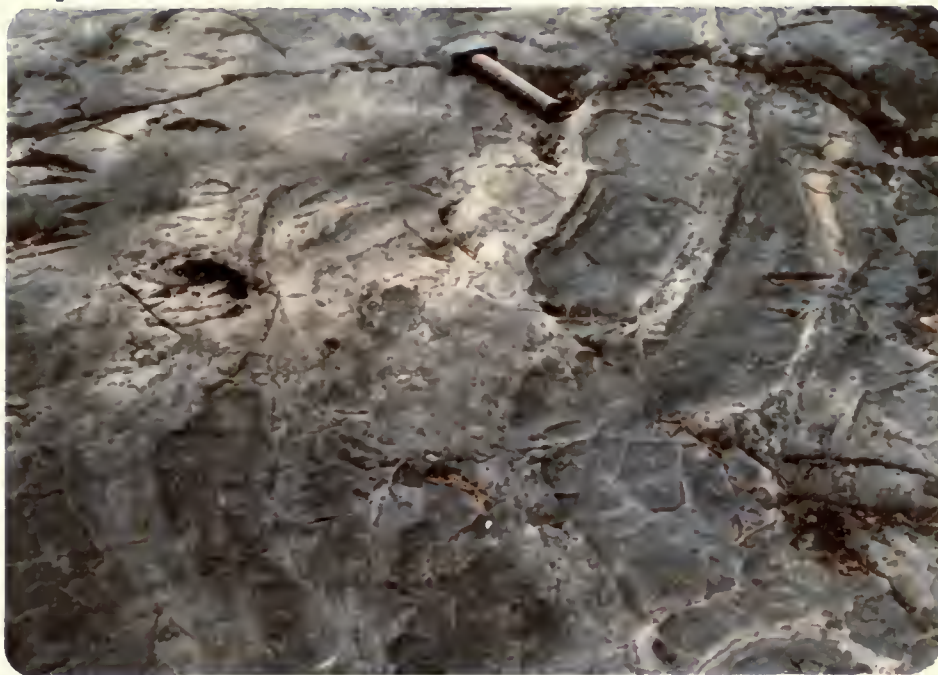
(b)   An irregularly folded spinifex-textured flow showing
      polyhedral jointing in the lower part of picture which
      is not observed in the upper part of the picture.
      Sample locations 247, 248, 249, 250, 251, 252, 253
                                        Grid Reference 799416
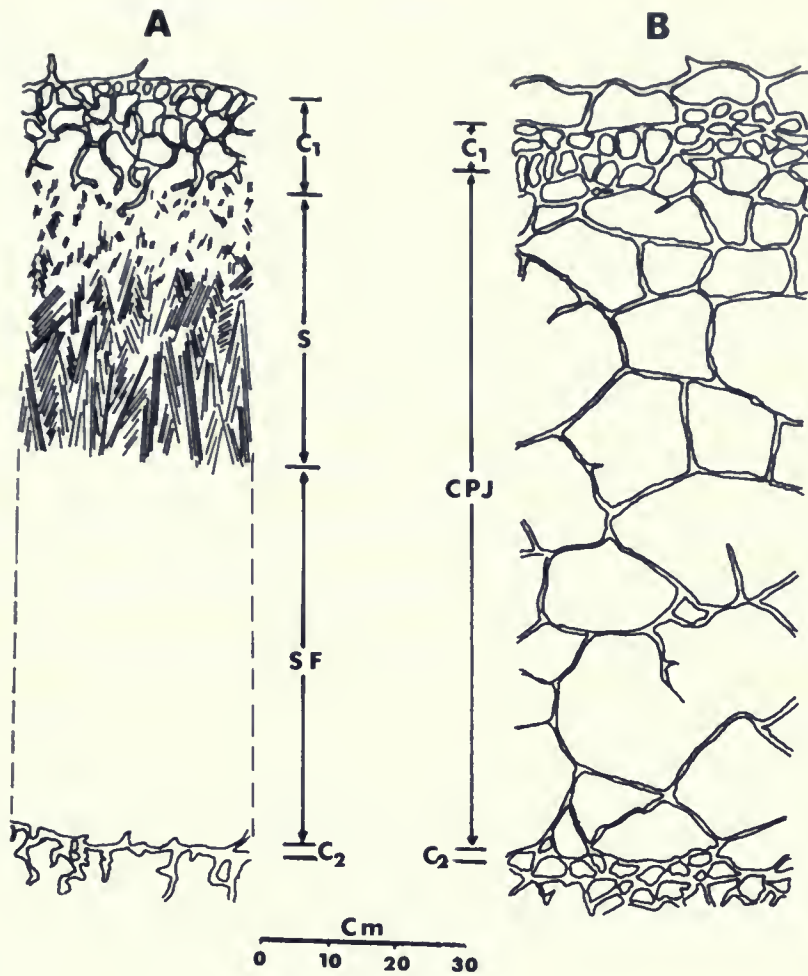
C_1	Upper chilled margin
S	Spinifex-textured zone
SF	Spinifex-free zone
C_2	Lower chilled margin
CPJ	Coarse polyhedral jointing

Figure 6   Diagramatic sections of two types of
            komatiitic lava flows: A, flow with
            spinifex texture; B, a flow without
            spinifex texture.

ascertain this: (a) The bladed olivine crystals progressively decrease in size toward the top; (b) The orientation of olivine blades in the upper part of the spinifex zone is random. In the lower part, the blades are arranged parallel to one another in booklets or sheeths that are oriented subperpendicularly to the plane of the flow (Arndt et al., 1977); and (c) Commonly, there is a tendency for the booklets to form a fan-like or cone-like arrangement with the apices pointing toward the top of the flow unit (Pyke et al., 1973). The lowest part of each flow unit is a thin, chilled margin (C2), overlain by various widths of spinifex-free zone (SF) which display a rough weathered surface. Many of the outcrops along the hydroline do not contain spinifex texture; however, they do exhibit coarse polyhedral jointing, as a main part of the flow and fine polyhedral joint- ing as a chilled flow top (Fig. 6B). Arndt et al. (1977) have reported this type of flow texture from ultramafic rocks in Munro Township, Ontario. In the McArthur Township, other outcrops display spinifex texture with an irregular pattern, where several relatively thin flow units are irregularly folded (Plate 6b). The width of the spinifex zone in the spinifex-textured flows varies from 10 cm in one of the outcrops along the hydroline to about 400 cm in flow units southwest of McArthur Lake. The length of blades varies from a few millimeters to 30 cm in different flow units. It seems that there is a tendency for thicker flows to contain a thicker spinifex zone with longer olivine blades. The lowest part of the flow units is almost uniform in all the outcrops and has a width of 12 to 30 cm.

Generally, the presence of this kind of flow texture is of great value in differentiating Ultramafic extrusive rocks from equivalent intrus- ive rocks. Furthermore, it is an accurate and reliable top indicator. In sample locations 120, 121, 122 (Fig. 3) numerous narrow asbestos veins were observed but are not present in sufficient quantities to be of any econom- ical value.

Petrography: Secondary minerals of the tremolite are the predominant minerals in most sections; however they do not exist in lava flows which contain more than 40% serpentine. Relict phenocrysts of olivine are present in a few thin sections. The olivine is anhedral and is commonly cut by irregular serpentine-and/or iron oxides-filled fractures. The largest olivine lath observed was 6.5 mm in length and 0.5 mm in width (Plate 7a). Serpentine pseudomorphs of olivine occur in many of the rocks. Two kinds of pseudomorphs are recognized: (1) The olivine has been entirely altered to serpentine with crystal boundaries marked either by carbonates or iron oxides (Plate 7b); (2) The second type is composed of tremolite in centers with serpentine rich rims (Plate 7c). The tremolite is extremely fine-grained and is always stained by brownish iron oxides. This type of pseudomorph is less than 0.3 mm in diameter; the boundaries are marked by minute magnetite and chromite grains. Microscopically the only relict volcanic texture present in these rocks is the spinifex-type. Olivine blades which have suffered alteration to fine-grained tremolite, range in length from 1 mm to 3.0 cm (Plate 7d). The presence of iron and chromium oxides along margins of the blades makes them easily distinguishable in plain light. In most thin sections tremolite pseudomorphing the olivine blades is finer-grained than other tremolite. The interstitial tremolites are arranged parallel to each other and are usually bent (Plate 7e). Equant pseudomorphs of olivine comprise lower parts of each flow unit (olivine accumulate zone) above the chilled base (Plate 7b). Tremolite with very fine-grained crystals is the predominant secondary ferromagnesian mineral. Its habit ranges from single needle-like fibers in the pseudo-morphs of olivine to fibrous accicular aggregates around spinifex blades. The individual tremolite crystals are achroic and most commonly show sweeping extinction under crossed nicols. Serpentine is the most abundant

PLATE 7

Goose Lake Formation

(a) Photomicrograph of a skeletal olivine crystal with serpentine in
     the fractures (crossed nicols, X 31).
     Sample 129

(b) Photomicrograph of an olivine accumulate zone, with serpentine
     pseudomorphing the olivine grains. Fine-grained magnetite is
     bordering the margins (plane light, X 31).
     Sample 123

(c) Photomicrograph of two olivine pseudomorphs (left central and top
     right). Fine-grained tremolite fills the central parts of the
     pseudomorphs while serpentine and magnetite make up the margins
     (crossed nicols, X 125).
     Sample 66

(d) Photomicrograph of skeletal olivine (now altered to tremolite) in
     the spinifex zone of a flow. The dark grey parts are devitrified
     glass (crossed nicols, X 31).
     Sample 256

(e) Photomicrograph of typical growth of tremolite crystals. Tremolite
     is finer-grained when pseudomorphs olivine, whereas it is coarser-
     grained and is commonly bent when replacing interstitial pyroxene
     (crossed nicols, X 31).
     Sample 89H

(f) Photomicrograph of antigorite (groundmass) and chrysotile (vein),
     in highly altered komatiite. Some carbonates present within chrys-
     otile (crossed nicols, X 125).
     Sample 78

PLATE 7
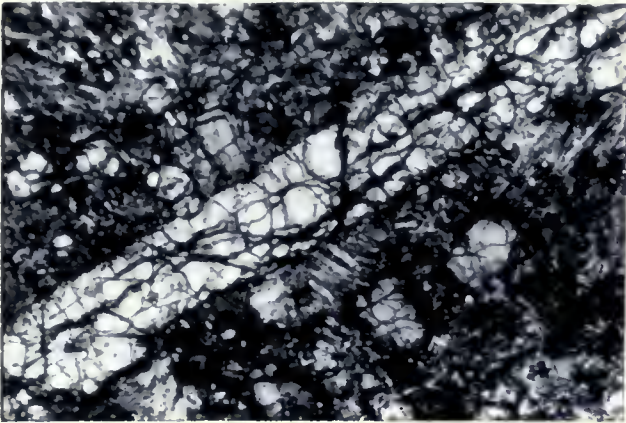
a
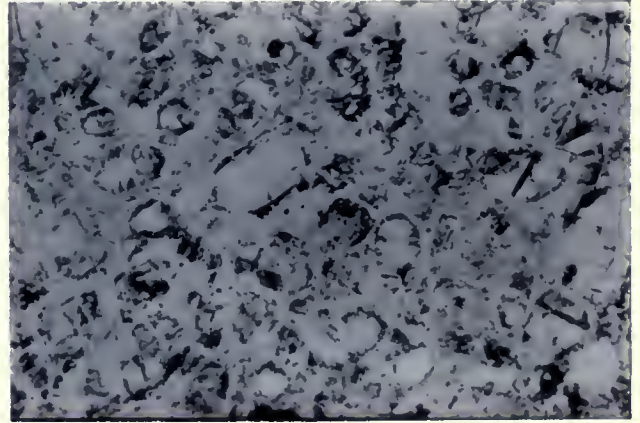
b
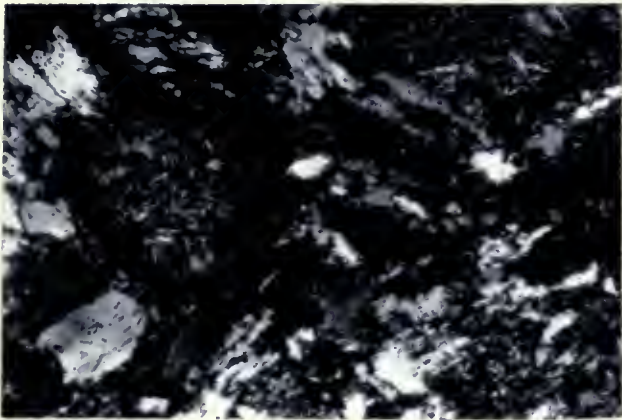
c
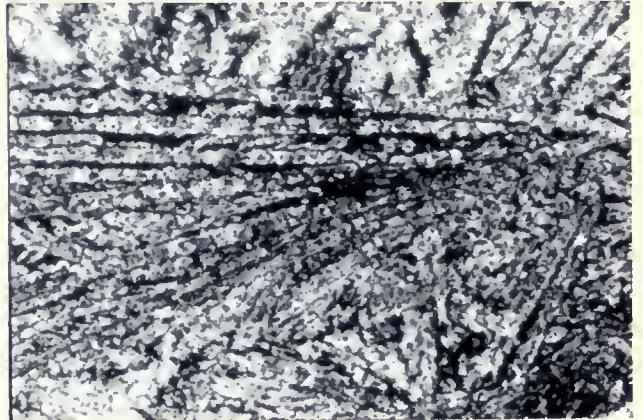
d
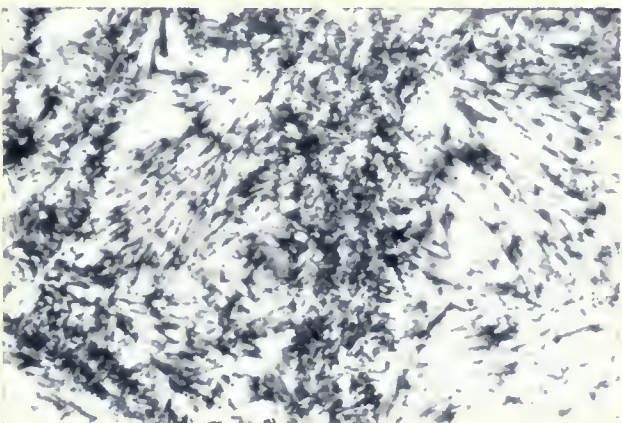
e
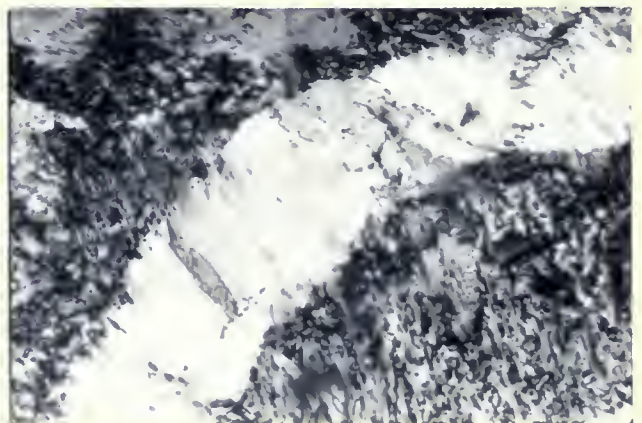
f

PLATE 8

Goose Lake Formation

(a) Photomicrograph of tremolite pseudomorphing olivine crystals. The dark parts are devitrified glass. The sample is taken from the spinifex zone of a flow unit (crossed nicols, X 31).
Sample 90H

(b) Photomicrograph of skeletal magnetite (plane light, X 31)
Sample 256

(c) Photomicrograph of anhedral albite (light grey, centre), chlorite (dark grey, right central on the edge) and tremolite (top left corner) (crossed nicols, X 125).
Sample 138

(d) Photomicrograph exhibiting three different stages of alteration in the rock and the fact that serpentinization has happened prior to the growth of tremolite. (crossed nicols, X 31).
The stages of occurrence are:
  1) Serpentinization of olivine (centre, dark grey)
  2) Development of cross-cutting carbonate veinlet of the olivine pseudomorph (upper centre)
  3) Growth of tremolite cross-cutting both olivine pseudomorph and carbonate veinlet (light to medium grey, upper centre).
Sample 259

Schumacher Formation

(e) Photomicrograph showing part of a variole (dark grey, right half) and groundmass (left half). The variole, compared to the groundmass is finer-grained and contains more saussurite and less actinolite and chlorite (crossed nicols, X 31).
Sample 81

(f) Photomicrograph of a banded specimen containing bands of hornblende alternating with saussuritized plagioclase (crossed nicols, X 125).
Sample 49

PLATE 8
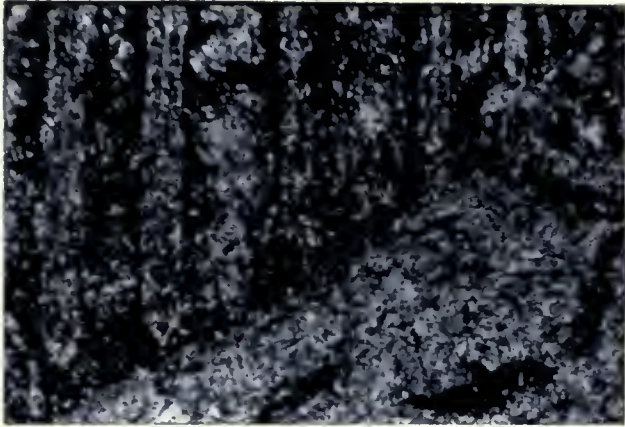
a
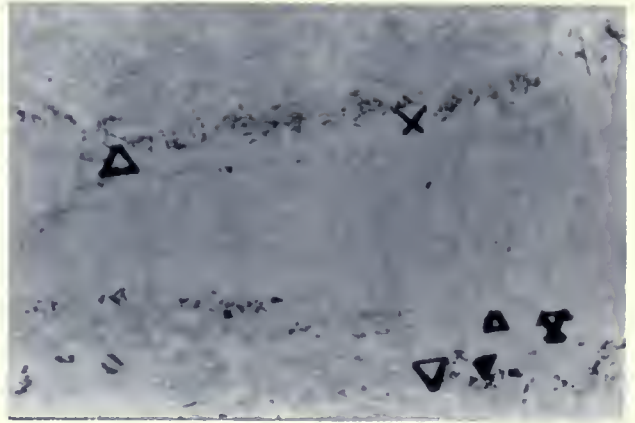
b
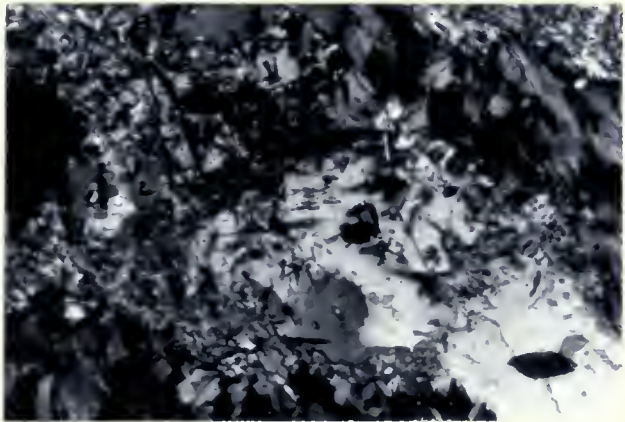
c
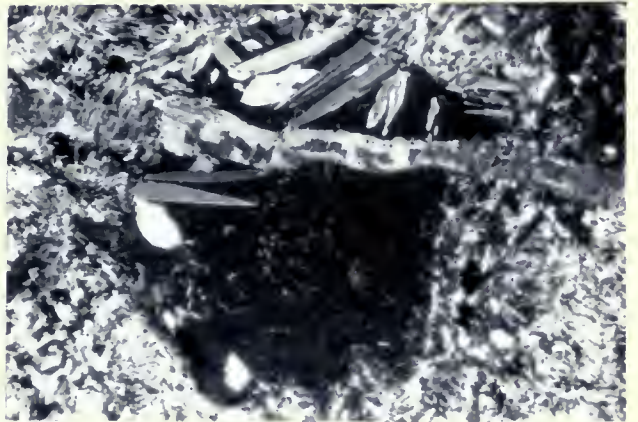
d
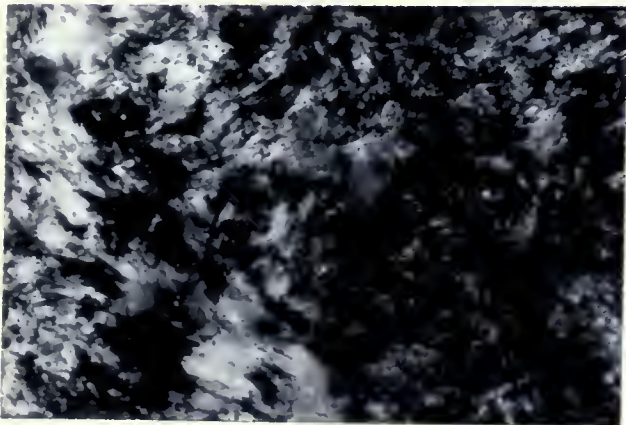
e
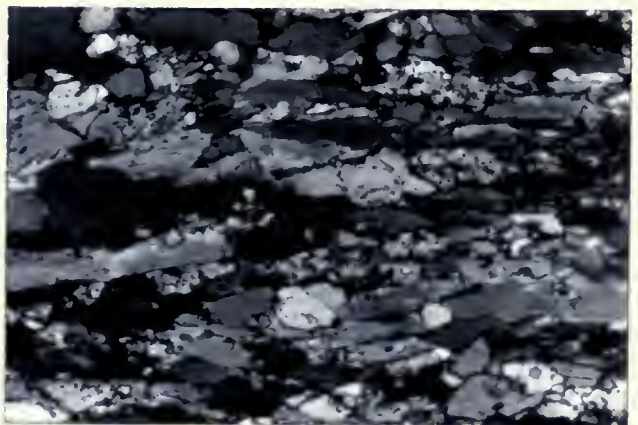
f

mineral in rocks with little or no tremolite. In some specimens the rocks have been entirely altered to serpentine; trace amounts of carbonates or magnetite mark the boundaries of the original crystals. Antigorite is the main constituent of serpentine and chrysotile occurring in cross-fiber veinlets in serpentinite (Plate 7f). Chrysotile is distinguished from antigorite by lower relief, higher birefringence and its fibrous habit. Varying amounts of devitrified glass exists in rocks taken from chilled margins and spinifex zones (Plate 8a). Interstitial to tremolite is fine-grained masses of chlorite recrystallized after glass. Chlorite predominately exhibits dark, greenish-brown or Berlin blue firefringences and is colorless to slightly green under the plain light. Most of the thin sections contain anhedral crystals of iron-rich chromite. Like those in the Donut Lake Formation, they have an opaque rim with a brownish, translucent center. A few of the sections contain numerous, tiny Magnetite crystals with skeletal structures. Skeletal magnetite shows various stages of growth from crossing bars to complete cubes of magnetite (Plate 8b). Anhedral albitized plagioclase is distinguished in one thin section accompanied by large amounts of chlorite, carbonate and minor tremolite (Plate 8c). Plate 8b shows the secondary growth of tremolite following the serpentinization of original lava.

SCHUMACHER FORMATION

General Relations: This formation, the youngest volcanic unit exposed in the study area, contains primarily basalt and basaltic andesitic flows. It is exposed both on the southwestern border of the Adams Pluton and between the Boomerang and Goose Lake Formations in the southwestern part of McArthur Township. In the zones of relatively intense deformation, the volcanics exhibit schistosity that resulted in compositional banding. All gradations between schistose metavolcanics and essentially altered but undeformed types, are present within outcrops. Attitudes of schistosity

suggests that it is the result of the intrusion of adjacent pluton, the contacts of which are parallel to folliation. The outcrops where samples 72, 73, 77 (Fig. 3) were taken, are distinctly layered. The stratigraphic units dip north-northeast at about 87°. The rocks exhibit varying shades of dark grey on weathered surfaces and dark green to dark grey on fresh surfaces. Sample 79, 80, and 81 (Fig. 3) have a tube-like or cigar-shaped variolites of white or light grey color, with an average diameter of 5 mm. The varioles are made up of concentric rings, with lighter toned inner rings. Some intermediate metavolcanic rocks form intercalations in the mafic flows of the Schumacher Formation.

Petrography: All of the metavolcanics in this formation have suffered alteration to secondary mineral assemblages. The predominant secondary mineral in less deformed rocks is actinolite, while hornblende pervades more deformed rocks. The volcanic rocks are divided into two groups as follows:

1) The first group of rocks contain an average of 55% actinolite crystals. Actinolite is pleochroic in most of the sections. The mineral occurs in a variety of habits, ranging from single, elongated prismatic grains to prismatic aggregates or from single, acicular fibers to fibrous aggregates. In some rocks actinolite displays wavy extinctions. Lineation of the actinolite crystals was observed in a few samples, but in most of the exposures the actinolite grains are randomly oriented. The crystals are most commonly fine-grained, but in two samples the grains were as large as 1.5 mm, causing a porphyritic texture. The presence of porphyritic texture indicates different cooling rates in the middle of these flows. Chloritization of actinolite in rocks from the exposures between Boomerang and Goose Lake Formation is evident. Chlorite is fine-grained and acts as

an interstitial mineral; it also was detected in small patches. The mineral is pleochroic and under crossed nicols displays brown interference color. Secondary albite crystals were observed in two thin sections; epidotization of plagioclase is widespread; an average of 30% zoisite was found in rocks devoid of plagioclase. Normally minor quantities of carbonate and sericite are present in most rocks in association with plagioclase and saussurite. Carbonates also occur in veinlets. Fine pleochroic brown biotite flakes present in the specimen taken from the outcrops in the southwest of McArthur Lake, where the flows are surrounded within three small intrusions. Prehnite (2.4%) occurs in veins in the rocks from the vicinity of the Adams Pluton. The grains within varioles are very fine-grained and are composed of highly saussuritized plagioclase with a few grains of actinolite and chlorite (Plate 8e). Centers of each varioles are marked by the presence of quartz crystals.

II) The second group of rocks contain 50-70% fine-grained hornblende. The preferred orientation of hornblende crystals imparts a banded appearance to the rocks (Plate 8f). Here the bands of fine-grained quartz or plagioclase alternate with hornblende rich bands. Hornblende is euhedral and shows strong pleochroism. Biotite may be present in some flows. Saussuritization is not as pronounced as in the former group. Chlorite and carbonates are absent and most of the plagioclase are sericitized. Minor amounts of prehnite are present in the veins. Accessory minerals in both groups of rocks are pyrite, magnetite, hematite, and trace amounts of sphene. On the edges, pyrite has oxidized to hydrous iron oxides.

ADAMS PLUTON

General Relations: Exposed on the north and northwestern section of

PLATE 9

Adams Pluton

(a) Photomicrograph of large twinned ca-plagioclase grain (grey, top
     left), quartz (light grey, bottom central), euhedral amphibole (light
     grey, bottom right corner), chlorite (dark grey, right central), and
     euhedral sphene (dark grey, top central), (crossed nicols, X 31).
     Sample 196

Peterlong Lake Complex

(b) Photomicrograph of biotite rich rock (light grey, right central) con-
     taining plagioclase (grey, bottom left), amphibole and quartz (top
     central on the edge), (crossed nicols, X 31).
     Sample 214

(c) Photomicrograph of hornblende (light grey, top left corner) which is
     partly altered to fine-grained actinolite. Apatite (grey, top central
     on the edges) is partly surrounded by magnetite (black), also, saus-
     suritized plagioclase is present (grey, bottom right corner), (crossed
     nicols, X 31).
     Sample 245

Quartz Diorite Sill

(d) Photomicrograph of fibrous uralite with hornblende crystals (grey,
     top centre), biotite flakes, quartz (grey, bottom center on the edge)
     and chlorite (dark grey, right center), (crossed nicols, X 125).
     Sample 118

Quartz Feldspar Porphyry

(e) Photomicrograph of sericitized anhedral plagioclase (left) and rounded
     quartz grain (right) enclosed in a matrix of fine-grained plagioclase,
     quartz and sericite (crossed nicols, X 31).
     Sample 166

Trondhjemite

(f) Photomicrograph of twinned plagioclase with minor amounts of chlorite
     (crossed nicols, X 31).
     Sample 146

PLATE 9
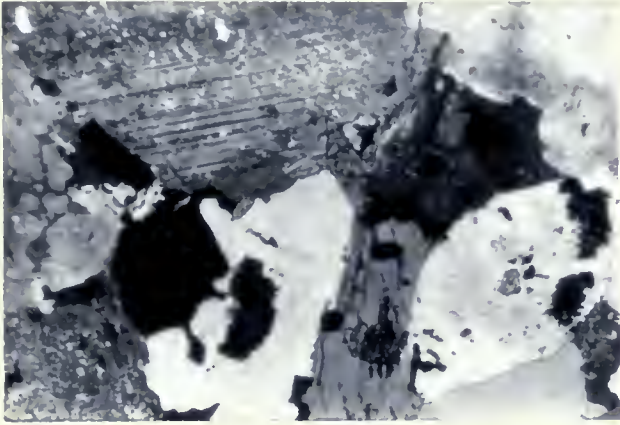
a
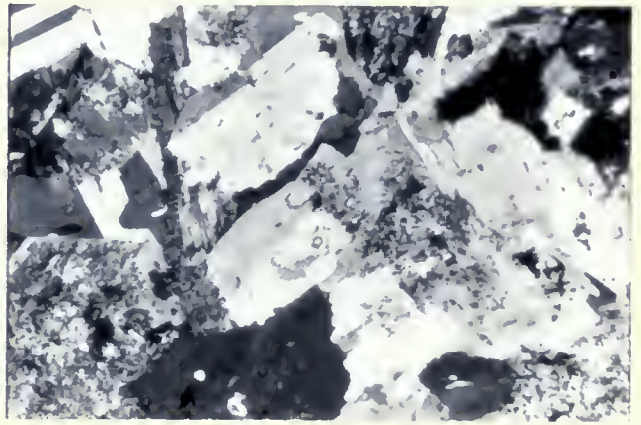
b
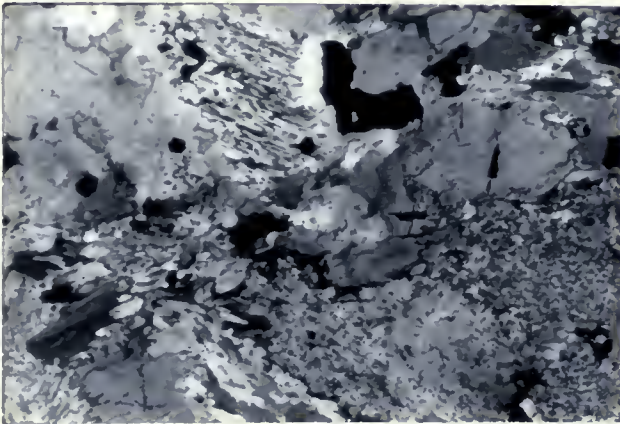
c
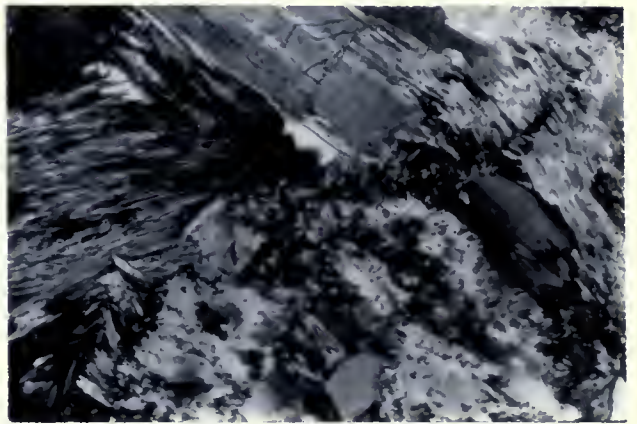
d
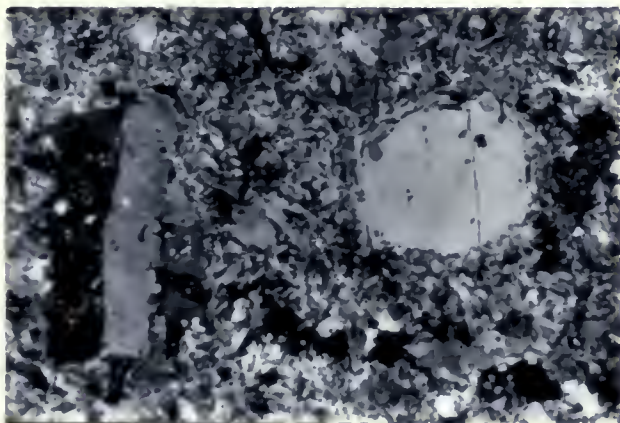
e

f

the area is a light pink, weathering porphyritic granodiorite. This plutonic stock has intruded the Schumacher Formation, and is therefore surrounded by basaltic rocks on the south, north, and east sides (Pyke, 1973), (Fig. 4). The intrusion had little effect on deforming the previously folded metavolcanics, except for the development of schistose foliation in nearby rocks. However, it has metamorphosed adjacent volcanics to amphibolite facies. Six out of eight samples selected were taken relatively near the edges of this pluton (less than 300 m). The rocks are coarse-grained and all of the grains are visible to the naked eye. They contain large phenocrysts of calcic plagioclase (up to 2 cm).

Petrography: Examination of thin sections reveals plagioclase to be the main constituent of these rocks. The large calcium-plagioclase crystals are generally altered, but some relict calcium-plagioclase still exists. Presence of Carlsbad and albite twinning in some calcium-plagioclase permits determination of the anorthite:albite ratio using the Fuque method. In most of the specimens the composition was An_{38} or less. Subhedral crystals of epidote (2-4%) and scattered amounts of sericite (1-2%) are alteration products of calcium-plagioclase. In addition, varying amounts of orthoclase and microcline, exhibiting gridiron structure occur. Alteration in alkali feldspars is much less severe than in plagioclase. Interstitial medium-grained quartz comprises from 10 to 17% of most thin sections. The major mafic mineral is hornblende (4-7%), the crystals of which are pleochroic green to brownish-green and showing well developed cleavage sets (56°, 124°), (Plate 9a); the crystals may be as large as 2 mm. A minimal percentage of fine-grained biotite is present in a few specimens. Chlorite is a ubiquitous alteration product of hornblende and biotite. An average of about one percent of small euhedral apatite grains

can be observed within feldspar crystals and interstitial groundmass. Euhedral grains of sphene and magnetite compose an average of 1% each.

PETERLONG LAKE COMPLEX

General Relations: A large batholith has intruded the metavolcanics in the southwestern corner of the study area (Fig. 4). This batholith surrounds the Donut Lake Formation and has a long border with basaltic rocks of the Redstone Formation. The age of the lavas, as determined from top directions, decreases away from the pluton; all lavas dip away from this batholith. Therefore it appears that intrusion of the Peterlong Lake Complex is the main cause of folding of the volcanic rocks. Furthermore, it is assumed that upward movement of the batholith has domed the stratigraphically lower volcanics and caused folding. All the selected samples are medium to coarse-grained and are weathered greenish-grey.

Petrography: Most of the sections are dominated by secondary minerals with plagioclase as the most abundant mineral in less altered rocks. Presence of albite twinning permits determination of the anorthite content of calcium-plagioclase, which is normally in the lower range of andesine. These crystals are coarse-grained and anhedral in habit. Sericitization and saussurization have had an extreme effect on plagioclase. Therefore in most of the cases calcium-plagioclase is altered to albite, white mica, and minerals of epidote group. Varying amounts of anhedral crystals of quartz occur in all of the specimens (2-25%). Also it is observed that rocks containing mica show higher amounts of quartz (Plate 9b). Crystals of microcline and orthoclase are found in one of the thin sections. The main mafic mineral, hornblende which is occasionally associated with actinolite (Plate 9c), is corroded on the edges, and more or less chloritized.

Fine-grained prismatic crystals of chlorite has grown around amphibole
grains, Samples taken from outcrops around Bartlett Lake (Fig. 3),
show about 15% aggregates of pleochroic brown biotite, which as a minor
phase was also recognized in some other rocks. Trace amounts of apatite,
carbonates, sphene and iron oxides were observed in a few of the sections.

QUARTZ DIORITE SILL

General Relations: The southern part of Goose Lake Formation is
intruded by a northwestern trending quartz diorite sill (Fig. 3). A
termination of the sill is along the southern shores of McArthur Lake
where samples were taken, but the sill continues for 3 km. toward north-
west (Pyke, 1973).

Petrography: The original mineralogy of the rocks has been destroyed.
The major ferromagnesian mineral is medium-grained, euhedral to anhedral
hornblende crystals which are pleochroic greenish brown with well developed
amphibole cleavage. Uralite, a fibrous light green amphibole, occurs in
one of the sections studied (Plate 9d). Amphiboles are slightly chlori-
tized. Chlorite (1-2%) is fine-grained and pleochroic pale green. Calcium-
plagioclase has entirely altered to albite, sericite and saussurite, but
the original crystal shape is preserved. Medium to fine-grained anhedral
crystals of quartz form 8 to 10% of the rocks. In addition trace amounts
of apatite, magnetite, sphene and leucoxene were detected. The close
petrographic resemblance of this sill with the Peterlong Lake Complex sug-
gests the same origin for both.

QUARTZ FELDSPAR PORPHYRY AND TRONDHJEMITE

General Relations: Two quartz feldspar porphyritic stocks and one trondhjemitic stock occur in the southeastern corner of the study area and along the southern shore of McArthur Lake. Pyke (1978) argues the occurence of these rocks as the high level-emplacement of the intrusions because of the presence of chilled margins, porphyritic texture, miarolitic cavities, minor granophyric texture, and abundant fracturing in these rocks. All the selected rocks from quartz feldspar porphyry are from chilled margins which are fine-grained. The quantity of larger quartz and feldspar phenocrysts increases towards the inside of the stocks. These rocks have a light pink color on the fresh surface but much darker in the case of the trondhjemite.

Petrography: All the sections reveal phenocrysts of oligoclase and of quartz in a finely granular groundmass of small, interlocking grains of quartz and feldspar (Plate 9e). Plagioclase phenocrysts are subhedral and about 1.5 mm. in length; quartz phenocrysts are subrounded and about 1 mm. in length. Groundmass is made of 60 to 70 percent plagioclase, which is albitic in composition and partly altered to white mica and carbonates, with an additional 20 to 30 percent fine-grained quartz. Chlorite and biotite are traced in two different sections. Iron oxides exist in small amounts. Trondhjemitic rocks are different in composition in such a way that they are less quartz rich (5-10%), richer in plagioclase by 65-80%, and contain 5 to 10% chlorite (Plate 9f). Plagioclase is partly altered to sericite and carbonates. Iron oxides are more abundant. Pyrite, sphene and apatite are also present.

GABBROIC SILLS

General Relations: One of the main components of the Abitibi

PLATE 10

Gabbro

(a)   Photomicrograph of a large anhedral hornblende crystal (grey, left
      side) which is partly altered to fine-grained actinolite (light
      grey, top left). Also a mixture of plagioclase and zoisite are
      present at right (crossed nicols, X 31).
      Sample 97

Diabase Dyke

(b)   Photomicrograph of a Precambrian diabase dyke. Pyroxene (grey,
      bottom right corner), biotite (light grey, top right corner), long
      prism of apatite (dark grey, center), amphibole (light grey, top
      left corner) and twinned plagioclase (left central, on the edge)
      (crossed nicols, X 31).
      Sample 52

Sedimentary Rocks

(c)   Photomicrograph of a banded sedimentary rock. Bands of hornblende
      alternating with plagioclase crystals (crossed nicols, X 31).
      Sample 240

(d)   Photomicrograph showing the porphyroblastic texture of a sedimentary
      rock: coarse-grained plagioclase crystals with zoning (right) and
      twinning (left). The black square in the centre is pyrite (crossed
      nicols, X 31).
      Sample 241

(e)   Photomicrograph showing elongated tourmaline crystals (dark grey,
      top left corner) and oriented in cross-section (black, right central)
      with some actinolite prisms (centre). The groundmass is a mixture
      of quartz plagioclase (crossed nicols, X 125).
      Sample 45

PLATE 10
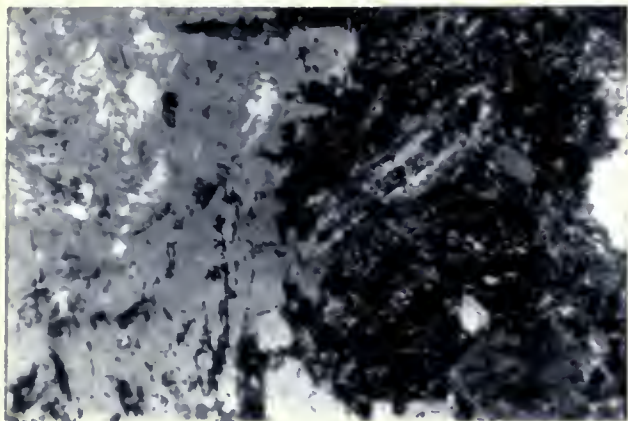
a
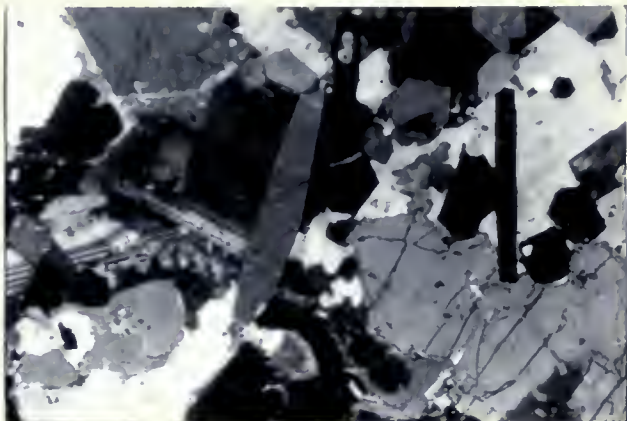
b
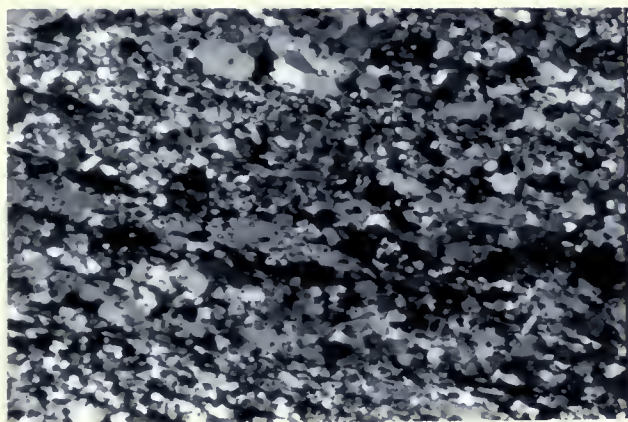
c
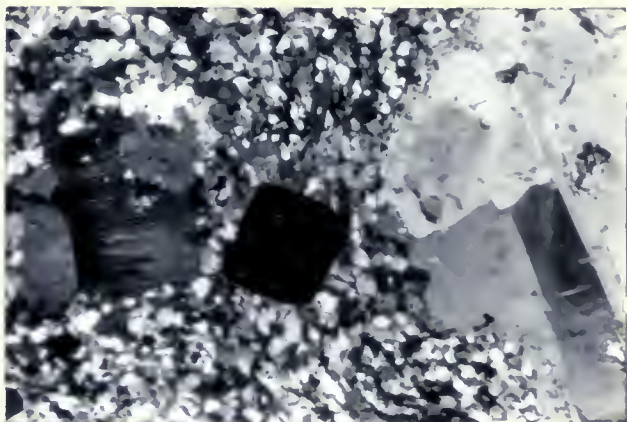
d
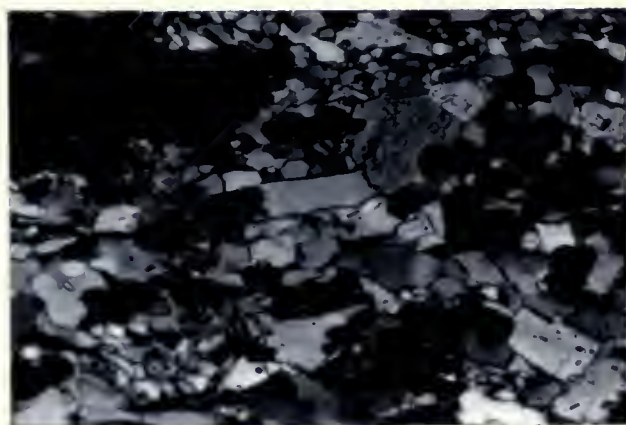
e

greenstone belt is medium to coarse-grained gabbroic sills which are associated with overlying or interlayered volcanic rocks. These greyish green weathered rocks are found mostly in the Redstone and Boomerang Formations, but a few were recognized in the Goose Lake and Schumacher Formations. The contact between gabbroic sills and the metavolcanics is exposed in only two locations in the Boomerang Formation (Plate 4b). Samples taken from these two locations are fine-grained. The largest gabbroic body in the area is approximately 3 km in width, with a tendency to be elongated in the direction of regional bedding. Because the gabbroic sills are considered possible reservoirs or vent channels for the lavas (Pyke, 1978; Jolly, 1977), they have almost the same age as extrusion of the lavas.

Petrography: Mineralogical relationship within the gabbroic sills are similar to those described for basaltic rocks of the Redstone Formation. The only differences are larger amphibole and feldspar grains, and extensive saussuritization of feldspar. Alteration of large anhedral hornblende crystals to fine-grained actinolite were observed in many of the sections (Plate 10a).

DIABASE DYKES

General Relations: Several diabase dykes of various ages traverse the area. The Early Precambrian dykes trend north to north-northwest, Middle Precambrian dykes trend northeast, and Late Precambrian dykes trend either east-northeast or northwest (Pyke, 1973). Pyke (1978) has called the Middle Precambrian dykes "quartz diabase" and Late Precambrian ones "olivine diabase". All of the selected specimens are medium to coarse-grained and weather dark greenish-grey.

Petrography: Large euhedral crystals of plagioclase are the main constituents of most diabase dykes. A major portion of the plagioclase are twinned according to Carlsbad and albite law. There is a general tendency for finer-grained specimens to show a higher anorthite content than coarser-grained samples from the same dyke. The anorthite content for Middle Precambrian dykes ranges between 30 to 80% and for the Late Precambrian dyke from 30 to 50%. The mineral assemblage for Middle Precambrian diabase is an average of 50% plagioclase, 28% clinopyroxene, 8% chlorite, 4% sericite, 2% biotite, 4% uralite, 5% magnetite and 2% quartz. Late Precambrian diabases consist of 40% plagioclase, 27% clinopyroxene, 8% magnetite and ilmenite, 6% olivine, 4% biotite and some chlorite, sericite, stipnomelane, uralite and sphene. Samples from central parts of the dykes show up to 7% euhedral apatite grains (Plate 10b). The diabase dyke on the southern shore of McArthur Lake is extensively altered having 12% plagioclase, 20% tremolite, 35% clinopyroxene, 8% chlorite, 18% sericite, 3% magnetite and 2% calcium-garnet.

METASEDIMENTS

General Relations: A minor sedimentary unit is located on the northwestern side of Quartz Lake (Fig. 4). Metasediments which resemble Timiskaming-type greywackes are thinly bedded (Plate 10c) but near the Peterlong Lake complex they change to Porphyroblastic texture (Plate 10d). It is evident that sediments predate the intrusion since they are highly metamorphosed. Several bands of iron formation, which can be generalized into two main units, are present within Boomerang Formation.

Petrography: Fine-grained anhedral plagioclase crystals build up about 50% of the banded rocks. Within the Porphyroblastic metasediments the

amount of plagioclase increases to about 65% by volume and also they grow in size up to 5 mm. Plagioclase is saussuritized in both banded and porphyroblastic metasediments but it is not twinned in the former. The abundance of quartz crystals decreases from 35 to 5% toward the intrusive contact. Minerals of epidote group increase toward the Porphyroblastic rocks but decrease in quantity toward the Peterlong Lake Complex. Fine flakes of biotite present in all the specimens (1-3%) however most of biotite has altered to chlorite (6%). Hornblende also shows a sharp increase in volume toward the batholith. Sphene, apatite, carbonates, iron oxides and zircon are detected in some of the thin sections.

Iron Formation: Several bands of iron formation, which can be generalized into two main units, are present within the Boomerang Formation. Bands of massive chert typically alternate with individual units. Iron occurs in fine-grained crystals of magnetite which in a few cases, are slightly rusted. Actinolite crystals commonly fill interstices between magnetite grains. Another characteristic is the presence of granular quartz crystals in zones of less magnetite concentration. The maximum concentration of magnetite is about 50% by volume. Sample 45 (Fig. 3), taken near the iron formation veins contains about 15% of subhedral prisms of dark, bluish-green iron-rich tourmaline (verdelite, Deer et al., 1974) which might represent contamination from sea water (Plate 10e).

DISCUSSION

The altered and metamorphosed nature of the entire lava pile is evident from thin section study of the extrusive rocks. The most significant findings are:

(1) The Donut Lake Formation is completely recrystallized to middle to upper amphibolite facies, therefore none of the primary phases or textures are preserved.

(2) The Redstone Formation contains secondary mineral assemblages ranging from the lower greenschist facies to amphibolite facies.

(3) The Boomerang Formation carries very small amounts of femic minerals, mostly of the greenschist facies. The rocks are predominantly recrystallized to secondary phases but some augite and calcium-plagioclase relics are also present in some specimens.

(4) The Goose Lake Formation is highly tremolitized and/or serpentinized (low-grade metamorphism). The lava flows, some of which exhibit spinifex textures contain a few relict olivine phenocrysts.

(5) The Schumacher Formation shows an extensive compositional banding of secondary hornblende and plagioclase.

(6) Intrusive rocks generally have preserved their original mineralogy except for gabbroic sills which resemble those in the metamorphosed Redstone Formation.

(7) Sedimentary rocks in the area include the low-grade metamorphosed Iron Formation with magnetite as the main constituent. Timmiskaming-type greywackes are either banded or porphyritic and are highly metamorphosed.

METAMORPHIC   SYNTHESIS

GENERAL

The volcanic rocks in the area contain the mineral assemblages which are indicators of the greenschist and amphibolite facies. The lava piles have suffered metamorphism primarily within the greenschist facies of regional metamorphism, with local upgrading to amphibolite facies along the borders of the granitic plutons in the area. The estimated 15600 m thickness of lava pile in this area (Pyke, 1978), suggests the total load pressure of about 4.5 kb with approximate temperatures ranging between 300 to 700°C (Winkler, 1974).

METAMORPHISM OF KOMATIITIC ROCKS

It is assumed here that komatiitic rocks, which were mainly composed of olivine and pyroxene, were altered to serpentine during the post eruptive cooling history of the lava.

1 Forsterite + 1 Enstatite + 2 $H_2O \rightleftharpoons$ 1 Serpentine
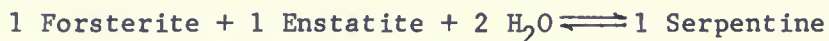
Due to later medium-grade metamorphism during the intrusion of plutonic bodies, serpentine changed to mineral assemblages containing orthropyroxene + olivine, that resemble those of the original lavas.

Metamorphism of the present serpentinite is a series of dehydration processes the extent of which depends on the pressure and temperature involved. For instance, in the case of sample 14 and 15, which contain tremolite + talc + chlorite assemblages, the rocks under P_{H_2O} between 1 to 5 kb were heated up to 650°C. To produce tremolite the rock should contain a

calcium-bearing phase (more likely diopside). Therefore:

(I)   5 serpentine + 2 diopside $\xrightarrow[P_{H_2O}=1-5\ kb]{T=400-500^{\circ}C}$ 1 tremolite + 6 forsterite + 9 H_2O.
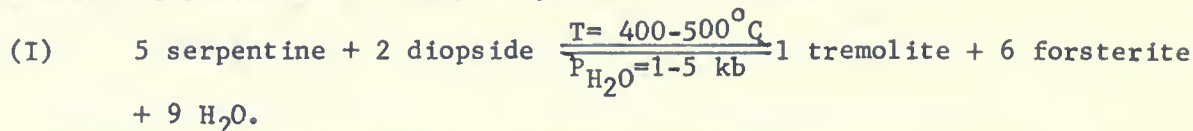
Later with increasing temperature the remainder of serpentine will be changed to talc:

(II)   5 serpentine $\xrightarrow[P_{H_2O}=2-5\ kb]{T=500-650^{\circ}C}$ 1 forsterite + 1 talc + H_2O.
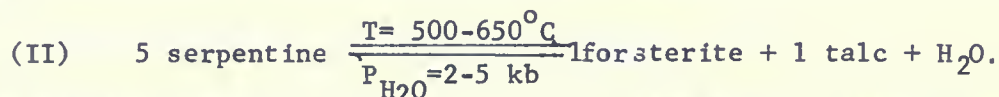
The Goose Lake komatiitic lavas contain the same mineral assemblages as these Donut Lake specimens, but do not carry talc. This indicates that they were not heated to higher temperatures than about $500^{\circ}C$ (the greenschist facies). Various amounts of chlorite present in these rocks is the product of post-metamorphic alteration of tremolite.

In the case of the samples taken around Donut Lake (267, 268, 269), first due to dehydration od serpentine, forsterite and talc is formed (Reaction II). Later as a result of degradation of metamorphosed rocks magnesite was introduced into the assemblage , or possibly because of introduction of carbon dioxide bearing weathering solutions to serpentine:

(III)   4 forsterite + 1 H_2O + 5 CO_2 $\xrightarrow[P_f=2\ kb]{T=500^{\circ}C}$ 1 talc + 5 magnesite
                                                                                        (Johannes, 1969).
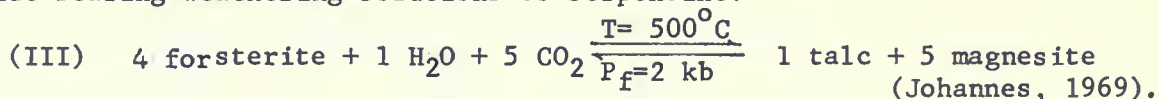
There is no petrographic evidence to distinguish whether talc + magnesite assemblage is the direct product of the metamorphism or not, however, the presence of serpentine and chlorite suggests retrogressive metamorphism of these rocks.

The assemblage cummingtonite + talc + magnesite + olivine + pyroxene found in a few of the rocks of Donut Lake Formation, is characteristic of the higher temperatures of metamorphism. Here, after the formation of talc + magnesite assemblage, some of the talc would react with forsterite to produce cummingtonite at temperatures more than $650^{\circ}C$.

(IV)   4 Forsterite + 9 talc ———→ 5 cummingtonite + 4H$_2$O.
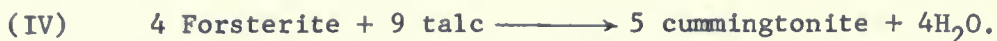
The rest of the samples contain cummingtonite + serpentine + pyroxene +
tremolite, which is again indicator of very high temperatures (about 700°C).
Serpentine is the product of the alteration of amphiboles and pyroxenes
present. Presence of the last two mineral assemblages depend on the extent
of occurance of reaction IV. The best supporting evidence for such assump-
tion is based on the fact that the rocks which carry more than 75% cumming-
tonite + serpentine by volume lack any talc and/or olivine.

METAMORPHISM OF MAFIC ROCKS

The Redstone and Schumacher Formations are exposed adjacent to the
Peterlong Lake Complex and Adams Pluton, respectively. This juxtaposition
has caused the rocks bordering the plutons to be metamorphosed to the
amphibolite facies. The interior volcanics, more remote from borders of
large plutons, metamorphosed to various degrees of the greenschist facies.
The transition from the amphibole facies to the greenschist facies in the
mafic rocks of regional metamorphic terranes is marked by the following
chemical events:

(1) A sudden change in the anorthite content of plagioclase. Plagio-
calse in most rocks of the greenschist facies is nearly pure albite (An$<$5)
whereas in the amphibolite facies the calcium content suddenly increases
to oligoclase or andesine (Turner, 1968; Hyndman, 1973; Seki et al., 1969).
Winkler (1974) agrees with such a jump, but places it 20 to 40°C lower than
the boundary between the greenschist facies and the amphibolite facies. In
addition the presence or absence of epidote group minerals in plagioclase +
hornblende + quartz paragenesis affect the plagioclase composition (Winkler,
1974).

(2) An increase in Al_2O_3 content of amphibole. The prominent amphibole in the greenschist facies is the poor alumina tremolite-actinolite, while in the amphibolite facies hornblende with Al_2O_3 greater than 5% (by weight) is the common amphibole.

(3) The disappearance of chlorite in the presence of muscovite and quartz (Winkler, 1974). However, the distinction between primary and secondary chlorite is a difficult problem, because chlorite can easily be formed by the secondary alteration of biotite and hornblende.

As discussed previously, the distinction between actinolite and common hornblende is based on some arbitrary criteria (page 17), because of quite similar optical properties of these two minerals. Furthermore, the secondary alteration and the deformation leave only a few twinned plagioclases for use in accurate An:Ab ratio determinations.

The rocks metamorphosed to the amphibolite facies were taken close to the contacts of the plutons. Post metamorphic alteration of the amphibolite facies rocks indicate that in most cases calcium-plagioclase was subsequently altered to albite, and hornblende was partly chloritized. Biotite, altered in part to chlorite, is present as a secondary mineral in a few samples. Other lavas more distant from the plutonic contacts were metamorphosed to the lower to upper greenschist facies.

Two zones are recognized within the greenschist facies of Redstone Formation. The first contains pale yellow to faint green actinolite, albite and relatively abundant in zoisite/epidote, quartz and chlorite, an assemblage characteristic of the lower greenschist facies. The other carries albite, biotite and amphibole with transitional composition between hornblende and actinolite, and less zoisite/epidote and chlorite. Most of these rocks were taken from the vicinity of the gabbroic sills and are considered to belong to the upper greenschist facies.

	Lower Greenschist	Upper Greenschist	Amphibolite
Quartz			
Plagioclase	An < 5	An < 5	An > 20
Epidote			
Actinolite			
Hornblende			
Sericite			
Biotite			
Chlorite			
Calcite			
Magnetite			
Sphene			

Figure 7   Paragenesis of some metamorphic minerals in the mafic volcanic rocks of the McArthur Township area.

	Greenschist Facies		
	Zone 1	Zone 2	Zone 3
Albite			
Quartz			
Actinolite			
White Mica			
Chlorite			
Biotite			
Clino/epidote			
Carbonate			

Figure 9   Paragenesis of some metamorphic minerals in the intermediate to felsic volcanic rocks of the McArthur Township area.
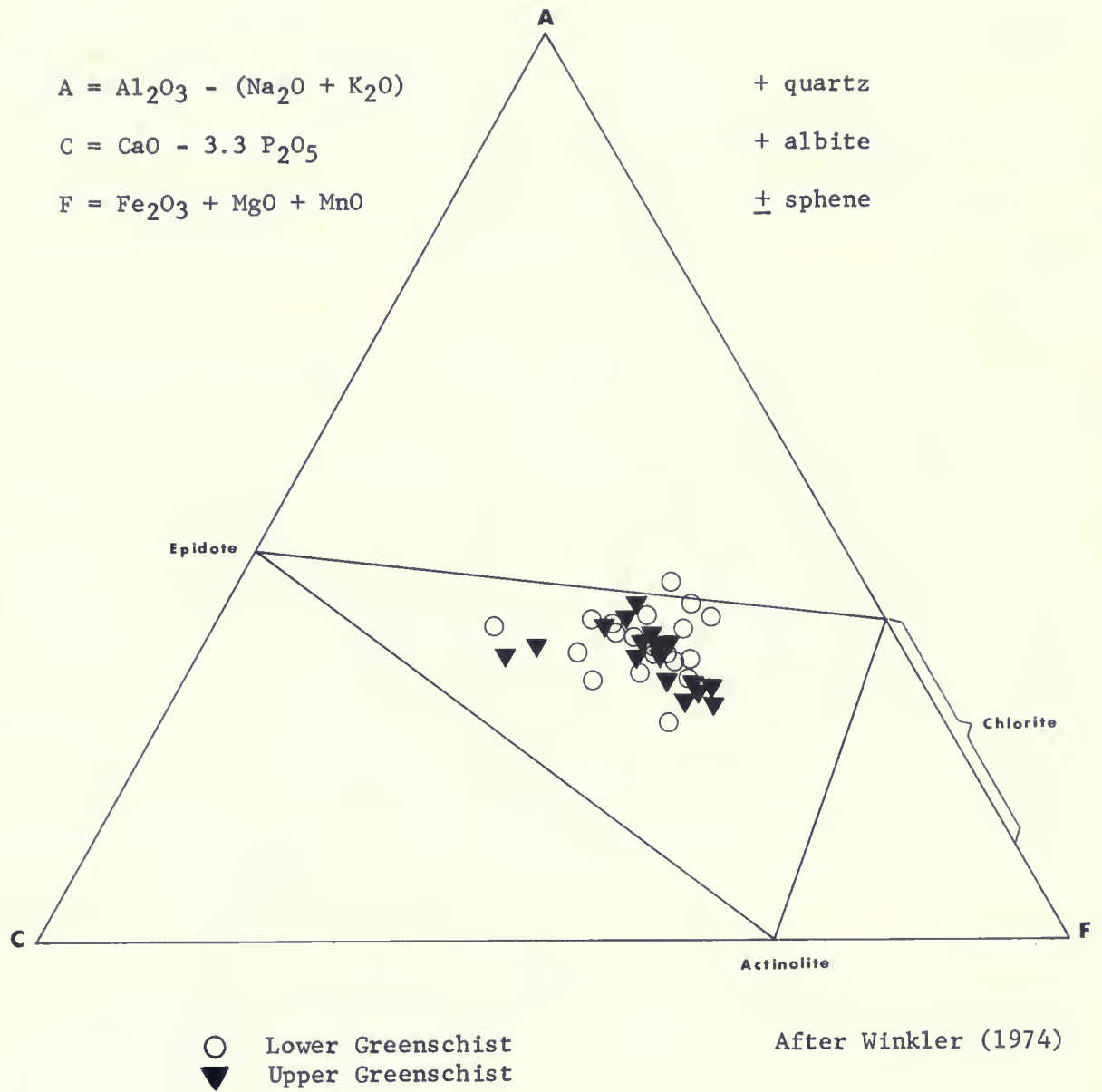
Figure 8   ACF diagram of the McArthur Township area mafic volcanic
            rocks.

The gabbroic sills in lower parts of the lava pile are comprised of amphiboles similar to those of the second zone in the Redstone Formation. This association could be attributed to: (a) higher load pressure applied to the rocks at the bottom of the lava pile; (b) the autometamorphism of the gabbro due to the alteration of the early formed crystals by a residual watery solution, in this case containing Al_2O_3 in addition.

The paragenesis of the mafic rocks of the area is presented in Figure 7. Figure 8 is the ACF diagram of the mafic rocks of the McArthur Township area metamorphosed to the greenschist facies.

METAMORPHISM OF INTERMEDIATE TO FELSIC ROCKS

The thin section study of the Boomerang Formation reveals that metamorphism up to the greenschist facies is abundant here. The following parageneses are recognized:

Zone 1) Albite + chlorite + white mica + clinozosite/epidote + quartz, carbonates. This assemblage is common in the rocks in the central and southern portions of this formation.

Zone 2) Albite + actinolite + carbonate + quartz + chlorite, clinozosite/epidote, white mica. This is the typical assemblage of the rocks around iron formation bands.

Zone 3) Albite + quartz + biotite + actinoliet, chlorite. This assemblage characterizes the northwestern lavas where they are much closer to Adams Pluton.

The overall distribution of the mineral assemblages indicate that metamorphic grade increases towards the northwest. The rocks are metamorphosed to the amphibolite facies where they are in contact with Adams Pluton. Figure 9 illustrates the paragenesis of the above zones. The Metamorphic map of the study area is presented in Figure 10.

50

LEGEND

A Amphibolite Facies

B Upper Greenschist Facies

C Lower

D Intrusive Body

N

0   1   2
     Km
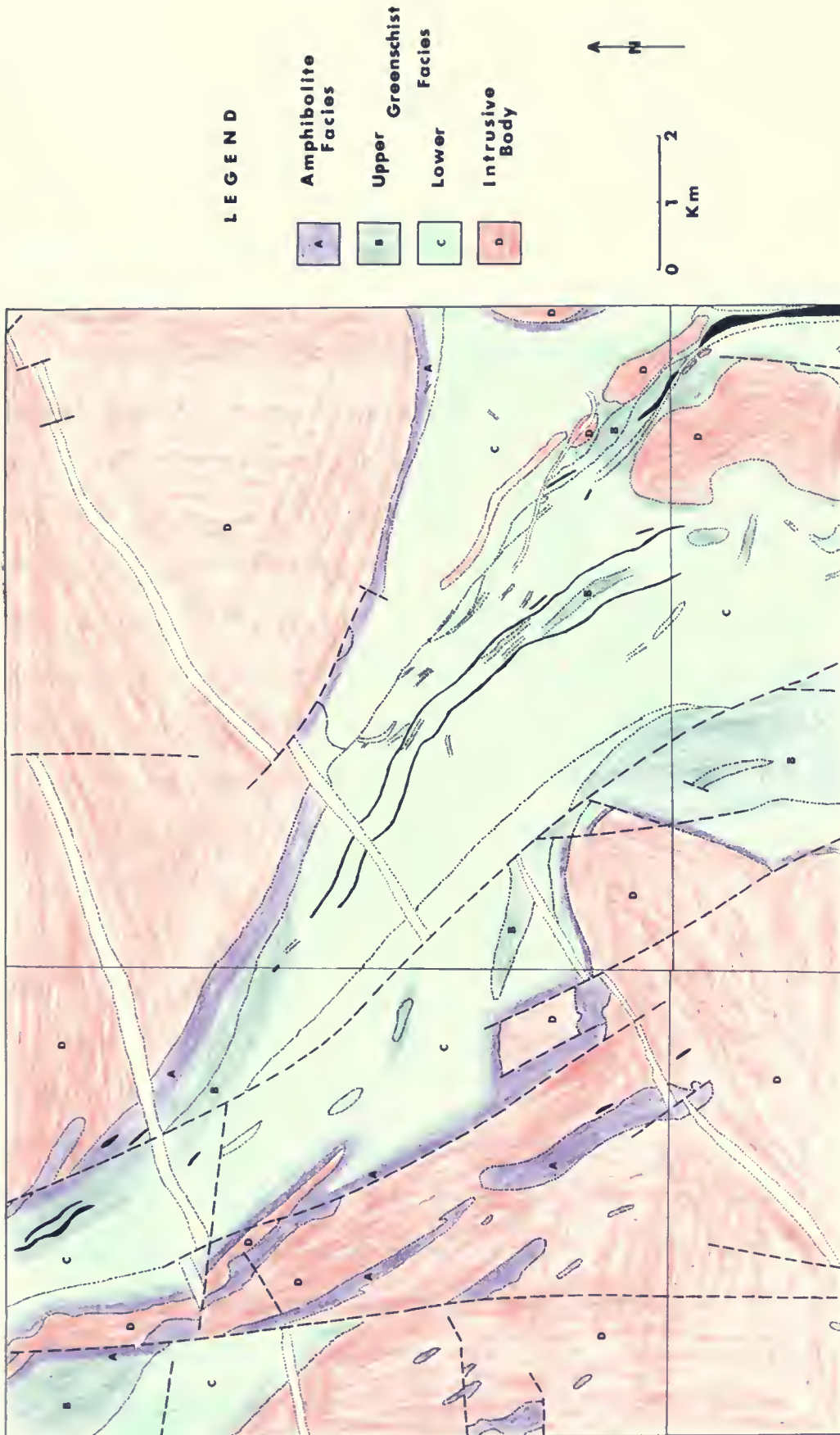
Figure 10   Metamorphic map of the study area

CHEMISTRY
OF THE ANALYZED ELEMENTS

GENERAL

The chemical analyses of the lavas in Appendix I do not represent the original compositions of these rocks because they have suffered chemical changes resulting from secondary alteration processes. To study such changes, the behaviour of each element in the lavas, their relative enrichment or depletion, and the effects of spilitization and widespread regional metamorphism will be discussed for individual elements. The elements are subdivided into six groups on the basis of geochemical behaviour and/or cation sizes. Within each group the arrangement is in order of increasing ionic radius. The following information is extracted from "Geochemistry" by Rankama and Sahama (1968), "Handbook of Geochemistry" by Wedepohl et al. (1969, 1970, 1972, 1974) and 'The Encyclopedia of Geochemistry and Environmental Sciences" by Fairbridge (1972).

ALKALI METAL ELEMENTS

The alkali metal elements have large radii and all form univalent positive ions.

Sodium: Na occurs only as univalent cation with radii of 0.98 $\overset{o}{A}$. The bulk of Na in igneous rocks must be found in the plagioclase feldspar and feldspathoids. Generally the amount of Na in igneous rocks increase toward the later stages of fractional crystallization, especially in the feldspathoid bearing rocks and to the lesser extent in granites. The well known exception is rhyolitic calc-alkalic flows which contain less Na_2O

L E G E N D

○   Donut Lake Formation

△   Redstone Formation

□   Boomerang Formation

●   Goose Lake Formation

◀   Schumacher Formation

■   Gabbroic Sills

N. B.   All subsequent diagrams use the same symbols as presented above unless otherwise specified.
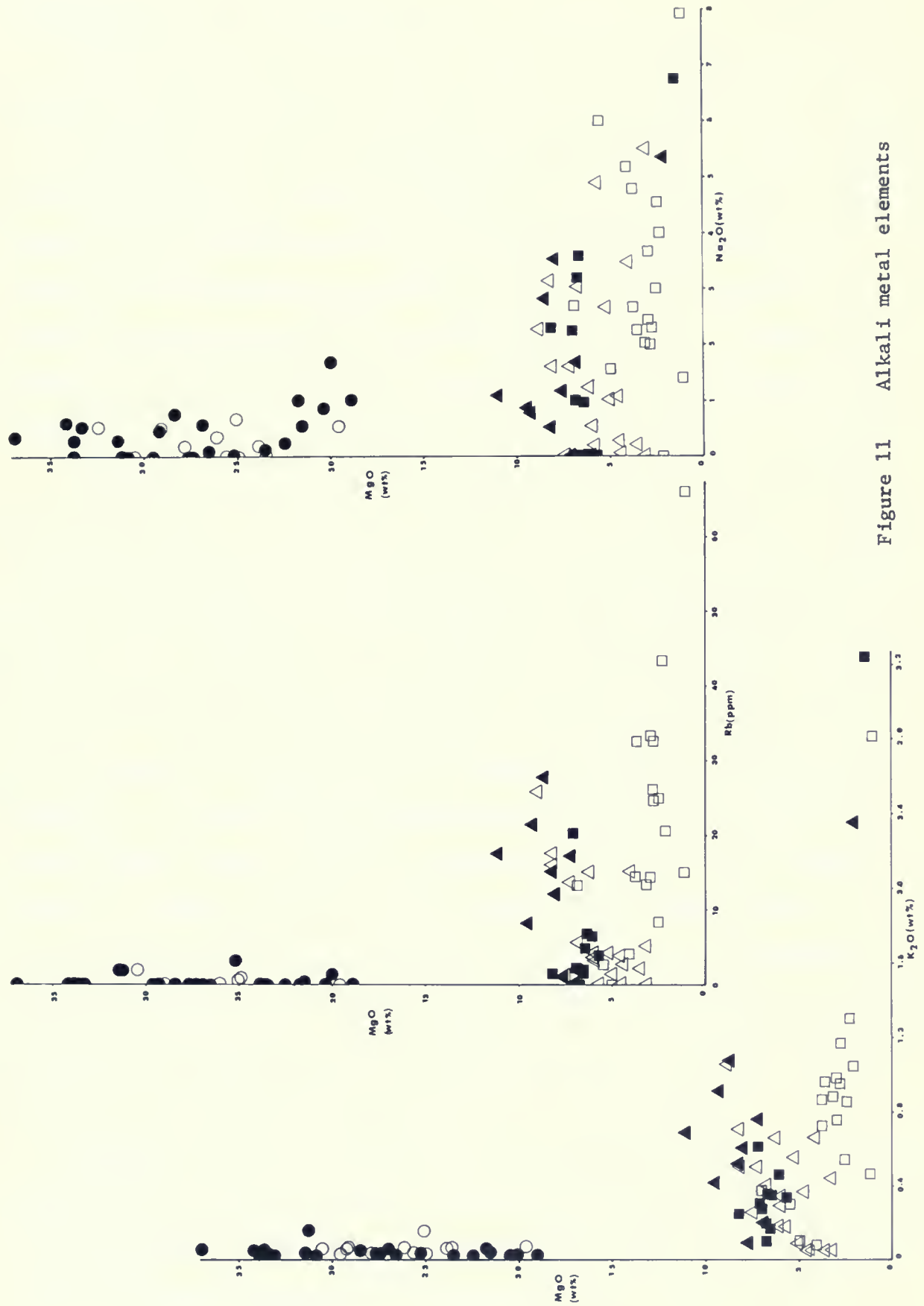
Figure 11   Alkali metal elements

than dacitic rocks of the same series.

There seems to be considerable movement of Na during the incipient stages of regional metamorphism (Smith, 1968; Watkins et al., 1970). There is a tendency for all of the calcium-plagioclase to change to albite during the greenschist facies metamorphism (Winkler, 1974). As expected, the Na_2O content of the rocks under the study increases from komatiitic through tholeiitic to calc-alkaline association (Fig. 11). Here the points are relatively widespread and off the fractionation trend. Many specimens concentrate at vanishingly low Na_2O content, indicating the high mobility of this element, perhaps through leaching by metamorphic fluids or sea water.

Potassium: This element is a univalent cation with radii of 1.33 $\overset{o}{A}$. The prime minerals carrying K are potash feldspars $KAlSi_3O_8$ and most common micas which form during the last steps of the main stage of crystallization. However potash feldspars and biotite may form at an earlier stage if the water content of the magma is very high. The oceanic tholeiitic basalt and some shield volcanic islands characteristically have much lower K content than continental tholeiitic basalts. Potassium appears to be mobile under conditions of low grade regional metamorphism (Cann, 1970) and higher grades (Kretz, 1972). After K was replaced during weathering it might react with alumina and silica to form clay minerals. However depletion of K is much slower than Na because potassium-feldspar is more resistant than plagioclase-feldspar (Siever, 1972). The mafic rocks of the McArthur Township area are like the Archean types from South Africa (Nisbet et al., 1977) rich in potassium, possibly as a result of metasomatism.

Rubidium: It has a radius similar to but larger than that of K^+, the preceding alkali metal in the periodic table. This similarity allows mutual substitution of these two elements. Rb is enriched in low temperature potassium minerals (potassium-feldspar, mica) and in fractional crystallization

it is concentrated in the residual liquid. Like other alkali metals, Rb is also brought into solution during weathering. Considerable movement of Rb is observed in granitic aureoles, where Rb culminates toward the granite contact (Bowler, 1959). Figure 11 displays the positive relationship of Rb versus MgO within the Schumacher and Redstone Formations. Like potassium, Rb is very low in many specimens of all types, suggesting leaching on a local scale. The similarity of K and Rb in Figure 11 indicates the close ties between these two elements.

ALKALI EARTH METALS

These belong to the second column of the periodic system, therefore are divalent and have large atomic radii.

Calcium: Approximately one half of the Ca in igneous rocks is present in the pyroxene and amphibole groups, and the other half is present in the plagioclase-feldspar. The Ca content of the plagioclase-feldspar increases with increasing metamorphic grade. Such an increase is furnished at the expense of other Ca minerals such as epidote. Most Ca minerals, particularly those of igneous and metamorphosed origin are relatively rapidly attacked by weathering and the Ca released to solution (Cann, 1970).

The CaO content of the rocks under study increases in komatiitic flows while it generally decreases in mafic lavas with decreasing MgO (Fig. 12). Four of the Redstone specimens contain very high CaO (17% by weight). These rocks are all metamorphosed to upper greenschist and contain high amounts of epidote group mineral and hornblende.

Strontium: The distribution of Sr in minerals and rocks is similar to a certain extent to that of calcium, which has an ionic radius of 0.99 $\overset{\circ}{A}$, close to that of Sr 1.12 $\overset{\circ}{A}$. Sr is usually found in greatest amounts in
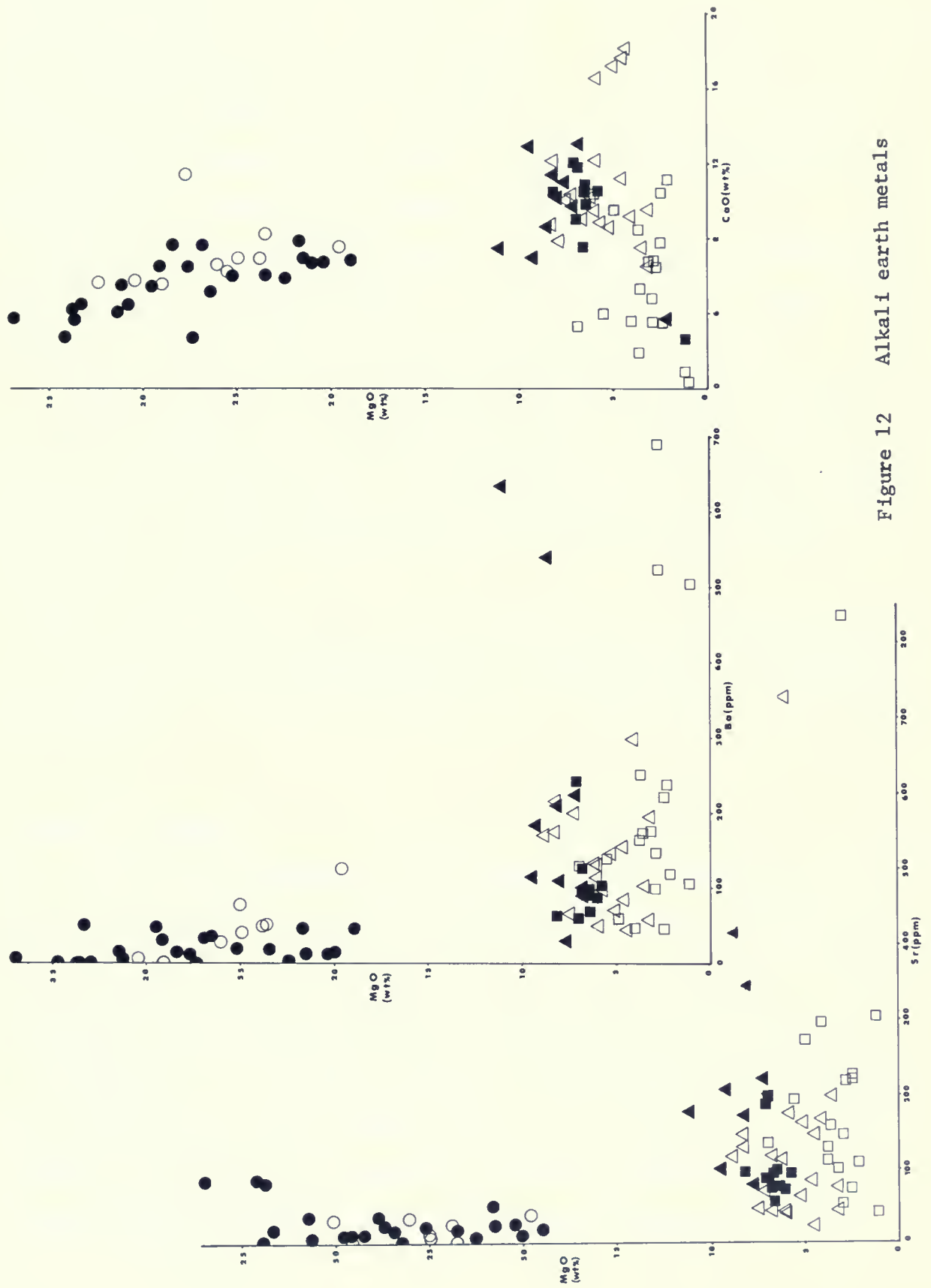
Figure 12   Alkali earth metals

calcium-rich minerals. The Ca/Sr ratio in plagioclase is lower than in pyroxene so magmas are more sensitive to plagioclase. Differing values of Sr concentration can be assigned to regional variation in the Sr content of the source magma, and to fractional crystallization and differentiation during formation of the rocks. Greenschist facies metamorphism often leads to a decrease in Sr (Cann, 1970).

There is no coherence of Sr with Ca in basaltic rocks of the area. However because of secondary changes, it seems that Sr values of the specimens drop with advanced fractional crystallization (Fig. 12).

Barium: Chemically Ba most commonly resembles strontium, but unlike Sr it has a tendency to substitute for K^+ ion and not Ca^{+2}. Ba content in igneous rocks series normally increases with increase in SiO_2 contents. It is mostly distributed among a number of silicate structures mainly feldspars and micas.

The characteristic increase in Ba content of the rocks under the study from komatiitic flows through tholeiitic to calc-alkaline may be observed in Figure 12.

RARE-EARTH ELEMENTS

Yttrium and the lanthanides are classified here as rare-earth elements. However this name is not consistent with their real abundance, especially the lanthanides with even atomic number which are more abundant than their odd-numbered neighbors, both in cosmic and in terrestrial surroundings.

Yttrium: Y is a strongly lithophile element which becomes enriched in the residual liquors during crystallization and is, therefore, plentiful in granites. The bulk of Y is concealed in minerals formed during the main stage of crystallization. Y could easily replace bivalent calcium ion
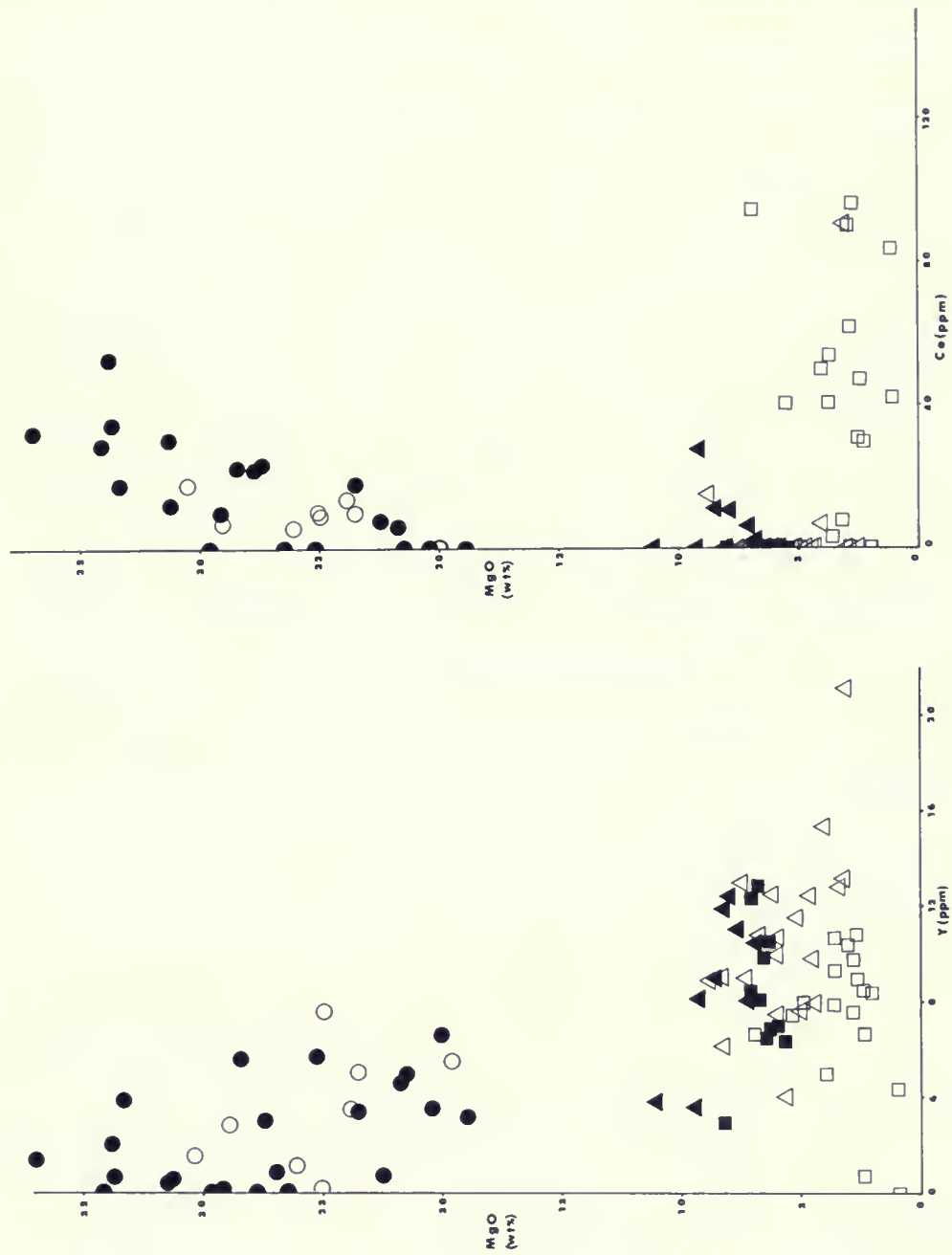
Figure 13   Rare-earth elements

because of radii similarity. Y behaves like the heavy rare-earths because it fits more easily into the pyroxene structure rather than the plagioclase.

The Y content of the analyzed rocks in McArthur Township area is very low averaging 2.6 ppm in komatiitic and 7 ppm in calc-alkaline associations. The enrichment trend extends from komatiite to tholeiite and then decreases toward the felsic members of calc-alkaline association (Fig. 13).

Cerium: Ce has very low content in the mantle but it is more abundant in basaltic rocks. If mantle garnet peridotite with low cerium content partially melts to yield a basaltic liquid, Ce will concentrate in the liquid. Ce like Y has a tendency to substitute Ca, therefore it is concentrated mainly in pyroxene and also plagioclase and hornblende. The similarity of the rare earth content of metamorphosed and non-metamorphosed rocks is the indication of a lack of influence of metamorphism on the composition of the different rare-earth minerals.

Cerium is much lower in later fractionates of each rock association within the area (Fig. 13). The Cerium content of the Redstone Formation and the gabbroic sills is vanishingly low. Such anomalies seem to be the result of a much lower precision limit of the XRF for this element.

FERROMAGNESIAN ELEMENTS

These comprise the group of trivalent and divalent elements which occur in 6-fold co-ordination with oxygen in silicates.

Aluminum: Al is strongly lithophile and its concentration increases towards the upper crust. The bulk of lithospheric Al is present in feldspar, with anorthite carrying double as much as do albite, and potassium-feldspar. Consequently, basic igneous rocks rich in the anorthite component, contain more Al than do the albite-rich plagioclase and potassium-feldspars of

acidic rocks. The little variation in Al content of different rock associations in the McArthur Township area can be distinguished by the MgO versus Al_2O_3 (Fig. 14) diagram. The small mobility of Al has been pointed out by Smith (1968) and Grant (1977).

Magnesium: In the crust it is concentrated in the basic and particularly ultramafic rocks. Mg is very strongly enriched in the dark silicate minerals which separated from the magma during the early stages of crystallization. The early olivines are rich in the Mg component, forsterite. During the main stage of crystallization Mg together with ferrous iron is the most important cation to become incorporated in femic minerals, which is due to almost equal size of the two ions ($r_{Mg^{+2}} = 0.66 \overset{o}{A}$; $r_{Fe^{+2}} = 0.75 \overset{o}{A}$).

Mg is not mobile because its energy of migration is high; this is because of the proper size of the Mg^{+2} ion to fill out completely the space between six oxygen ions in contact with one another, without pushing them apart. Consequently a strong bond is generated between Mg and oxygen ions. Forsterite and enstatite, the early-crystallized constituents of ultrabasic rocks, often succumb to autometamorphism and react with aqueous solutions, whereby serpentine and talc and often also chlorite, amphibole, and still other minerals are formed. The chemical peculiarity of differentiation is the decrease of MgO and increase of Fe/Mg + Fe ratio toward the later stages of crystallization. Therefore MgO and Fe/Mg + Fe ratio are used to determine the crystallization trends of the various lava suites.

Nickel: Ni is one of the typical constituent elements of the early magmatic sulfide segregations of the pyrrhotite-pentlandite assemblage. However, the bulk of Ni found in igneous rocks is incorporated in ferromagnesian silicate minerals, especially olivine, being concealed in their structures. Ni silicates are closely related to corresponding Mg minerals,
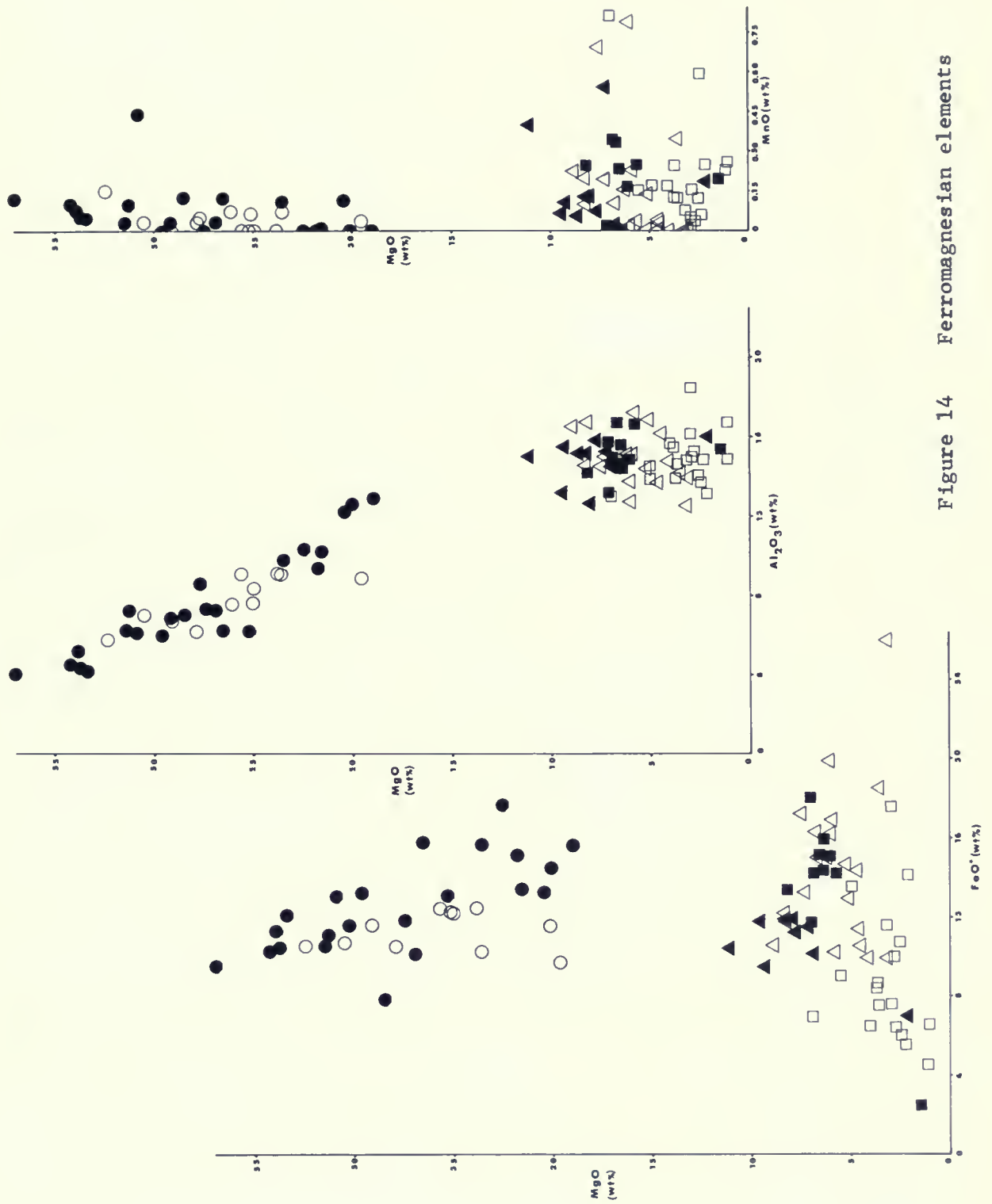
Figure 14   Ferromagnesian elements

61
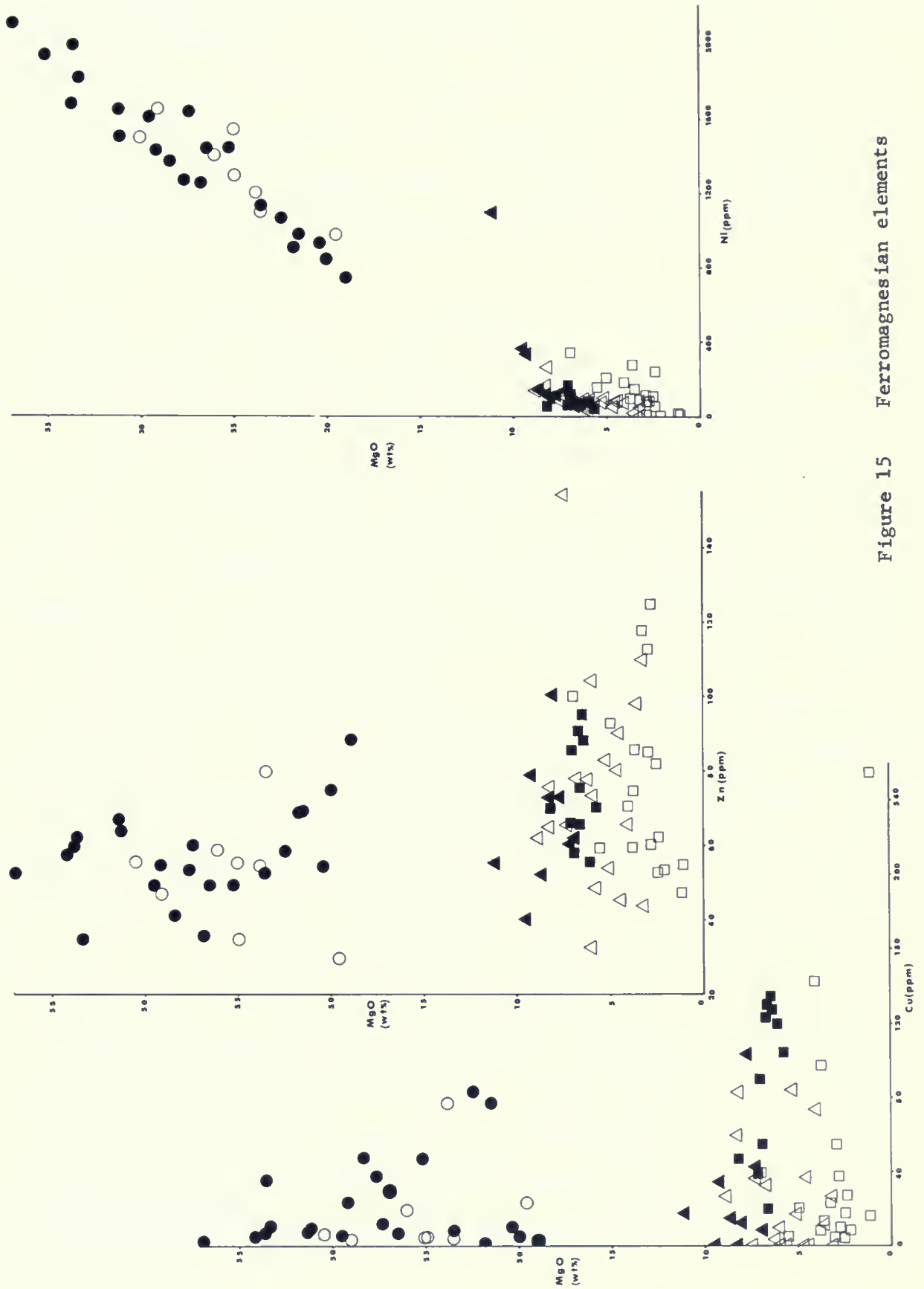
Figure 15   Ferromagnesian elements

both structurally and chemically, because of the ionic radii similarities
of Ni^{+2} and Mg^{+2}. Within the McArthur Township area the lava pile shows
systematic linear Ni depletion with increasing fractionation (Fig. 15). The
basaltic komatiite and tholeiitic rocks follow the main trend extending from
komatiitic association. On the other hand calc-alkaline flows ensue a dif-
ferent trend which occurs on the right side of the main crystallization
trend.

Copper: Cu is most commonly enriched in late magmatic hydrothermal
stages of magmatic crystallization. The behaviour of Cu during weathering
and sedimentation may be compared usefully with that of Zn. Cu goes into
ionic solution during the weathering, being afterward largely precipitated
as sulfide. The behaviour of Cu during contact metamorphism has been in-
vestigated by Brookins and Dennon (1964). On the traverses through contacts
between different magmatic rocks Cu concentration do not change as abruptly
at the contact as those of Ni and Co.

The behaviour of the Cu as well as Zn in the study area is unusual. The
Zn and Cu content increase with fractionation till it reaches the intermediate
members of each association where their abundance suddenly drop (Fig. 15).
This could suggest, perhaps the separation of an immiscible Cu and Zn sulphide
phase during crystallization or separation of a S-rich gas or fluid (Ewart et
al., 1973). This may have some bearing on Abitibi ore deposits, which are
thought to arise from S, Cu, Zn rich fumaroles.

Zinc: Zn is more substantial constituent of those parts of the sulfide
ores which were the last to crystallize and which often intrude the surround-
ing rocks. The manner of occurence of Zn is determined by its property of
diadochically replacing ferrous iron and magnesian in mineral structures.
Lundergardh (1948) found the highest Zn content in the more acidic products

of differentiation. The range of variation in Zn contents of basaltic rocks is mainly controlled by scattering of the iron content and not by the magma type of basalt. In general, Zn^{+2} ion is very mobile due to weathering and its concentration increases relatively with increasing decomposition. In the greenschist and amphibolite facies metamorphism no systematic change in zinc content is recorded (Kamp, 1970).

Iron: In the early-formed silicate rocks the content of iron is rather low (11%). The highest content of Fe is met at the outset of the main stage of the crystallization. Fe:Mg ratio changes during the differentiation and iron finally becomes enriched in regard to magnesium during the last steps of the main stage of crystallization. In an environment in which the oxidation of Fe^{+2} cannot take place, the residual liquor will be rich in iron. Igneous iron minerals undergo weathering and disappear in the order shown by Goldich (1938) to be: olivine first, followed by pyroxene, amphibole and biotite. Magnetite is much more resistant to chemical weathering than iron silicates but it can undergo oxidation to hematite.

The Redstone Formation flows display a strong iron enrichment trend while the Boomerang lavas contain much lower iron and its amount drastically decreases toward the more felsic end members (Fig. 14). Some of the rocks in the Boomerang Formation are distinctly off the main trend of fractionation.

Manganese: Mn is related to iron in its chemical properties and is a member of the iron family. Actually it resembles iron in many respects as far as its manner of occurence in nature is concerned. Unlike ferric hydroxide and oxide, which in metamorphic processes are readily converted into magnetite Fe_3O_4 the manganese oxides and hydroxides only exceptionally form housmannite Mn_3O_4. Silicate minerals of Mn often result from the metamorphic changes.

This element seems to drop in amount in the latest fractionates of each association but it is more enriched in mafic rocks of the area (Fig. 14).

THE LARGE HIGHLY CHARGED CATIONS

These include elements with valencies of 4, 5 and 6 which have a difficulty in entering common mineral lattices because of valency difficulties.

Titanium: Like iron, Ti shows a distinct tendency to become separated from the crystallizing magma at an early stage and to become enriched on the onset of the crystallization. Ilmenite, rutile and sphene are the most abundant of the independent Ti minerals. During weathering, Ti consequently remains largely in the resistates. Ti is much more resistant in ilmenite and rutile than sphene and femic minerals carrying Ti.

There is a close similarity between the abundance trend of TiO_2 and FeO* in the area. Titanium is highly enriched in the latest fractionates of the Redstone Formation lavas (Fig. 16).

Zirconium: The content of Zr is low in the early crystallates, but during the main stage of crystallization, this metal shows a tendency to become enriched in the last rocks to crystallize. Zr is contained in zircon in igneous rocks, a mineral which is one of the first phases to crystallize from an igneous magma and shows great stability toward ordinary hydrothermal solutions and the crystal remains unmodified during rock metamorphism.

The Zr content of the komatiitic flows of the area remains constant during most parts of the fractionation. It shows an increase in the intermediate and felsic flows of the area (Fig. 16).

THE SMALL CATIONS

This group includes the small cations occurring in 3 and/or 4-fold
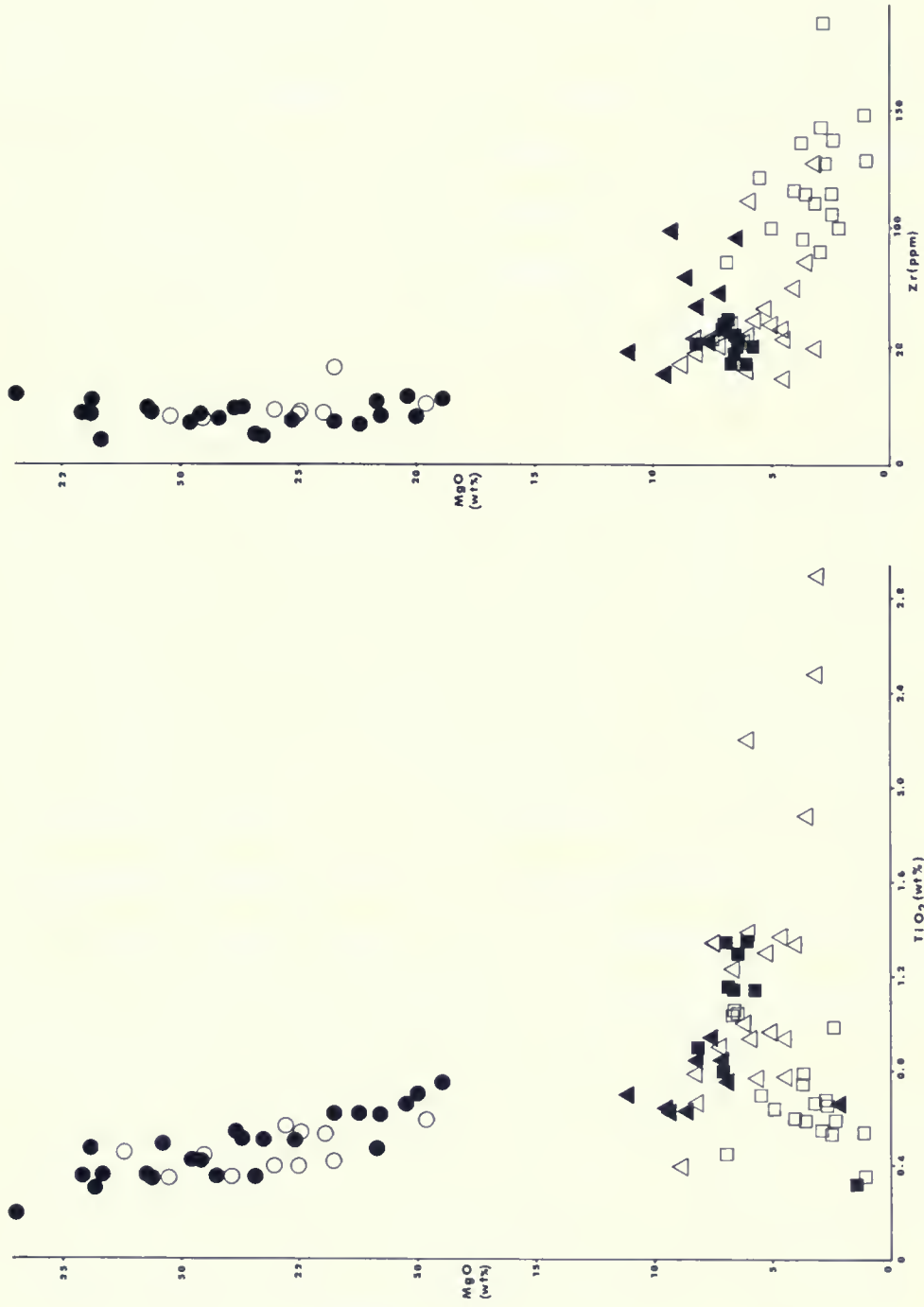
Figure 16   The large highly charged cations

co-ordination with oxygen in silicates.

Phosphorus: With the atomic radius of 0.35 Å, P is mainly concentrated in apatite which is one of the most common accessory constituents of igneous rocks. The fact that P follows very closely the coarse of Ti during the magmatic differentiation was first pointed out by Vogt (1931). Phosphorus like Ti starts to separate from the magma during the earliest steps of the main stage of crystallization. However, in the early separated silicates such as dunite, P and Ti are relatively rare. The P in igneous rocks is slowly   mobilized by weathering processes.

The lavas under the study show a slight increase toward the latest fractionate rocks (Fig. 17).

Sulfur: This element has an ionic radii of 0.35 Å and in igneous rocks occurs in sulfide which necessitates reducing conditions. A sulfide melt and silicate melt are only partially miscible particularly at lower temperatures. Therefore the sulfides are separated from the magma at an early stage of the crystallization before the main stage sets in, and a great number of elements having high affinity for sulfur thus become sep-arated from the magma in the sulfide phase (eg. Fe, Zn, Ni, Cu). The rocks formed during the main stage of the crystallization contain little sulfur. S is a highly mobile element and may be expelled as a fluid from the magma when its concentration is driven above the equilibrium point by progressive fractionation of a magma body (Ewart et al., 1973).

Figure 17 shows the inconsistency of sulfur values in various associations. A significant feature is very low sulfur concentration of the Boomerang lava, which may be the result of segregation of S-rich gas before calc-alkaline differentiation of the magma starts (Naldrett et al., 1978).
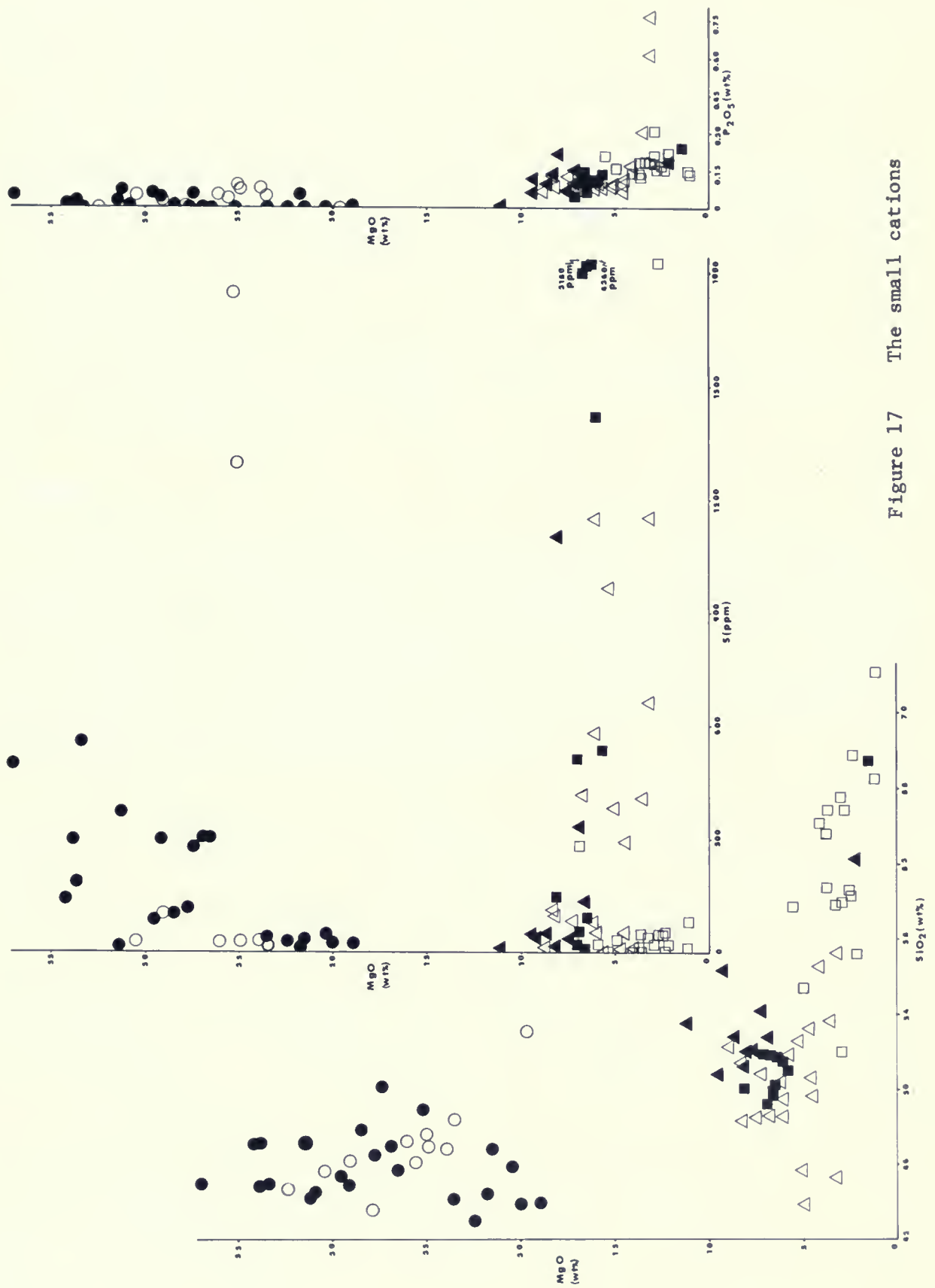
Figure 17   The small cations

Silicon: The 4 valent Si^{+4} has an atomic radius of 0.40 Å and is strongly enriched toward the last phases of the main stage of crystallization. Formation of orthopyroxene in early stages of the fractionation causes the much stronger silica enrichment of the remaining liquid. The bulk of Si, perhaps more than 90%, remains in the solid products formed during weathering and only a small portion is brought into solution. The quartz veins of varying grades of purity are common in igneous and metamorphic terranes.

The silica content of the McArthur Township area increases toward the end of each volcanic cycle (Fig. 17).

SUMMARY

The degree of solubility of the elements and their tendency to become mobilized during low to medium-grade metamorphism are summarized as follows: Na, K, Rb, Ba, Sr, Ca and S are highly mobile; Zn, Cu, Mn, Y, Ce, P and Si are moderately to slightly mobile; and Ni, Fe, Mg, Al, Zr and Ti exhibit little sensitivity to metamorphic processes.

PETROCHEMISTRY
OF THE ROCKS

GENERAL

Introduction: A total of 132 rocks were analyzed for the major oxides contents. The best 125 analyses, 86 extrusive and 39 intrusives were selected for study here. Most of the discarded analyses were from the vicinity of iron formation bands and carried unusually high iron content. Furthermore, all the volcanic rock analyses with values of over 102.60 and below 97.40 are omitted from consideration. About one hundred (80 extrusive, 24 intrusives) of the specimens analyzed for major oxides were also analyzed for trace elements. The major oxides include SiO_2, Al_2O_3, $FeO*$, MgO, CaO, Na_2O, K_2O, TiO_2, MnO, P_2O_5, and trace elements are Ba, Ce, Cu, Ni, Rb, S, Sr, Y, Zn, and Zr.

In choosing samples, care was taken to select the least altered rocks and also those with no fracture, vein, or void filling materials, to overcome the problem of major element dilution. To avoid chemical variation due to fractional crystallization of some mineral phases during flow consolidation, fine-grained metavolcanics were analyzed:

Method: Major and trace element analyses were carried out by x-ray fluorometer analysis, using a Philips 1450/20 sequential automatic x-ray spectrometer. Homogeneous glass discs and powder packs were used to determine major oxides and trace elements respectively. Each determination was repeated at least twice, and in some cases the average values were used.

For callibration of the XRF determination, U.S.G.S. standard powders were used (Flanagan, 1969). To obtain MgO values in the range of the komatiitic flows combinations of standards were also prepared (Appendix II).

Classification: Figure 18 is an alkali-silica plot for all the volcanic rocks. All the rocks plot under the dividing line, therefore the rocks are subalkaline. This field includes komatiitic, tholeiitic and calc-alkalinic volcanic series. Some of the salient differences in major element chemistry between the Redstone and Boomerang Formations are illustrated on an $A(Na_2O + K_2O) - F(FeO^*) - M(MgO)$ diagram (Fig. 19). This diagram demonstrates the tholeiitic affinity of the Redstone Formation and the calc-alkaline nature of most of the Boomerang lavas. A few of the Boomerang Formation specimens are transitional between tholeiitic and calc-alkaline associations. Furthermore, a number of rocks plot abnormally near the upper half of the joining F - M line. This feature is seen also in MgO - Na_2O and MgO - K_2O diagrams (Fig. 11) can be explained by a strong depletion in Na_2O and K_2O content of these rocks (Jolly, 1978). It should be noted that the conventional geochemical diagrams like total alkaline versus SiO_2 and AFM diagrams require caution in use. This is a result of changes in alkaline contents of the rocks by the widespread low grade metamorphism. To demonstrate the contrasting differentiation trend of these associations, Figures 20a and 20b are employed. Here TiO_2 and total iron content of the rocks as FeO are plotted against FeO*:MgO ratio. These figures indicate the iron and titanium enrichment of the tholeiitic flows with advancing fractional crystallization, especially in the early stages. On the other hand, calc-alkaline magmas monotonously decrease in Fe and Ti contents. To separate komatiitic flows from the other types, Al_2O_3 is plotted against the FeO/(FeO + MgO) 100 ratio of the rock, in which total iron is calculated as FeO (Fig. 21). All the samples within the Donut Lake, Goose Lake and Schumacher Formations and some of the Redstone Formation specimens plot on the left side of the inclined line, therefore belong to the komatiitic association.
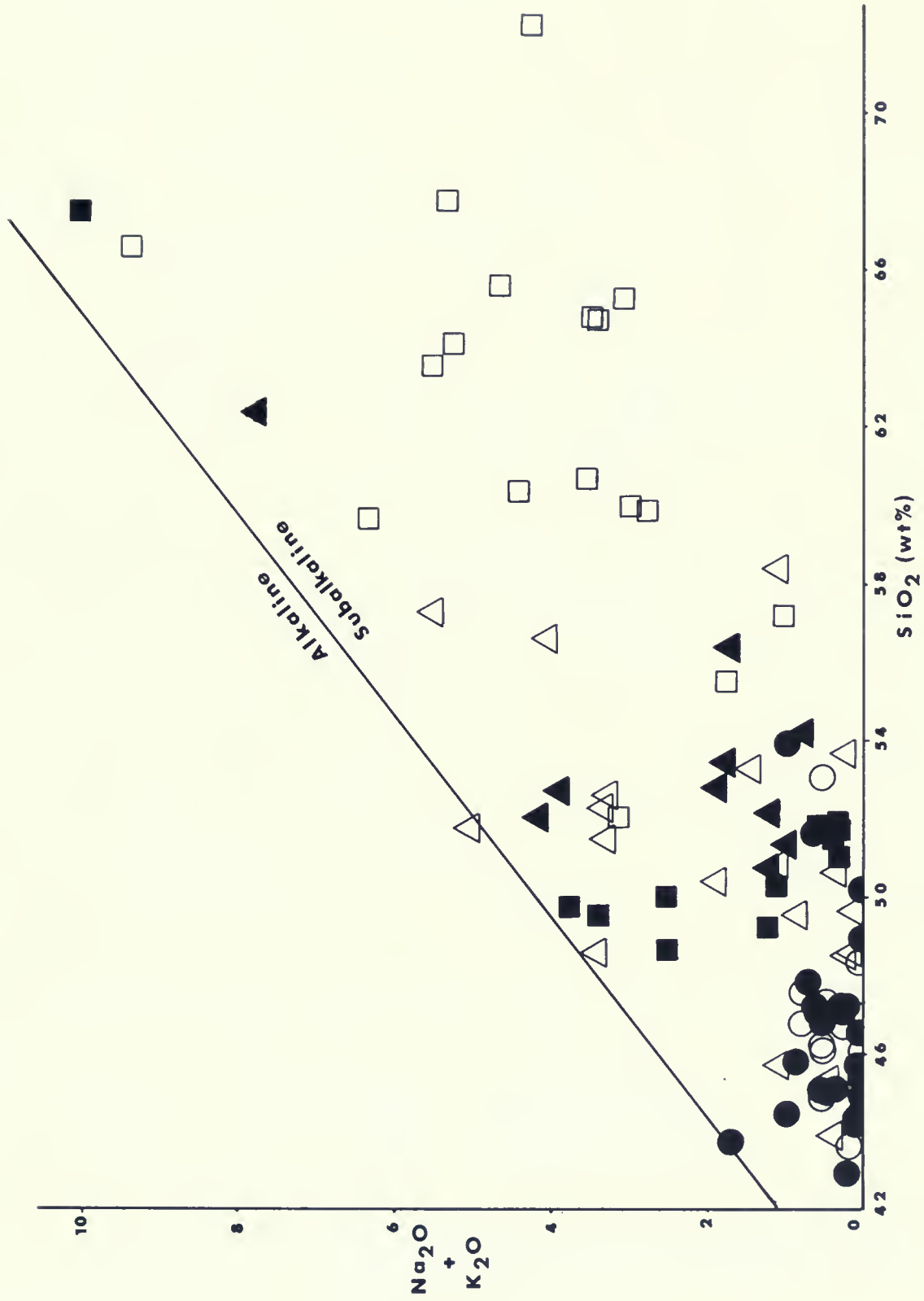
Figure 18   Alkalies – silica plot for volcanic rocks and gabbroic sills of the McArthur
Township area. Dividing line after MacDonald (1968).
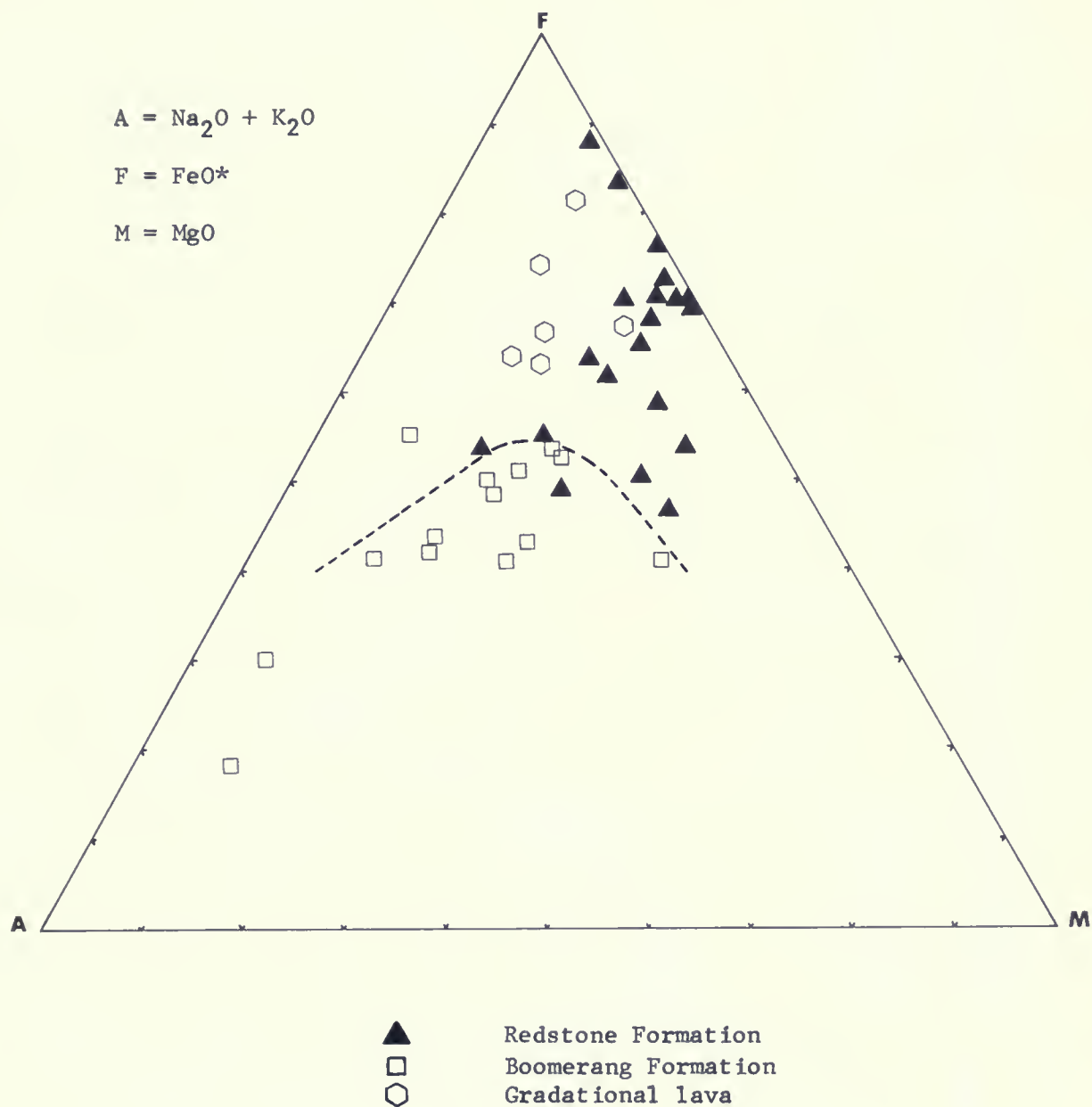
Figure 19   AFM diagram for the mafic and intermediate to felsic volcanic rocks of the McArthur Township area. Dividing line after Irvine and Baragar (1971).
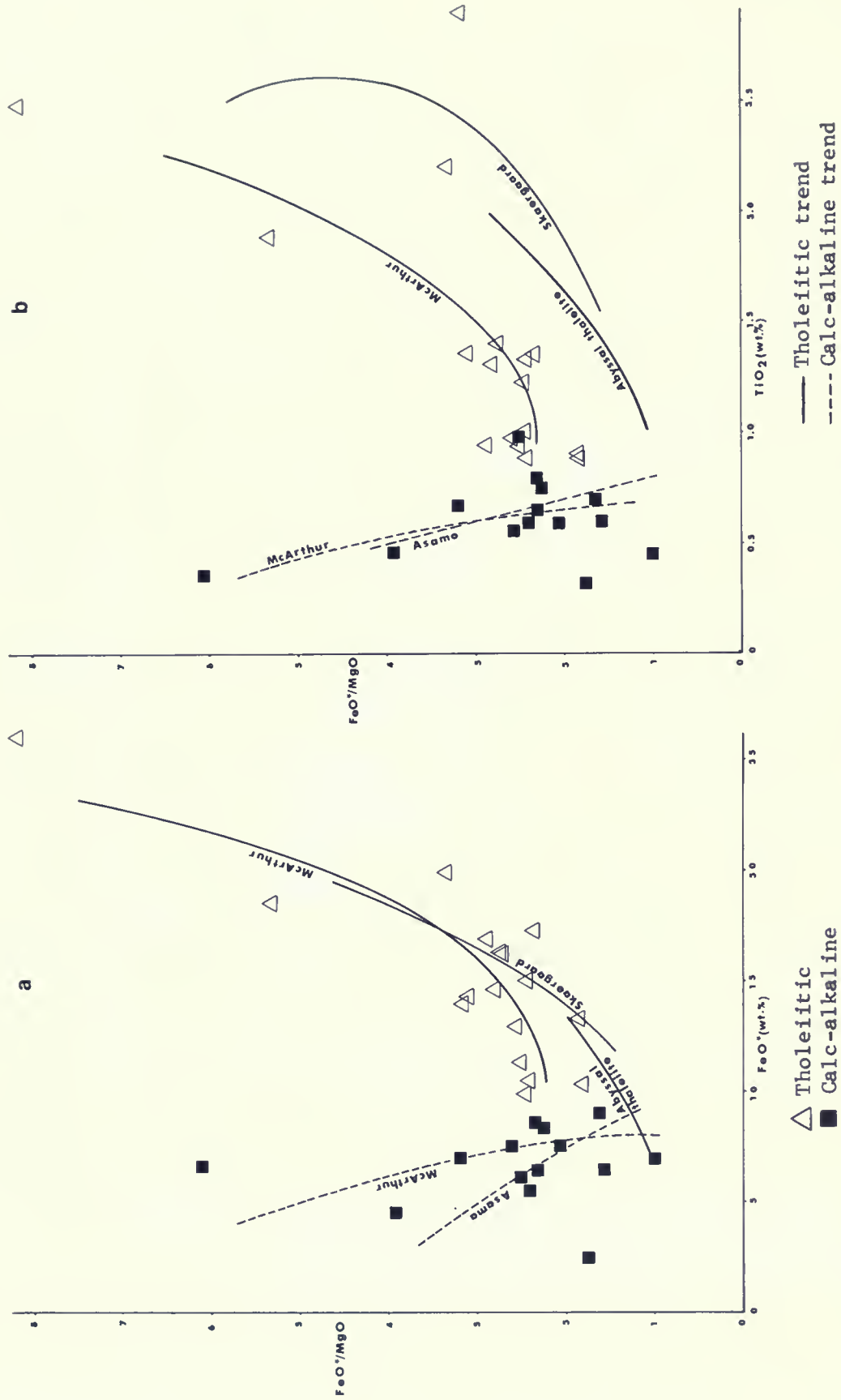
Figure 20   Variation of FeO* and TiO$_2$ contents of tholeiitic and calc-alkaline rocks of
the McArthur Township area with increasing FeO*/MgO. Other trends after
Miyashiro (1975).
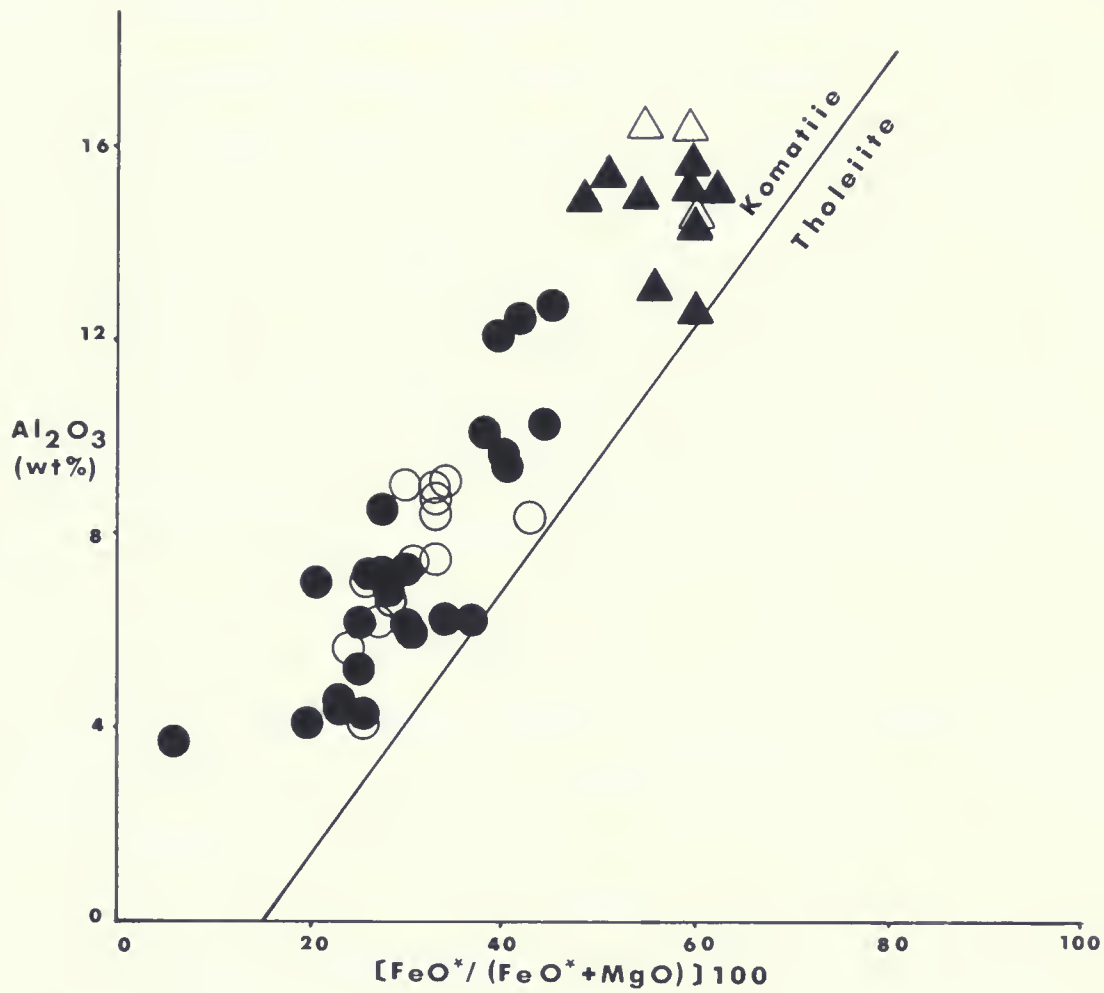
Figure 21   Variation of Al_2O_3 with $[FeO*/(FeO* + MgO)]$ 100
             weight percent ratio, showing the rocks belonging
             to the komatiitic association. Dividing line
             after Naldrett and Cabri (1976).

Immobile element diagram: Traditional geochemical diagrams used for classification of different associations could not accurately be applied to altered, metamorphosed and metasomatized rocks. The most common of these diagrams is the AFM diagram which utilized highly mobile Na and K and slightly mobile Fe. To find a diagram analogous to the AFM diagram without employing any of the highly mobile elements, a ternary diagram was developed incorporating the relatively immobile elements Zr, Ti, and Ni (Fig. 22). The similarity of this ternary diagram, referred to hereafter as a ZTN plot, to that of the AFM diagram becomes more apparent when the geochemical properties of the pairs Zr - K_2O and Na_2O, TiO_2 - FeO* and Ni - MgO are compared. Generally, Zr tends to be enriched during magmatic fractionation, as are the alkalis. Also, TiO_2 and FeO* display similar patterns during the differentiation processes, both exhibit enrichment in the intermediate members of the tholeiitic series. Finally, the continual depletion of Ni and MgO during magmatic differentiation of magma is similar especially within the komatiitic series.

On the ZTN plot, the differentiation of the lavas occur in at least three subparallel trends, all of which initiate from the Ni apex and move toward the TiO_2 apex with various degrees of inclination; finally, all swing sharply toward the Zr apex.

The three distinct trend lines marked in ZTN diagram (Fig. 22) are obtained by available Archean chemical analyses from different greenstone belts. The trend line 1 is representative of tholeiitic rocks and the trend 3 is indicative of fractionation of most felsic calc-alkaline rocks. The trend 2 could be divided into 2 segments: 2a represent fractionation trend of komatiitic series which joins the low TiO_2 tholeiite segment of the trend, 2b. All the rocks above the trend 2b are of tholeiitic nature. All the calc-alkalic rock series plot below the trend line 2, but the mafic end-members

LEGEND

Calc-alkaline

▽   Hallberg, Johnston, and Bye (1976)   (23)

☐   Jolly (unpublished data)   (47)

○   Naqvi and Hussain (1973)   (14)

Tholeiitic

▲   Nesbitt and Sun (1976)   (7)

⬢   Hallberg, Carter and West (1976)   (5)

■   Jolly (unpublished data)   (42)

●   Naqvi and Hussain (1973)   (6)

Komatiitic

⬡   Hallberg, Carter, and West (1976)   (11)

▼   Nesbitt and Sun (1976)   (16)

Total   171
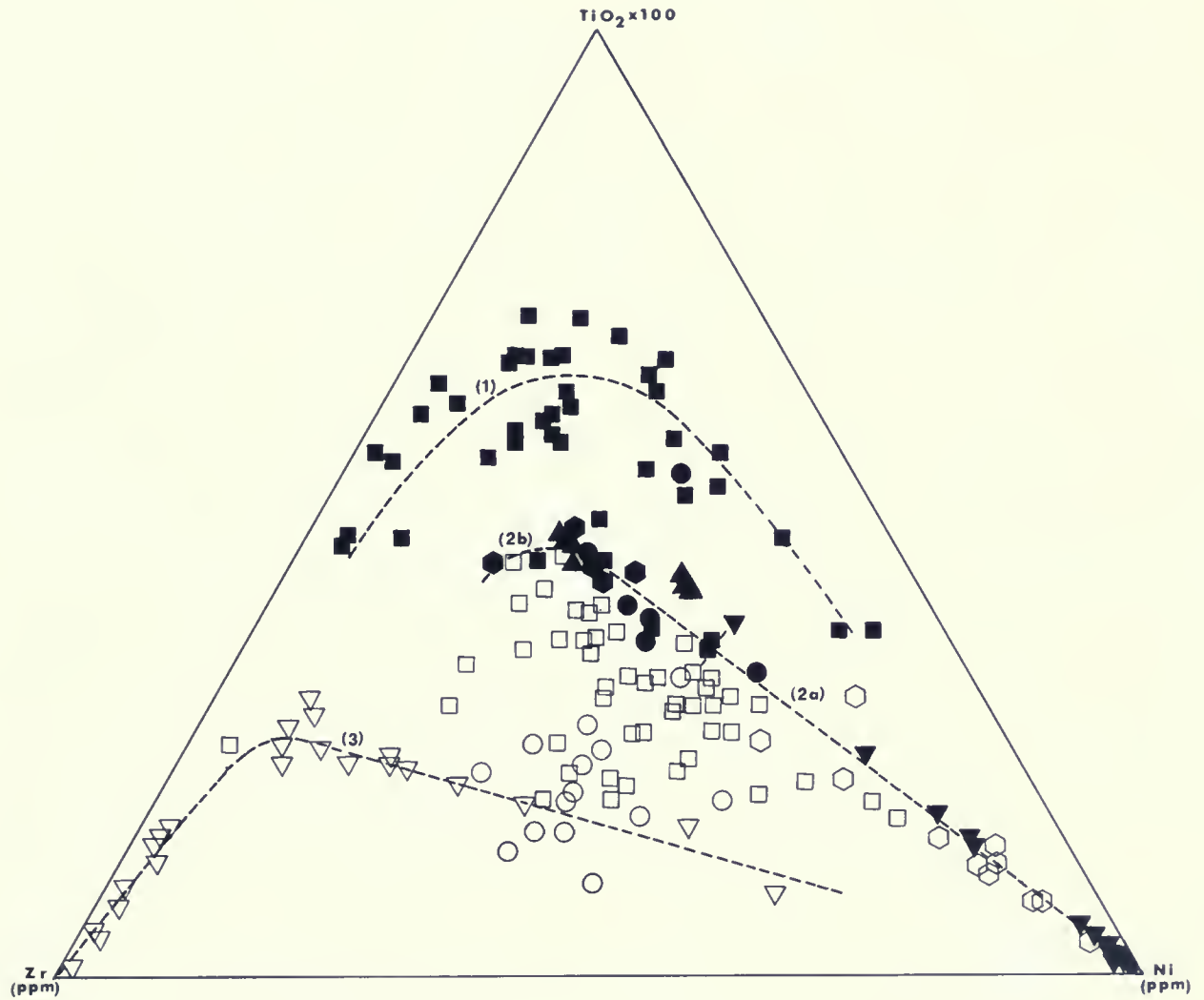
Figure 22   ZTN diagram for Archean volcanic associations.
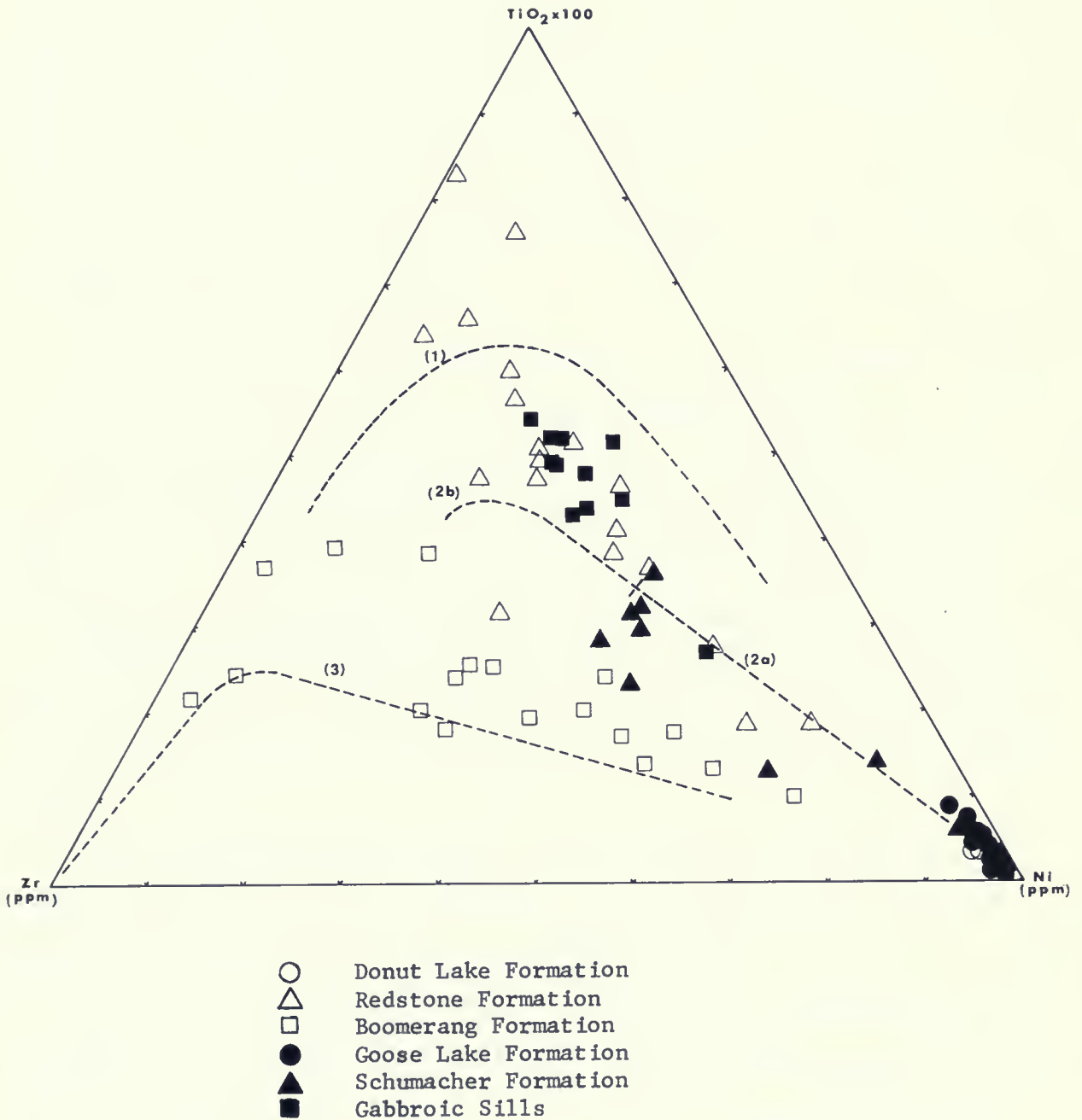
Figure 23   ZTN diagram for various rock associations in the
            McArthur Township area. Trend lines from Figure 22.

of this volcanic series intermingle with the tholeiitic and komatiitic volcanic series.

According to this figure the Chitaldrug Archean metabasalt (Nagvi and Hussain, 1973) which contain less than 1.2% by weight TiO_2 are of calc-alkalic nature, while those with greater than 1.2% are tholeiitic. Most of the low Mg of high Mg series of Nesbitt and Sun (1976) fall between trend 1 and 2b. Figure 23 exhibits the tholeiitic nature of the Redstone Formation with the exception of 3 of them which have a komatiilic affinity. The Donut Lake, Goose Lake and Schumacher Formations are komatiitic and Boomerang Formation is calc-alkaline.

In general, the rocks in McArthur Township area are chemically divided into three different associations, with one gradational member.

The komatiitic association has high MgO and NiO contents with normally high CaO/Al_2O_3 and low $FeO*/(FeO* + MgO)$ ratios and low TiO_2 contents (Arndt et al., 1977). Ultramafic and basaltic rocks predominate this association.

The tholeiitic association of the volcanic rocks are characterized by predominance of mafic members, displays significant absolute iron-enrichment with respect to magnesium in the intermediate members and carries high TiO_2 contents.

The calc-alkaline association is characterized by continual iron and titanium depletion and alkali enrichment during fractionation. Andesite and dacites prevails other classes in this association.

In each association, there is a wide range of SiO_2 content which is used to subdivide the associations. Ultramafic rocks have SiO_2 contents of lower than 47 percent; basalts range from 47 to 52 percent; andesite range from 52 to 62 with a subgroup of basaltic andesites (low - Si) with 52 to 56 percent; dacite with SiO_2 ranging from 62 to 70 percent, and rhyolite with

SiO_2 higher than 70 percent. Both the name of the rock and the name of the association are used for classification here (ie. basaltic komatiite or tholeiitic andesite). Iron is expressed in all of the tables and diagrams on the basis of total Fe as FeO (FeO*). In the case of using Fe_2O_3 contents for certain diagrams and norm calculations, the equation suggested by Irvine and Baragar (1971) is employed where: $\%Fe_2O_3 = \%TiO_2 + 1.5$. For classification and all the plottings, recalculated results to 100% without the volatiles are utilized.

CHEMISTRY OF EXTRUSIVES

Komatiitic Association : The term komatiite was introduced by Viljoen and Viljoen (1969) to cover a suite of rocks ranging in composition from dunite through peridotite to basalt in the Barberton Mountain Land of the South Africa. Before this, the existence of ultramafic liquids had not gained general acceptance because of the requirement of extremely high temperature to generate a liquid containing high normative olivine. However, the pioneer work of Viljoen and Viljoen (1969) and later Pyke et al. (1973), Green (1975) and Arndt et al. (1977) and others, provided reasonable explanations for the mechanism of extrusion of komatiite during the Archean. Viljoen and Viljoen (1969) described komatiite as the series with high MgO (ranging from 32% to 6%), high Fe/Mg ratio and high CaO/Al_2O_3 ratio for which the mean of 1.59 was quoted. The latter ratio has been the subject of many papers since that time (Brooks and Hart, 1972, 1974: Williams, 1972; Green, 1975; Green et al., 1975; and Nesbitt and Sun, 1976). As a result, Arndt et al. (1977) have redefined the chemistry of komatiite as having a low FeO*/FeO* + MgO ratio at given Al_2O_3 values, low TiO_2 at given SiO_2 and high MgO, NiO and Cr_2O_3 content, and some high CaO/Al_2O_3 ratios with the average of 0.84.

The Donut Lake komatiite is predominantly ultramafic in composition. Three of the samples are basaltic and one of them is basaltic andesite. The MgO content of the Donut Lake komatiite does not drop as drastically as those reported from the other greenstone belts in transition from ultramafic to basalt. Here, MgO averages 25.11% with a range of 17.50 to 32.35 weight percent which increases toward the top of the flow. This average amount is similar to a spinifex-textured peridotitic komatiite from Munro Township, about 90 km away in the northeast of the area studied here, reported by Arndt et al. (1977) but it is approximately 5% lower than that which Nesbitt & Sun (1976) have described from Australian spinifex-textured peridotites. Alumina has a mean value of 7.17% in ultramafic rocks, but increases to 8.04 in basaltic komatiite. Al_2O_3 content of these rocks on average is about 0.8% higher than those mentioned in literature from other parts of Canadian Shield (Arndt et al., 1977). Rhodesian greenstone belt (Nisbet and others, 1977) and the Eastern Goldfield region of Australia (Halberg, 1972). CaO, for most specimens, ranges between 5 to 8 percent but it increases up to 19% in the case of the altered sample 16 with about 10% calcite by volume. The same sample shows very low alumina which results in a very high CaO/Al_2O_3 ratio (5.23). The TiO_2 content averages 0.43 weight percent for ultramafic and 0.40 for basalt. Similar values are reported from Munro Township locality (Nesbitt and Sun, 1976). However, for a given SiO_2 value, these rocks contain higher amounts of TiO_2 in comparison to other greenstone belts, which roughly averages 0.30 percent by weight.

When comparing all data with the typical komatiite of Naldrett and Cabri (1976), Nesbitt and Sun (1976) and Arndt et al. (1977) there is a general suggestion that for a given value of SiO_2, all the oxides, with the exception of magnesian oxide, show higher values. In other words, the SiO_2 contents of Donut Lake komatiite is depleted in correlation to the SiO_2

contents of most of the komatiitic associations in other parts of the world. This is reflected in CIPW normative calculation of these lavas presented in Appendix I. Sample 16 and 266 were undersaturated, so no values are indicated for them. All of the specimens, with the exception of sample 18 (basaltic andesite in composition), are olivine and hypersthene normative. Hypersthene values dominate over olivine values in almost half of the samples. Samples 16 and 17, which display extensive alteration, show a considerable displacement from the general komatiitic trend in most of the MgO variation diagrams. Therefore these altered samples are not plotted in any of the figures.

Trace-element contents of these rocks are given in Appendix I, and all are plotted against MgO in Figures 11 to 17. Nickel follows a distinguishable positive relationship to MgO over a wide range of MgO content. The negative relationship of MgO to Y, Ba, Zn, Cu is observed in Figures 12, 13, 15 whereas there is a decrease in Ce values when MgO decreases (Fig. 13). Ti/Zr ratio of these rocks averages to 107.

Goose Lake Formation lavas are either ultramafic or basaltic; no felsic end-members are present. The average SiO_2 content of ultramafic rocks is 45.01% and of basaltic rocks is 48.02 weight percent.

The high magnesium and low aluminum content of this formation causes the rocks to plot distinctly separate from other associations in variation diagrams. The MgO and Al_2O_3 contents average 26.94 and 8.06 weight percent for ultramafic and 29.60 and 6.13 for basaltic rocks, respectively. The higher Al_2O_3 average of ultramafic rocks seems to be due to several diamond drill cores which are taken from spinifex-textured flows with high Al_2O_3 contents. The mean total iron content of Goose Lake Formation decreases from 12.90 in ultramafic rocks to 11.30 in basaltic rocks. Again, the FeO* contents of ultramafic rocks in this formation is about 2% higher than in the Donut Lake

Formation which is presumably because of the higher iron contents of drill cores. The Goose Lake CaO content averages 6.01 weight percent for ultramafic and 5.26 for basaltic rocks. Such low amounts of CaO for a given MgO content are not reported from any other spinifex-textured rocks in other komatiitic lavas. TiO_2 is generally higher than komatiite in Munro Township (Arndt et al., 1977; Nesbitt and Sun, 1976), and Belingine Green-stone Belt, Rhodesia (Nisbet et al., 1977). The comparison between published data from other areas and the present study reveals that these rocks are enriched in most major oxides but show a slight depletion in SiO_2 and CaO contents. Samples 138, 249, 250, 253 show an unusually high Na_2O contents, (more than 0.85%). It has been found that sample 138 (Fig. 3) is the only one in the area containing plagioclase. The presence of about 5% albite by volume enriches the rock in Na_2O contents. Also in spite of Arndt et al's. (1977) classification where komatiites carrying plagioclase, should contain less than 12% MgO, this rock contains almost 22 percent by weight magnesium oxide. Samples 249, 250 and 253 (Fig. 3) are the diamond drill cores taken from the spinifex-textured part of a flow unit and all of them have more than 30% chloritized and devitrified glass. Arndt et al. (1977) have published the microprobe analyses of interstitial devitrified glass for 42 different samples. The soda content of their analyses ranges from 0.75% to 3.08% with an average value of 1.80%.

Normative calculation indicates olivine rich nature of these rocks. Besides that all are hypersthene normative too with the exception of sample 253 which contains no hypersthene but very small amount of nepheline.

In different MgO variation diagrams trace elements of Goose Lake Formation display the same pattern as Donut Lake Formation. However, there are some minor differences. In this formation, Y, Zn, and Ba have a tendency to be

enriched in rocks with lower MgO, while Ni and Ce exhibit the opposite trend. In a comparison, komatiite of the McArthur Township carry more Ba and less Y than those indicated by Nesbitt and Sun (1976). The Ti/Zr ratio of the Goose Lake Formation averages to about 134.

Goose Lake Formation komatiite, in addition to petrographic differences, such as presence of abundant spinifex-textured lavas and lack of any medium or coars grained rocks, show the following specific geochemical characteristics when compared with the Donut Lake Formation: (1) CaO content of Goose Lake Formation is more than 2% lower, while the Al_2O_3 content does not show any significant change (Table 1); (2) Goose Lake Formation exhibits pronounced higher iron and magnesium content (Fig. 14) (Table 1); (3) Goose Lake Formation is enriched in Ni, Ce and Cu and depleted in Ba in comparison to the Donut Lake komatiite (Table 3). Komatiite in McArthur Township area, like other well studied komatiitic rocks have a low FeO*/MgO and FeO*/FeO* + MgO ratio. For both formations, FeO*/MgO ratios range from 0.27 to 0.83 and FeO*/FeO* + MgO between 0.20 and 0.45. In most of the variation diagrams the Goose Lake Formation shows much wider ranges for the above ratios than the Donut Lake Formation. The MgO content of these two formations never drops below 17.5% by weight. CaO/Al_2O_3 ratio of these rocks varies in a wide range but averages to about 0.85.

Thirteen diamond drill cores taken from the three different spinifex-textured flows were studied chemically. Figure 3 ahows the sample locations; major and trace element data are presented in Appendix I. Stratigraphic chemical variations in MgO, Al_2O_3, CaO, Ni, and Y through one of the flows are shown in Figure 24. The components can be divided into two distinct groups: Those of group one which show an abrupt decrease and those of group two which show a sharp increase, across the contact from the S to SF
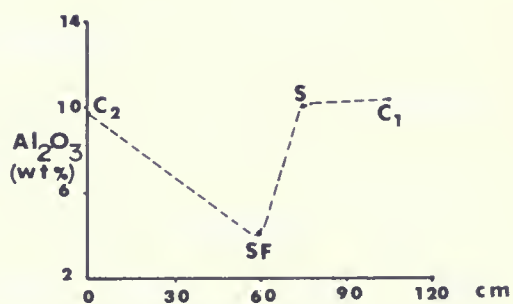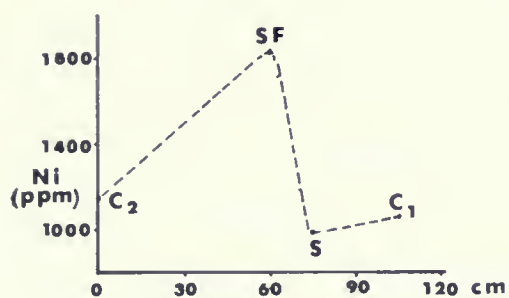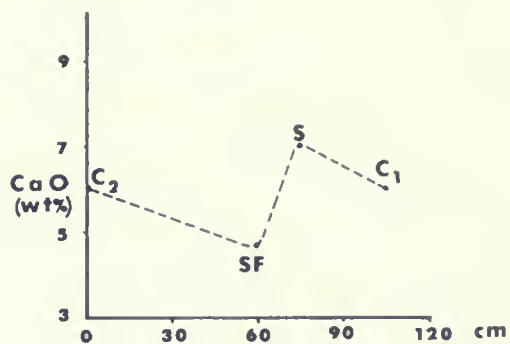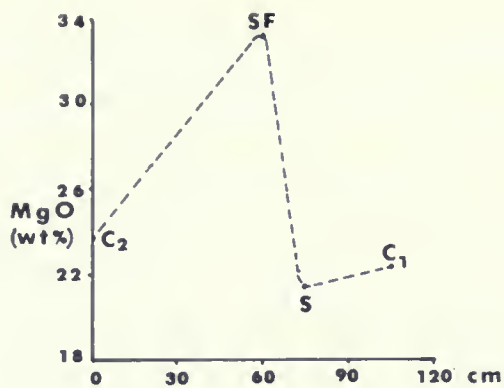
C₁   Upper chilled margin
SF   Spinifex-free zone
S   Spinifex-textured zone
C₂   Lower chilled margin
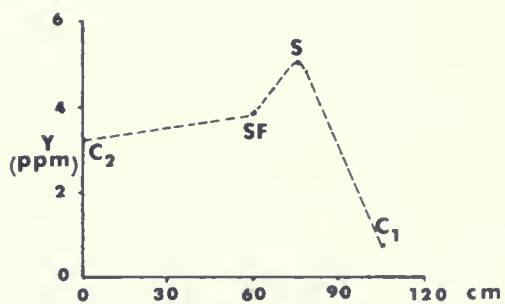
Figure 24   MgO, CaO, Al₂O₃, Ni and Y variations in a spinifex-textured flow from the Goose Lake Formation.

zone. MgO, Ni are in the first group and CaO, Al_2O_3 and Y are in the second. The profiles in both the first and second group show (a) a progressive increase for group one and decrease for group two from a lower chilled margin toward the SF zone, (b) a sudden decrease for group one and increase for group two at the contact between SF and S zones, and (c) a slight increase for group one and decrease for group two toward the top chilled margin. The significant point is low CaO/Al_2O_3 ratio of the spinifex-textured zones and higher CaO/Al_2O_3 ratio of the spinifex-free zones, within all the flow units.

The basaltic komatiite of <u>Schumacher Formation</u> partly surrounds the komatiitic lavas of Goose Lake Formation, both in the north and northwest and the south and southeast. No petrographical and geochemical gradation exist at the contacts of these two formations. The Schumacher Formation lavas are komatiitic in composition since they all plot on the left side of the inclined line in Figure 21. Furthermore, because they contain less than 12% MgO they are classed as basaltic komatiite (Arndt <u>et al</u>., 1977). In addition to these rocks, the uppermost flows of the Redstone Formation display basaltic komatiite characteristics. Payne (1978) has divided the lavas in the Schumacher Formation of Timmins area (approximately 30 km north of the study area) into two different units on the basis of TiO_2 content: The lower unit contains less than 1.20% TiO_2 for which the average of 0.89% is calculated. It also carries higher MgO (6.70%) and lower FeO* (11.92%) than the upper unit. The basaltic lavas of the upper unit have an average of 1.41% TiO_2, 13.69% FeO* and 5.19% MgO. As a result, it is suggested that only the lower part of the Schumacher Formation is exposed in McArthur Township, or that the upper unit of this formation pinches out before reaching the area.

The basaltic and basaltic andesitic flows predominate in the formation. The MgO content of the basalts average 8.51 weight percent and those of basaltic andesites and andesites average 8.30 and 9.28%, respectively. These values are (about 1.5%) lower than Barberton type basaltic komatiite of South Africa (Viljoen and Viljoen, 1969) and Munro basaltic komatiites (Arndt et al., 1977). Similar values are reported from magnesium basalts of tholeiitic units of Destor and Deguisier (Gelinas et al., 1977). The modern analogue of the rocks with such a high MgO content is mid-oceanic ridge basalt (Sun and Nesbitt, 1977) and abyssal tholeiite (Melson and Thompson, 1970). Alumina content of these rocks is 14.89 for average basalt, while it increases to 14.97 and 15.43 for basaltic andesites and andesite respectively. Comparable values are published by Arndt et al. (1977) and Naldrett and Cabri (1976).

The average content of total iron as FeO and CaO of the rocks is 11.10 and 9.99 respectively, which decreases with increasing SiO_2 and Al_2O_3. TiO_2 values are much lower than tholeiitic rocks of the area. Averages of 0.74, 0.72 and 0.63 percents characterize the basalts, basaltic andesites and andesites of the basaltic komatiite in McArthur Township. The closest values in literature are reported from Abitibi belt by Brooks and Hart (1974) and Arndt et al. (1977). High magnesium-tholeiite of Jolly (1978) and magnesian basalt of Nisbet et al. (1977) contain identical TiO_2 content.

The data presented here when compared to basaltic komatiite of Naldrett et al. (1976) and Arndt et al. (1977) shows one main contrasting difference: the low K_2O content of basaltic komatiite, which always averages less than 0.28%. Schumacher basaltic komatiite contains average of 0.62 weight percent K_2O which is more than twice the maximum K_2O content of the typical basaltic komatiite (Naldrett and Cabri, 1976). In spite of the fact that

Table 1   Average major oxide compositions of different groups in weight percent. All values have been recalculated less volatiles.

KOMATIITIC ASSOCIATION

Donut Lake Formation	Total	MgO > 30	MgO < 30
No.[1]	(13)	(3)	(10)
SIO2	46.82	45.51	47.22
AL203	7.49	6.46	7.81
FEO*	11.06	10.82	11.81
MGO	25.11	30.62	23.46
CAO	8.61	5.73	9.48
NA20	0.31	0.33	0.30
K20	0.05	0.04	0.05
TIO2	0.44	0.40	0.45
MNO	0.06	0.06	0.06
P205	0.05	0.03	0.05

Goose Lake Formation	Total	MgO > 30	MgO < 30
No.[1]	(23)	(8)	(15)
SIO2	45.77	45.62	45.84
AL203	7.57	5.24	8.83
FEO*	12.41	10.94	13.19
MGO	27.60	33.18	24.62
CAO	5.65	4.19	6.42
NA20	0.41	0.26	0.48
K20	0.03	0.04	0.02
TIO2	0.48	0.36	0.54
MNO	0.07	0.13	0.04
P205	0.02	0.03	0.02

Schumacher Formation[2]	Total	Non-variolitic	Variolitic
No.[1]	(12)	(10)	(2)
SIO2	52.28	52.68	52.20
AL203	14.98	15.23	14.94
FEO*	11.10	11.69	10.98
MGO	8.46	7.67	8.61
CAO	9.99	10.52	9.88
NA20	1.60	0.24	1.86
K20	0.62	0.64	0.62
TIO2	0.72	0.85	0.69
MNO	0.16	0.33	0.13
P205	0.10	0.14	0.09

THOLEIITIC ASSOCIATION

Redstone Formation	Total	Olivine Normative	Quartz Normative
No.[1]	(17)	(4)	(13)
SIO2	50.37	47.48	51.26
AL203	14.67	15.94	14.26
FEO*	14.87	14.09	15.11
MGO	5.23	5.85	5.02
CAO	11.31	12.92	10.83
NA20	1.49	2.26	1.26
K20	0.30	0.24	0.33
TIO2	1.40	1.01	1.54
MNO	0.16	0.12	0.17
P205	0.18	0.08	0.21

CALC-ALKALINE ASSOCIATION

Boomerang Formation[3]	Total
No.[1]	(14)
SIO2	64.65
AL203	14.94
FEO*	6.64
MGO	3.13
CAO	4.13
NA20	4.32
K20	1.18
TIO2	0.60
MNO	0.23
P205	0.16

Gradational Lava	Total
No.[1]	(6)
SIO2	57.53
AL203	15.08
FEO*	12.94
MGO	3.09
CAO	7.81
NA20	1.85
K20	0.71
TIO2	0.64
MNO	0.13
P205	0.21

1   Number of analyses
2   Including 3 samples from Redstone Formation (41, 199, 201)
3   Including 1 sample from Schumacher Formation (157) and 1 from gabbroic sills (186)

Table 2 Average trace element compositions of different groups
in parts per million.

KOMATIITIC ASSOCIATION

Donut Lake Formation	Total	MgO > 30	MgO < 30
No.[1]	(9)	(2)	(7)
BA	49.7	4.1	62.7
CE	8.9	13.8	7.5
CU	16.6	4.4	20.1
NI	1295.5	1577.7	1214.8
RB	0.4	0.9	0.3
S	419.3	68.8	519.5
SR	22.4	14.4	24.7
Y	3.2	2.3	3.4
ZN	51.0	52.1	50.7
ZR	24.4	20.2	25.7

Goose Lake Formation	Total	MgO > 30	MgO < 30
No.[1]	(22)	(7)	(15)
BA	17.8	10.5	21.2
CE	14.3	29.7	7.2
CU	21.0	9.5	26.4
NI	1403.9	1821.6	1208.9
RB	0.4	0.6	0.3
S	249.7	295.4	228.4
SR	25.2	44.5	16.2
Y	2.3	1.2	2.8
ZN	57.3	57.0	57.4
ZR	21.2	23.0	20.4

Schumacher Formation[2]	Total	Non-variolitic	Variolitic
No.[1]	(12)	(10)	(2)
BA	225.0	226.5	217.2
CE	6.2	6.8	2.9
CU	33.8	36.2	21.4
NI	255.7	280.6	131.0
RB	15.1	14.9	16.1
S	163.4	191.9	20.8
SR	181.9	179.2	195.4
Y	8.6	8.3	10.0
ZN	66.0	66.0	66.2
ZR	61.9	60.4	69.2

THOLEIITIC ASSOCIATION

Redstone Formation	Total	Olivine Normative	Quartz Normative
No.[1]	(17)	(4)	(13)
BA	121.1	77.2	133.2
CE	6.0	0.0	7.4
CU	27.5	12.5	30.9
NI	65.6	72.8	59.9
RB	4.9	2.5	5.4
S	369.4	212.9	420.6
SR	134.8	295.4	90.2
Y	11.0	8.3	12.0
ZN	75.3	63.0	80.8
ZR	60.8	72.4	59.2

CALC-ALKALINE ASSOCIATION

Boomerang Formation[3]	Total
No.[1]	(12)
BA	220.6
CE	55.5
CU	56.0
NI	137.3
RB	25.6
S	43.9
SR	182.0
Y	7.0
ZN	67.3
ZR	121.4

Gradational Lava	Total
No.[1]	(16)
BA	199.2
Ce	16.5
CU	18.9
NI	90.8
RB	13.8
S	590.7
SR	249.8
Y	7.7
ZN	97.0
ZR	116.2

1   Number of analyses
2   Including 3 samples from Redstone Formation (41, 199, 201)
3   Including 1 sample from Schumacher Formation (157) and 1 from
    gabbroic sills (186)

Table 3   Average major oxide compositions of McArthur Township
          area volcanic classes in weight percent. All values
          have been recalculated less volatiles.

KOMATIITIC ASSOCIATION

Donut Lake Formation	Ultra-mafic	Basalt	Basaltic Andesite	Andesite	Dacite	Rhyolite
No.[1]	(9)	(3)	(1)			
SIO2	45.84	47.70	53.02			
AL203	7.17	8.04	8.81			
FEO*	11.11	11.32	9.70			
MGO	25.81	24.87	19.62			
CAO	9.21	7.13	7.61			
NA20	0.28	0.34	0.48			
K20	0.04	0.07	0.06			
TIO2	0.43	0.40	0.60			
MNO	0.06	0.07	0.03			
P205	0.05	0.06	0.01			

Goose Lake Formation	Ultra-mafic	Basalt	Basaltic Andesite	Andesite	Dacite	Rhyolite
No.[1]	(16)	(7)				
SIO2	45.01	47.49				
AL203	8.06	6.47				
FEO*	12.90	11.30				
MGO	26.94	29.11				
CAO	6.01	4.79				
NA20	0.46	0.29				
K20	0.03	0.02				
TIO2	0.50	0.44				
MNO	0.07	0.06				
P205	0.02	0.02				

Schumacher Formation[2]	Ultra-mafic	Basalt	Basaltic Andesite	Andesite	Dacite	Rhyolite
No.[1]		(4)	(7)	(1)		
SIO2		50.41	52.76	56.32		
AL203		14.89	14.97	15.32		
FEO*		11.91	10.85	9.49		
MGO		8.51	8.30	9.28		
CAO		11.29	9.68	6.97		
NA20		1.50	1.77	0.76		
K20		0.53	0.64	0.91		
TIO2		0.74	0.72	0.63		
MNO		0.12	0.20	0.10		
P205		0.10	0.10	0.11		

THOLEIITIC ASSOCIATION

Redstone Formation	Ultra-mafic	Basalt	Basaltic Andesite	Andesite	Dacite	Rhyolite
No.[1]	(3)	(9)	(3)	(2)		
SIO2	44.94	49.80	53.15	56.86		
AL203	14.85	14.87	14.07	14.35		
FEO*	18.57	14.44	15.81	9.92		
MGO	4.71	6.02	4.45	3.60		
CAO	14.42	11.79	9.12	7.90		
NA20	0.39	1.28	1.29	4.41		
K20	0.28	0.29	0.33	0.36		
TIO2	1.46	1.20	1.52	2.11		
MNO	0.12	0.22	0.11	0.00		
P205	0.27	0.10	0.15	0.48		

CALC-ALKALINE ASSOCIATION

Boomerang Formation	Ultra-mafic	Basalt	Basaltic Andesite	Andesite	Dacite	Rhyolite
No.[1]				(3)	(10)	(1)
SIO2				60.22	65.86	72.20
AL203				14.09	15.17	14.87
FEO*				7.82	6.32	6.55
MGO				3.88	2.93	1.08
CAO				7.59	3.19	0.31
NA20				4.41	4.30	1.43
K20				0.67	1.31	2.81
TIO2				0.81	0.55	0.35
MNO				0.33	0.20	0.26
P205				0.17	0.16	0.13

1   Number of analyses
2   Including 3 samples from Redstone Formation (41, 199, 201)

Table 4   Average trace element compositions of McArthur Township
area volcanic classes in parts per million.

KOMATIITIC ASSOCIATION

Donut Lake Formation	Ultra-mafic	Basalt	Basaltic Andesite	Andesite	Dacite	Rhyolite
No.[1]	(5)	(3)				
BA	33.3	52.2				
CE	11.2	8.2				
CU	20.0	8.5				
NI	1324.0	1354.3				
RB	0.7	0.2				
S	217.7	456.8				
SR	24.4	15.0				
Y	3.3	2.1				
ZN	46.9	65.2				
ZR	21.9	28.2				

Goose Lake Formation	Ultra-mafic	Basalt	Basaltic Andesite	Andesite	Dacite	Rhyolite
No.[1]	(15)	(7)				
BA	22.0	8.6				
CE	10.6	22.2				
CU	22.0	18.9				
NI	1312.5	1599.7				
RB	0.2	0.7				
S	199.6	357.2				
SR	19.1	38.5				
Y	2.1	2.6				
ZN	57.9	55.9				
ZR	20.8	22.1				

Schumacher Formation[2]	Ultra-mafic	Basalt	Basaltic Andesite	Andesite	Dacite	Rhyolite
No.[1]		(4)	(7)	(1)		
BA		178.8	257.4	182.8		
CE		0.6	6.4	27.1		
CU		35.7	32.6	34.2		
NI		224.0	66.0	335.4		
RB		14.1	14.8	21.5		
S		64.2	238.2	36.0		
SR		135.3	205.0	203.3		
Y		7.7	9.1	8.2		
ZN		63.0	66.0	73.2		
ZR		50.8	63.1	98.4		

THOLEIITIC ASSOCIATION

Redstone Formation	Ultra-mafic	Basalt	Basaltic Andesite	Andesite	Dacite	Rhyolite
No.[1]	(3)	(9)	(3)	(2)		
BA	104.5	107.7	134.5	177.5		
CE	0.0	0.0	0.0	48.0		
CU	14.9	26.3	32.3	37.0		
NI	64.3	68.2	46.3	62.0		
RB	3.2	5.1	3.2	7.7		
S	528.8	296.3	461.7	340.9		
SR	311.3	86.4	136.1	117.6		
Y	10.5	9.4	12.3	18.2		
ZN	78.5	77.6	86.5	54.4		
ZR	72.9	50.5	69.4	88.7		

CALC-ALKALINE ASSOCIATION

Boomerang Formation	Ultra-mafic	Basalt	Basaltic Andesite	Andesite	Dacite	Rhyolite
No.[1]				(3)	(8)	(1)
BA				292.5	191.6	506.7
CE				46.8	60.4	41.8
CU				5.7	50.0	254.5
NI				116.0	162.5	0.0
RB				17.4	23.5	66.5
S				0.3	55.4	82.5
SR				183.0	199.2	40.9
Y				7.6	7.7	0.0
ZN				61.7	71.0	54.8
ZR				107.0	125.9	128.3

1   Number of analyses
2   Including 3 samples from Redstone Formation (41, 199, 201)

Table 5   Average major oxide compositions of mafic and felsic
intrusions and metasediments in weight percent. All
values are recalculated less volatiles.

Peterlong Lake Complex	Total	Biotite rich	Biotite poor
No.[1]	(9)	(3)	(6)
SIO2	58.56	65.63	56.46
AL203	15.38	15.90	15.35
FEO*	7.67	4.97	8.47
MGO	5.27	1.13	6.61
CAO	6.83	4.27	7.58
NA20	4.16	5.49	3.75
K20	1.19	1.72	0.84
TIO2	0.70	0.65	0.69
MNO	0.08	0.06	0.08
P205	0.16	0.18	0.16

Diabase Dyke	Total	Olivine diabase	Quartz diabase
No.[1]	(7)	(4)	(3)
SIO2	48.42	46.05	51.57
AL203	14.07	12.46	16.22
FEO*	14.36	14.49	14.20
MGO	8.30	10.83	4.93
CAO	10.81	11.13	10.38
NA20	0.80	1.15	0.35
K20	0.61	0.64	0.57
TIO2	1.75	2.01	1.40
MNO	0.20	0.20	0.20
P205	0.67	1.04	0.18

Adams Pluton	Total	Quartz Diorte Sill Total	Gabbroic Sill Total
No.[1]	(5)	(1)	(11)
SIO2	68.66	57.92	50.49
AL203	15.70	14.52	15.06
FEO*	2.18	8.09	14.68
MGO	0.54	8.66	6.71
CAO	2.39	6.39	10.19
NA20	7.27	2.49	1.20
K20	2.81	1.04	0.30
TIO2	0.28	0.58	1.12
MNO	0.06	0.20	0.14
P205	0.12	0.12	0.10

Qtz-Feldspar Porphyry	Total	Trondhjemite Total	Timiskaming Sedimentary Rock Total
No.[1]	(1)	(1)	(2)
SIO2	75.76	61.08	64.24
AL203	13.23	16.44	16.25
FEO*	0.99	8.24	5.85
MGO	0.38	1.49	2.68
CAO	1.20	2.65	3.60
NA20	6.82	8.32	5.71
K20	1.44	0.50	0.77
TIO2	0.06	1.03	0.63
MNO	0.08	0.00	0.07
P205	0.04	0.23	0.19

Table 6   Average trace element compositions of mafic and felsic
intrusions and metasediments in parts per million.

Peterlong Lake Complex	Total	Biotite rich	Biotite poor
No.[1]	(3)	(1)	(2)
BA	275.7	333.9	246.6
CE	36.8	83.2	13.6
CU	19.6	10.4	24.2
NI	197.5	48.2	272.1
RB	41.8	56.7	34.2
S	109.8	50.7	139.3
SR	211.9	249.4	193.2
Y	13.3	21.7	9.1
ZN	73.3	61.9	78.9
ZR	115.0	221.9	61.5

Diabase Dyke	Total	Olivine diabase	Quartz diabase
No.[1]	(5)	(3)	(2)
BA	260.5	434.2	53.1
CE	18.8	18.6	19.0
CU	94.0	81.2	113.2
NI	501.3	254.9	871.0
RB	9.6	11.0	7.5
S	442.9	670.4	101.7
SR	186.0	363.0	70.4
Y	11.0	13.8	6.8
ZN	71.7	72.4	70.7
ZR	86.1	117.0	39.6

Adams Pluton		Quartz Diorte Sill	Gabbroic Sill
	Total	Total	Total
No.[1]	(3)	(1)	(11)
BA	803.5	220.6	102.6
CE	113.2	27.9	ND
CU	16.5	28.8	90.3
NI	14.9	302.7	79.3
RB	89.6	26.9	4.6
S	38.0	63.4	1012.5
SR	989.7	227.2	102.3
Y	15.5	9.3	8.4
ZN	65.1	71.8	74.2
ZR	233.3	108.9	50.9

Qtz-Feldspar Porphyry		Trondhjemite	Timiskaming Sedimentary Rock
	Total	Total	Total
No.[1]	(1)	(1)	(1)
BA	661.7	118.2	189.0
CE	163.1	170.9	44.6
CU	34.4	165.5	85.0
NI	ND	24.8	69.3
RB	53.8	23.0	38.2
S	263.8	3100.0	257.5
SR	220.2	264.8	228.1
Y	10.9	10.1	13.3
ZN	ND	10.8	108.2
ZR	141.1	238.5	157.5

potassium should increase with fractionation, due to the potassium meta-
somatism of basaltic komatiite and tholeiitic associations of this area,
it displays a distinctive decrease (Fig. 11). Hart (1969) reports the
increase in K and Rb of submarine basalt due to sea water alteration.

Normative calculation of these lavas indicates that all of the Schumacher
Formation lavas are quartz and hypersthene normative while komatiitic rocks
belonging to the Redstone Formation are olivine normative.

Trace element results of basaltic komatiite demonstrate a gradual de-
crease of Zr, Sr, Zn, Cu, Ni, and Rb in the rocks with more mafic composi-
tion. Trace element analyses of basaltic komatiite from other areas are
scarce. However, comparison of the data with basaltic komatiite of Arndt
et al. (1977) and high magnesium-metabasalts of Nesbitt and Sun (1976),
with average MgO contents of about 10 and 12% respectively, reveals higher
Zr, Ni, Sr and Rb and lower Y contents of the Schumacher Formation of the
McArthur Township.

The mean whole rock analytical result of variolitic flows in Schumacher
Formation is presented in Tables 1 and 3. Note the higher Al_2O_3, FeO*, MnO,
Rb, Zr, and Y and lower MgO, Na_2O, Ni and sulfur contents of the variolitic
flows compared to non-variolitic ones. Brooks (1977) has analyzed the matrix
fractions of some Abitibi variolites, all of which carry high iron contents
(up to 24 weight % FeO*).

There is more than 7% gap between MgO content of the komatiitic and
basaltic komatiitic rocks present in the area (Fig. 11 to 17). A gap be-
tween 16% to 20% MgO is reported from the Belingive greenstone belt, Rodesia
(Nisbet et al., 1977), also the MgO variation diagrams of Nesbitt and Sun
(1976) show just one sample between 15 to 20% MgO. Payne (1978) reports
a gap between 8 to 14% from the Goose Lake Formation of Timmins area,

while Arndt et al. (1977) and Arndt (1977a) data from the Fred's flow
in Munro Township do not show any gap. In general, the reported MgO gaps
in the literature seem to reflect inadequate local and regional sampling.

Tholeiitic Association: Most of the lava flows in the Redstone Forma-
tion and some of the flows in the Boomerang Formation display tholeiitic
affinities. Figure 14 demonstrates the strong iron enrichment trend of
these rocks in FeO total versus MgO plots. Note that some show an excep-
tionally high iron content. The iron enrichment trend of tholeiitic lava
in the McArthur Township area, compared to average primitive tholeiitic
lavas of Abitibi greenstone belt (Jolly, 1978), shows maximum enrichment
of iron in rocks with 6% MgO rather than 4%. The similar iron enrichment
trends are reported by Gelinas et al., (1977) from the Deguisir tholeiitic
units, Abitibi (Fig. 25).

Ultramafic lavas, basalts and basaltic andesites are the most prominant
lava types of the tholeiitic association in the area. The lavas vary con-
siderably in TiO_2 values but average 1.40%. TiO_2 contents of this association
averages 1.46% for ultramafic rocks and 1.20 for basalts, while those for
basaltic andesite average 1.52 and for andesites 2.11. These values are
generally higher than those reported from greenstone belts in India
(Naqvi and Hussain, 1973) in western Australia (Hallberg, 1972), and in
Manitoba (Green, 1975). On the other hand values reported by Jolly (1977,
1978) from Abitibi belt are slightly higher than TiO_2 values here. However,
comparable TiO_2 contents from Abitibi greenstone lavas are reported by
Baragar (1968); Goodwin (1977); Gelinas et al. (1977); and Grant (1978).
TiO_2 has received much attention as a tool to discriminate between different
modern volcanic suites, Pearce and Cann (1973) report an average TiO_2 content
of 0.86% for low-K tholeiite, and 2.71 and 2.53 for ocean island basalt and
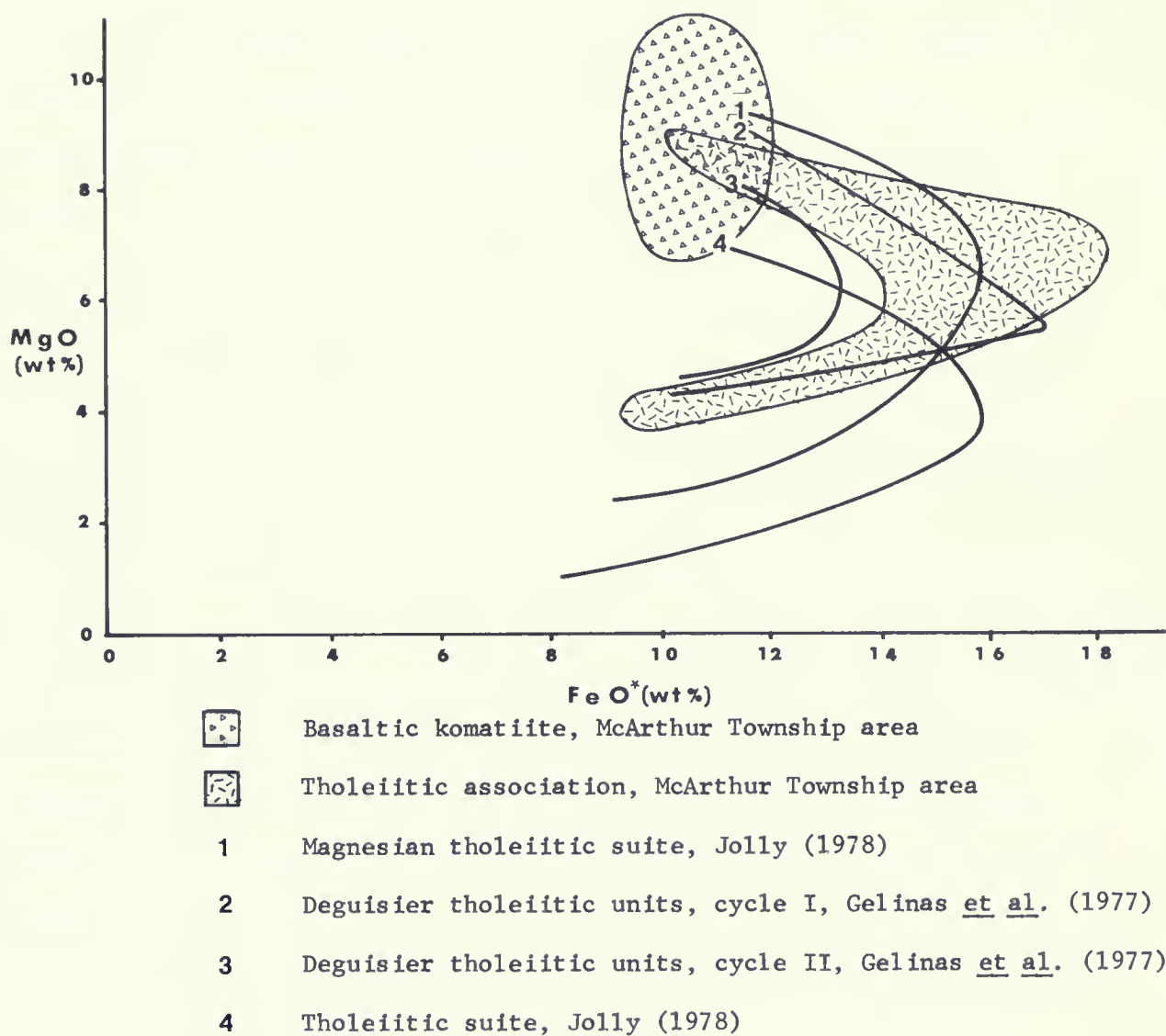
Figure 25   Some tholeiitic iron enrichment trends of the Abitibi belt.

continental basalt, respectively. Chayes (1964) divides the oceanic and
circum oceanic basalt on the basis of whether it contains, respectively,
more or less than 1.75 percent TiO_2. Comparable TiO_2 contents to those
of McArthur tholeiite characterize the island arc tholeiite of which the
Japan arc tholeiite is the prime example (Pearce and Cann, 1971).

Aluminum oxide content of the tholeiitic association for various classes
is about 14 weight percent, with a very slight decrease towards the less
mafic rocks. Identical alumina values are cited from several Archean vol-
canics, Abitibi (Gelinas et al., 1977; Goodwin, 1977), Yellowknife
(Baragar, 1966), Island Lake greenstone belt (Delaney, 1976), western
Australia (Hallberg, 1972) and India (Naqvi and Hussain, 1973). Modern
oceanic tholeiite contains comparable Al_2O_3 to the rocks under the study
here.

The CaO trend drops sharply from mafic to felsic rocks. The average
value of 11.31 calculated for tholeiitic rocks of the area is conspicuously
higher than those of the other areas.

P_2O_5 content of the samples 32 and 36 compared to the average rock is
very high. These rocks and other rocks which contain more P_2O_5 than the cited
average (0.18%) are distinctively enriched in TiO_2 also. These facts suggest
that although apatite, ilmenite and sphene were precipitating from the
beginning of crystallization or soon after, they became abundant cumulus
minerals in the middle of flows as later crystallization products of the
cooling lava.

MgO averages 4.71 weight percent for ultramafic, 6.02 for basaltic,
4.45 for basaltic andesite and 3.60 for andesitic lavas. These values
are much lower than oceanic tholeiite while it resembles that of island
arc tholeiite.

McArthur Township area tholeiite like other Archean tholeiitic rocks is marked by very low K_2O content which is analoguous to K_2O content of the low K tholeiite of island arc series.

Trace-element values for tholeiitic rocks are presented in Appendix I. Ba, Ce and Rb increase progressively in values with decreasing SiO_2 contents. Sulfur is relatively abundant in tholeiitic rocks. No relationship has been observed between sulfur and transition metals (Ni, Cu, Zn) abundances. Zr (60.8) and especially Y (11.0) abundances in tholeiitic rocks are considerably lower than those reported in literature from other greenstone belts. The closest Zr content (70 ppm) is from the basaltic and andesitic tholeiites of the Superior Province described by Goodwin (1977). Yttrium has never been reported in such small amounts, however, Yttrium content of depleted Archean tholeiite of Condie (1976) is the same as those in McArthur Township area. An overall similarity is apparent between lavas under study here and arc tholeiite when major and trace elements is compared. In contrast, however, McArthur tholeiite has much more Ni than its arc tholeiite analogues which reflects the possible higher olivine in its source areas. On the basis of the CIPW normative calculation the tholeiite of the McArthur area will be divided into two distinctive groups:

(1) Olivine Normative Tholeiite: These rocks contain an average of about 13% normative olivine and therefore are enriched in MgO and NiO, both of which are largely controlled by olivine in the residue during the partial melting (Gast, 1968; Nesbitt and Sun, 1976) or fractionation. They are also enriched in Al_2O_3 and the alkalies. Two of the rocks in this group contain small amounts of normative nepheline.

(2) Quartz Normative Tholeiite: These rocks contain about 6% quartz in the norm and as expected, they are enriched in SiO_2, FeO*, TiO_2, P_2O_5, Y and Ba.

All the rocks in both two groups contain normative hypersthene, too.

The presence of 1 to 2 percent quartz observed in thin sections taken from picritic lavas indicated that at least some of the observed quartz in other rocks of the area are secondary.

FeO^*/MgO and $FeO^*/(FeO^* + MgO)$ ratios of the McArthur area tholeiites are high and quite distinctive compared to the komatiitic rock series. These ratios are 3.01 and 0.75 for average quartz normative rocks, respectively. CaO/Al_2O_3 ratios of these rocks are slightly lower than komatiitic lavas.

Calc-alkaline Association: A typical calc-alkaline lava is characterized by monotonous depletion of iron and titanium and enrichment of silicon and alkalies during the fractional crystallization. Figure 20 shows the calc-alkaline nature of more than two thirds of the sampled specimens in Boomerang Formation. In addition, minor intermediate to felsic lavas of calc-alkaline affinities are intercalated within gabbroic sills and basaltic komatiites of the area. The AFM diagram (Fig. 19) shows the alkali rich nature of these rocks in a trend nearly perpendicular to $MgO - FeO^*$ join. Andesite, dacite and rhyolite are the prominent lava types of the calc-alkaline association. The population of rhyolite in the area is very small and most of the lavas are of dacitic composition.

Low FeO^*, as well as low TiO_2 is the most distinctive factor of this association. FeO^* values are always below 10% (average 6.64) and shows a decrease towards the felsic rocks. The average TiO_2 content of andesite is 0.81 weight percent, averages of 0.55% and 0.35% characterize dacite and rhyolite. These values are very much like those reported by Goodwin (1977) from the Superior Province, Ontario, and by Hallberg et al., (1976) from Marda Complex, Australia. Higher values were reported by Jolly (1977) and

Gelinas et al. (1977) from Abitibi belt. In modern volcanic rocks such
a low FeO* and TiO_2 trends are reported from different island arc calc-
alkaline series, between which Dominica Island of Lesser Antilles (Brown
and others, 1977) and Viti Levu of Fiji (Gill, 1970, 1974) are the best
examples.

MgO content of calc-alkaline rocks is considerably lower than tholeiitic
rocks of the area. The mean MgO contents of andesitic rocks is 3.88 weight
percent, while it drops to 2.93 and 1.08 in dacites and rhyolite. These
values are consistent with those indicated by Jolly (1977) from the Abitibi
greenstone belt and by Hallberg et al. (1976) from Marda Complex. Similar
MgO trends are reported from Lesser Antilles (Brown and others, 1977) and
Fiji (Gill, 1970, 1974).

The Al_2O_3 content of average calc-alkaline rocks is 14.94 which is
nearly the same as the tholeiitic rocks of the area. This low average is
the main contrasting difference which exists between McArthur calc-alkaline
rocks and those in modern island arcs. Alumina contents of most of the
Archean calc-alkaline rocks reported from other areas resemble their modern
island arc counterparts. The average CaO value is less than half of the
tholeiitic rocks of the area, and slightly lower than modern calc-alkaline
rocks.

Normative calculation of the geochemical results shows that half of the
rocks contain corundum, which might be an indicator of calcium and alkali
depletion for a given Al_2O_3 content.

Trace element values of calc-alkaline association are much different
than those of tholeiitic series in the area. In spite of about 30% decrease
in Yttrium contents, Ba and Zr show almost 100% increase in value, Ni 50%,
Rb 300%, and Ce 900% compared to tholeiitic rocks.

The calc-alkaline association of the McArthur Township area, like other Archean calc-alkaline rocks, contains higher Ni content than the calc-alkaline series of orogenic belts. To distinguish the Archean calc-alkaline association from the typical island arc counterparts, it was suggested by Jolly (1975) to designate the former as "primitive calc-alkaline".

Gradational lavas: These include the data points which fall off the normal calc-alkaline trend in the FeO* - MgO variation diagram (Fig. 14). These lavas are included within the Boomerang Formation and all characterized by twice as high an iron content as that of the calc-alkaline rocks of the same formation. CaO, K_2O, Zr, Ni, and Ce content of these rocks are between the calculated averages of calc-alkaline and tholeiitic associations.

CHEMISTRY OF INTRUSIVES

Gabbroic sills are identical in chemical composition to basaltic tholeiite of the Redstone Formation. Therefore, all plot in the tholeiitic field of the AFM diagram. Consequently because of the small compositional variation of the gabbros, in most of the plottings they fall in clusters. The comparison of the chemical composition of the gabbroic sills and available data from the basaltic rocks of the upper Schumacher Formation in the Timmins area (Payne, 1978) indicates relative higher MgO and FeO* and lower TiO_2 of the gabbros.

Calculation of the CIPW norms of the specimens indicates that rocks taken from the chilled margin of the sills contains normative olivine.

The geochemistry of Peterlong Lake Complex, as well as its petrography,

indicate the existence of at least two phases in this batholith. The specimens with higher SiO_2, Na_2O, K_2O, Zr, Y and Ce are biotite and quartz rich (quartz diorite) while those with small amounts of biotite and quartz contain higher FeO*, MgO, CaO, Cu and Ni diorite.

The Adams Pluton is very poor in iron, magnesium, nickel and copper content but enriched in alkalies, barium, zirconium, strontium, and cerium. Reported chemical values from Geikie Pluton (Pyke, 1978), southeast of the study area, are analogues to Adams Pluton analytical results.

The most silica rich rocks in the area belong to quartz-feldspar porphyry with SiO_2 = 75.76 weight percent. Furthermore, these rocks are characterized by very small amounts of CaO, FeO*, and MgO and 6.82 and 1.44 percent Na_2O and K_2O respectively. Na_2O is present in albitic plagioclase and most of the K_2O is concentrated in secondary sericite. The trondhjemitic intrusion is depleted in SiO_2, K_2O, Rb and Ba, but enriched in FeO*, MgO, TiO_2, P_2O_5, Al_2O_3, Zr, Cu, and Ni relative to the quartz-feldspar porphyry which reflects a lower quartz content and higher amounts of chlorite, iron oxides and sphene as mentioned in the previous chapter.

The chemistry of olivine diabase dykes is quite different from that of quartz diabase. Olivine diabase is enriched in MgO and depleted in SiO_2 and Al_2O_3. Sample 52 (Fig. 3) is drastically enriched in TiO_2 (5.28%) and P_2O_5 (3.20%). Thin section study of this rock indicates the presence of about 7% apatite and 8% ilmenite by volume.

CHEMISTRY OF THE SEDIMENTS

Two of the sedimentary samples are analyzed and the average of these two are presented in Tables 5 and 6. The chemistry of the sediments is

very close to the average composition of the calc-alkaline rock associ-
ation of the study area (Tables 1 and 2). This similarity might indicate
that the Boomerang and Krist Formations as a source of the sediments.

SUMMARY

The lavas of the McArthur Township area are subdivided into komatiitic,
tholeiitic and calc-alkaline associations, with some members seemingly
transitional between the last two. The lava pile was erupted during two
cycles of volcanism, each of which was initiated by eruption of komatiitic
flows. Tholeiitic lavas were then erupted, but during the first cycle the
MgO content of the rocks increased and TiO_2 decreased upward so that the
latest flows exhibit komatiitic affinities. The calc-alkaline rocks
occupy the upper third of each cycle of volcanism.

In general there is an overall evolution in volcanism from lavas of
ultramafic to mafic characteristics lower in the pile to more felsic
derivations at higher levels.

DISCUSSION

The primary mineralogy of most of the lavas of the McArthur Township area was destroyed by the previous greenschist to amphibolite grade metamorphism that occurred mostly during Kenoran time. Similarly, many geochemical components, such as the alkalies, have been redistributed by metamorphic activity during metamorphism. However, a few components, (MgO, FeO^*, TiO_2, Al_2O_3, Ni and Zr) appear to have been relatively immobile during metamorphism. Characteristic of the rocks are low Al_2O_3 and very low Y. The lavas are arranged in two superimposed cycles, each of which grade from ultramafic types at the base to felsic pyroclastics at the top.

The combined study of the major and trace element geochemistry is used here in evaluating the petrogenesis of McArthur Township area. To provide a liquid with a composition similar to komatiitic flows from a mantle with garnet peridotite composition temperatures of at least $1650^\circ C$ (Green et al., 1975) are required. With the present average geothermal gradient of the earth such a liquid could be produced at the depth of 400 km. A higher Archean geothermal gradient is hypothesized by many authors (Nisbet et al., 1977; Green, 1975); such estimates generally allow derivation of parental magma from depths in excess of 150 km. The linear Ni/MgO variation observed in Figure 14 points to the existence of a high Ni phase, presumably olivine, which controls the Ni variation in high-Mg komatiitic liquids. The presence of abundant olivine in chilled flow bases has suggested to some (Nesbitt and Sun, 1976; Arndt, 1977b) that some of the olivine was entrained upward so rapidly from depth, along with the ultramafic liquids, that fractionation could not occur.

The water content of the erupted liquid may have been much lower than those presently observed in the lava. Green et al. (1975) demonstrated

103

the dry nature of komatiitic liquids ($<0.2\%$ H_2O) by quenching komatiitic liquids of various water contents. It was found that dry magmas are the only ones that do not crystallize any olivine prior to the eruption. This, and the presence of some olivine in erupted liquid indicated before, suggests the water content of about 1% and slightly lower eruption temperature than that suggested by Green et al. (1975). Kushiro (1972) argued in favor of the wet melting of the peridotite to produce komatiitic liquid, because such a process provides a higher stability field for olivine.

If the melting is viewed as taking place within an upward rising convective mantle diapir as suggested by Wyllie (1968) and others, the process may have been polybaric, with higher degrees of partial melting at greater depth. The model for the formation of ultramafic lavas accepted here includes the rise of a partially molten mantle diapir from a depth of at least 150 km. During the rise, the volume of liquid increased due to the lower load pressures in upper mantle. Most of the magma would then have gradually separated from the refractory residue and incorporated into the surrounding zone. A second stage of melting in the residual phase are thought to have yielded the komatiitic lavas. Such a process is favoured by Arndt (1977b); Nisbet et al. (1977); Bickle et al. (1977); Sun and Nesbitt (1978) and Jolly (1978). The argument about a two-stage process is strongly supported by reported light rare-earth element depletion in the komatiite relative to tholeiite.

The residual chrome-spinel present in the Donut Lake and Goose Lake Formations, and orthopyroxene are the Cr-rich phases controlling Cr variation schemes reported by Nesbitt and Sun (1976) and Nisbet et àl. (1977). Furthermore, as the residual spinel does not exist if partial melting of garnet peridotite exceeded 50% (Hawkesworth and O'Nions, 1977)

leaves the conclusion that the partial melting of a mantle source in the
case of the komatiite under study probably was between 35 to 50%.

On the basis of field relations, pillow structures, polyhedral flow
tops and spinifex textures, Biljoen and Viljoen (1969); Nesbitt (1971);
Pyke et al. (1973) and Arndt et al. (1977) have suggested submarine extrusion
of the ultramafic rocks. The mechanism of crystallization and formation of
komatiitic flows are described in the literature as in situ rapid crystalliz-
ation of a liquid which was initiated with downward crystallization of olivine
blades, giving rise to the spinifex texture. Figure 24 illustrates the varia-
tion of five different elements in a spinifex-textured flow in the area. MgO
and Ni show more concentration in spinifex free zone which will reflect its
higher olivine contents. On the other hand CaO, Al_2O_3, and Y are concentrated
in the spinifex part of a flow, which contains a higher volume of pyroxene. The
pyroxene which are interstitial to olivine grains have a diopsidic augite compos-
ition and are highly aluminous (Pyke et al., 1973; Arndt et al., 1977). The high
tendency of Y to replace Ca^{+2} has enriched yttrium in this zone.

The basaltic komatiite is presumed to be the result of lower amounts
of partial melting at lower P - T conditions, resulting in enrichment of
Ti, K, Rb, Ba and Sr in the melt.

The McArthur Township area tholeiite and generally the Archean tholeiite
are probably derived through relatively low degrees of melting at a shallower
depth in the upper mantle after the incorporation of parts of the surrounding
mantle (high light rare-earth contents) into the diapir. Low Y, Zr, K, Rb
and Ce contents all suggest that the source was relatively primitive.

The absence of mafic members of the calc-alkaline association in the
McArthur Township area prevents the effective evaluation of their petro-
genesis. However, the high nickel contents of these rocks indicate a

higher olivine concentration in the source than the modern calc-alkaline generating magmas.

A few theories concerning the origin of calc-alkaline lavas have been proposed. The one that seems more applicable to the area is the fractional crystallization of a parental basaltic magma suggested by Osborn (1959, 1962), who indicated the controlling role of oxygen. Under a high oxygen fugacity, much magnetite would crystalize, leading to depletion of the residual magma in iron and titanium and complementary silica enrichment. This theory is supported by a very small amount of Fe - Ti oxides observed in the lavas.

Diapiric deformation of the gneissic basement probably originated by compressional forces that were compounded by the upward transfer of plutonic bodies from depth as a result of Kenoran Orogeny. The presence of biotite and absence of potash feldspars in most of the granitic plutons indicates their wet intrusion.

The following is the summary of the processes that are viewed as leading to the magmatic evolution of the McArthur Township area:

(1) The partial melting of an Archean mantle at a depth of at least 150 km.

(2) The upward movement of the diapir accompanied by increase in volume of the liquid.

(3) Separation of the first liquid from refractory residual minerals and incorporation into the surrounding mantle, at relatively shallow depth, resulted the strong light rare-earth depletion of the residue.

(4) Partial melting (35 to 50%) of the residual phases and eruption of the light rare-earth depleted komatiites. The basaltic komatiite flows were formed by a lower degrees of partial melting of the residual source. Incorporation of parts of the surrounding mantle into the melt in later stages is responsible for the higher light rare-earth contents of the tholeiitic flows.

(5) An increase in P_{O_2} of the magma chamber followed by calc-alkaline eruptions.

(6) Continued pulses of partial fusion of the komatiitic parental magma were responsible for a cyclic nature of the volcanism.

(7) Partial melting of the wet gneissic basement introduced the granitic plutons into the area.

CONCLUSION

The McArthur Township area consists of an assemblage of Archean vol-
canic and sedimentary rocks which have been intruded by two large granitic
plutonic stocks. The lavas and sedimentary rocks are predominantly com-
posed of secondary mineral assemblages characterizing the greenschist facies
with upgrading to the amphibolite facies along the intrusive margins.
Regional metamorphism of these rocks occurred during the Kenoran Orogeny.

The petrochemical evaluation of the rocks were accomplished by using
relatively immobile elements (Fe, Mg, Ti, Al, Ni, and Zr). Three different
volcanic associations were distinguished by employing relatively immobile
Zr, Ti and Ni in a ternary diagram (ZTN).

The komatiitic association is characterized by high MgO (6.5 to 37.0%),
high Ni (110 to 2100 ppm), low TiO_2 (0.85%) and low FeO*/(FeO* + MgO)
ratios. The Cao/Al_2O_3 ratios of these rocks are not high and average about
0.85. The ultramafic members of this association commonly exhibit spinifex
texture.

The tholeiitic association contains high FeO* (11 to 26%), high TiO_2
(0.9 to 2.9%) and exhibit a distinct iron and titanium enrichment in the
intermediate members.

The calc-alkaline association displays a significant iron and titanium
depletion trend, with maximum FeO* and TiO_2 contents of 10% and 1%, respec-
tively. The lavas contain relatively higher Ni values than the tholeiitic
association.

In general, two cycles of volcanism, two periods of sedimentation and
one episode of magmatic intrusion are recognized in the study area. The
komatiitic lavas occupy the basal sequence of each volcanic cycle which is

108

followed by tholeiitic and calc-alkaline associations toward the top. The numerous gabbroic sills found in the area were possibly the feeders for the tholeiitic lavas of the second cycle of volcanism (upper Schumacher Formation).

The lavas were formed by partial melting of the mantle under a wide range of P - T conditions.

The sedimentary units were deposited after both the first (iron formation) and second (greywacke) cycles of volcanism in the study area but before the intrusion of the granitic plutons.

COMPARISON BETWEEN ARCHEAN LAVAS AND MODERN TYPES

Comparison between the Archean lava flows present in the McArthur Township area and modern volcanic series was partly done in a previous section, where it was suggested that the FeO*, MgO, TiO_2 and K_2O contents of the tholeiitic and calc-alkaline associations are similar to their counterparts in the modern island arc volcanic series. The modern analogues of the komatiites are found in rifting zones (Clarke, 1970), but they lack spinifex-textured rocks, and none of them are associated with nickel sulfide deposits. Oceanic tholeiites contain higher amounts of TiO_2, CaO and Y than any of the Archean volcanic associations. In addition, the Ni content of island arc calc-alkaline suites is at least five times lower than its Archean counterpart.

The application of the ZTN diagram to modern volcanic series (Fig. 26) and its comparison to Archean rocks (Fig. 22) indicates that the fractionation of the Archean volcanic series was strongly controlled by Ni, because the major part of each fractionation trend is subperpendicular to the Z - T join. Magmatic fractionation in modern volcanic rocks is not restrained by Ni because of its initially low concentrations. This might indicate a lack of enough heat in the "modern" mantle to form such mafic melts.

In conclusion, the possible sialic basement underlying the Abitibi greenstone belt, evidences for submarine eruptions of these rocks and similarity of the tertiary basalts of Baffin Bay (Clarke, 1970, 1975) to the Archean komatiite and tholeiite suggests that the two may have originated by rifting induced by a tensional force, perhaps generated by diapiric convection within the Archean mantle.
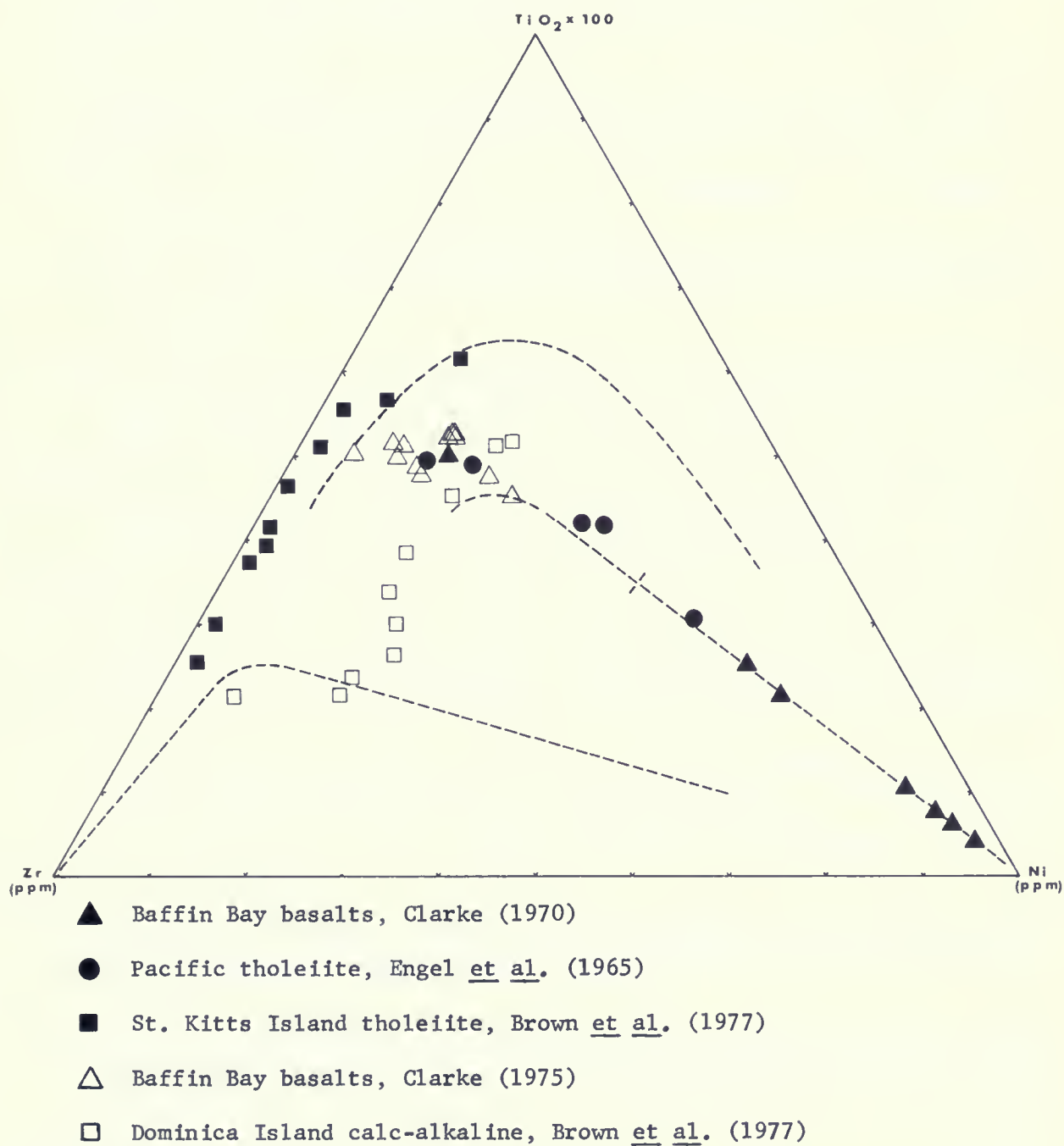
Figure 26   Application of ZTN diagram to modern volcanic rocks.

REFERENCES

Arndt, N. T., 1977a, Thick, layered peridotite-gabbro lava flows in Munro Township, Ontario: Can. Jour. Earth Sci., v. 15, n. 11, p. 2620-2637.

_____, 1977b, Ultrabasic magmas and high-degree melting of the mantle: Contrib. Mineral.Petrol., v. 64, p. 205-221.

Arndt, N. T., Naldrett, A. J., and Pyke, D. R., 1977, Komatiitic and iron-rich tholeiitic lavas of Munro Township, northeast Ontario: Jour. Petrol., v. 18, n. 2, p. 319-369.

Baragar, W. R. A., 1966, Geochemistry of the Yellowknife volcanic rocks: Can. Jour. Earth Sci., v. 3, p. 9-30.

_____, 1968, Majo-element geochemistry of the Noranda volcanic belt, Quebec, Ontario: Can. Jour. Earth Sci., v. 5, n. 4, pt. 1, p. 773-790.

Bickle, M. J., Ford, C. E., and Nisbet, E. G., 1977, The petrogenesis of peridotitic komatiites: evidence from high-pressure melting experiments: Earth Planet. Sci. Let., v. 37, p. 97-106.

Bowler, C. M. L., 1959, The distribution of the five alkali elements and fluorine in some granites and associated aureoles from the southwest of England. Ph. D. dissertation, University of Bristol.

Brookins, D. G., Dennen, W. H., 1964, Trace element variation across some igneous contacts: Trans. Kansas. Acad. Sci., v. 67, p. 70.

Brooks, C., 1977, Archean variolites: source of iron in the Precambrian environment: Can. Jour. of Earth Sci., comm., v. 14, n. 3, p. 511-513.

Brooks, C., Hart, S. R., 1972, An extrusive basaltic komatiite from a Canadian metavolcanic belt: Can. Jour. Earth Sci., v. 9, p. 1250-1253.

_____, 1974, On the significance of komatiite: Geology, v. 2, p. 741-748.

Brown, G. M., Holland, J. G., Sigurdsson, H., Tomblin, J. F., and Arculus, R. J., 1977, Geochemistry of the Lesser Antilles volcanic island arc: Geochim. Cosmochim.Acta, v. 41, p. 785-801.

Bruce, E. L., 1926, Geology of McArthur, Bartlett, Douglas and Geikie Townships (Redstone River area), District of Timiskaming: Ont. Dept. Mines, v. 35, p. 37-56 (published 1927). Accompanied by Map 35h, scale 1 inch to 3/4 mile.

Cann, J. R., 1970, Rb, Sr, Y, Zr and Nb in some ocean floor basaltic rocks: Earth Planet. Sci. Let., v. 10, p. 7-11.

Chayes, F., 1964, A petrographic distinction between Cenozoic volcanics in and around the open oceans: Jour. Geophy. Res., v. 69, n. 8, p. 1572-1588.

Clarke, D. B., 1970, Tertiary basalts of Baffin Bay: possible primary magma from the mantle: Contrib. Mineral. Petrol., v. 25, p. 203-224.

_____, 1975, Tertiary basalts dredged from Baffin Bay: Can. Jour. Earth Sci., v. 12, p. 1396-1405.

Condie, K. C., 1976, Trace element geochemistry of Archean greenstone belts: Earth Sci. Reviews, v. 12, p. 353-417.

Deer, R. A., Howie, and Zussman, J., 1974, An introduction to the rock-forming minerals: Longman, London, 528 p.

Delaney, G. D., 1976, A reconnaissance study of the metamorphic petrology and volcanic chemistry of a portion of the Island Lake greenstone belt, Manitoba: Unpublished M. Sc. thesis, Brock University.

Dimroth, E., Boivin, P., Goulet, N., and Laroche, M., 1973, Tectonic and volcanic analytical studies in the Rouyn-Noranda area: Open file rept., Dept. Nat., Rec. Quebec.

Dunbar, W. R., 1948, Structural relations of the Porcupine ore deposits: in structural geology of Canadian ore deposits. Can. Mining and Met. Symposium, p. 442-456.

Engel, A. E. J., Engel, C. G., and Havens, R. G., 1965, Chemical characteristics of oceanic basalts and the upper mantle: Geol. Soc. Am. Bull., v. 76, p. 719-734.

Ewart, A., Bryan, W. B., Gill, J. B., 1973, Mineralogy and geochemistry of the younger volcanic islands of Tonga, S. W. Pacific: Jour. Petrol., v. 14, pt. 3, p. 429-465.

Fairbridge, R. W., 1972, Encyclopedia of geochemistry and environmental sciences, v. 4: Nostrand Reinhold, Toronto, 1321 p.

Ferguson, S. A. et al., 1968, Geology and ore deposits of Tisdale Township: Ont. Dept. Mines Geological Rept. 58.

Flanagan, F. J., 1969, U. S. Geological Survey standards - II. First compilation of data for the new U.S.G.S. rocks: Geochim. Cosmochim. Acta, v. 33, p. 81-120.

Gast, P. W., 1968, Trace element fractionation and origin of tholeiitic and alkaline magma types: Geochim. Cosmochim. Acta., v. 32, p. 1057-1086.

Gelinas, L., Brooks, C., Perrault, G., Carignan, J., Trudel, P., Grasso, F., 1977, Chemo-stratigraphic divisions within the Abitibi volcanic belt, Rouyn-Noranda, Quebec. in: Geol. Assoc. Can. Special Paper 16.

Gill, J. B., 1970, Geochemistry of Viti Levu, and its evolution as an island arc: Contrib. Mineral. Petrol., v. 27, p. 179-203.

_____, 1974, Role of underthrust oceanic crust in the genesis of a Fijian calc-alkaline suite: Contrib. Mineral. Petrol., v. 43, p. 29-45.

Goldich, S. S., 1938, A study in rock-weathering: Jour. Geol., v. 46, p. 17.

Goodwin, A. M., 1973, Archean iron-formations and tectonic basins of the Canadian Shield: Econ. Geol., v. 68, p. 915-933.

_____, 1977, Archean volcanism in Superior Province, Canadian Shield, in: Volcanic regimes in Canada, Geol. Assoc. Can. Special Paper 16.

Grant, R. W. E., 1977, Geochemistry of metavolcanic rocks of the Timmins region, northwestern Ontario: Unpublished M. Sc. thesis, Laurentian University, Sudbury, Ont.

Green, D. H., 1975, Genesis of Archean peridotitic magmas and constraints on Archean geothermal gradient and tectonics: Geology, v. 3, n. 1, p. 15-18.

Green, D. H., Nicholls, I. A., Viljoen, M. I., and Viljoen, R. D., 1975, Experimental demonstration of the existence of peridotitic liquids in early Archean magmatism: Geology, v. 3, n. 1, p. 11-14.

Green, N. L., 1975, Archean glomeroprphyritic basalts: Can. Jour. Earth Sci., v. 12, n. 12, p. 1770-1784.

Hallberg, J. A., 1972, Geochemistry of Archean volcanic belts in the Eastern Goldfields region of Western Australia: Jour. Petrol., v. 13, pt. 1, p. 45-56.

Hallberg, J. A., Carter, D. W., and West, K. N., 1976, Archean Volcanism and sedimentation near Meekatharra, Western Australia: Precambrian Research, v. 3, p. 577-595.

Hallberg, J. A., Johnston, C., Bye, S. M., 1976, The Archean Marda igneous complex, Western Australia : Precambrian Research, v. 3, p. 111-136.

Hart, S. H., 1969, K, Rb, Cs contents and K/Rb, K/Cs ratios of fresh and altered submarine basalts: Earth Planet. Sci. Let., v. 6, p. 295-303.

Hawkesworth, C. J., O'Nions, R. K., 1977, The petrogenesis of some Archean volcanic rocks from southern Africa: Jour. Petrol., v. 18, pt. 3, p. 487-520.

Hopkins, P. E., 1912, Notes on McArthur Township: Ontario Bureau of Mines, v. 21, n. 2, p. 278-280.

_____, 1924, Notes on gold in McNeil and other Townships: Ont. Dept. Mines, v. 33, pt. 3, p. 37-40.

Hyndman, D. W., 1972, Petrography of igneous and metamorphic rocks: McGraw-Hill, New York, 532 p.

Irvine, T. N., and Baragar, W. R. A., 1971, A guide to the chemical classification of the common volcanic rocks: Can. Jour. Earth Sci., v. 8, p. 523-548.

Johannes, W., 1969, An experimental investigation of the system $MgO-SiO_2-H_2O-CO_2$: Am. J. Sci., v. 267, p. 1083-1104.

Jolly, W. T., 1975, Subdivision of the Archean lavas of the Abitibi area, from Fe-Mg-Ni-Cr relations: Earth Planet. Sci. Let., v. 27, p. 200-210.

_____, 1977, Metamorphic history of the Archean Abitibi belt. in: Volcanic regions in Canada, Geol. Assoc. Can. Special Paper 16.

_____, 1978, Development and degradation of Archean lavas, Abitibi area, Canada, in light of major element Geochemistry: in press.

Kamp, P. C. van de, 1970, The green beds of the Scottish Dalradian series: geochemistry, origin, and metamorphism of mafic sediments: Jour. Geol., v. 78, p. 281-303.

Kretz, R., 1972, Potassium: element and geochemistry. in: The encyclopedia of geochemistry and environmental sciences., v. 4A, edited by: R. W. Fairbridge, Van Nostrand Reinhold, Toronto, p. 970-972.

Krogh, T. E., and Davis, G. L., 1971: Zircon U-Pb ages of Archean metavolcanic rocks in the Canadian Shield: Carnegie Inst. Wash. Geophysical Laboratory Annual Rept. 1970-1971, p. 241-270.

Kushiro, I., 1972, Effect of water on the composition of magmas formed at high pressures: Jour. Petrol., v. 33, p. 311-334.

Lundegardh, P. H., 1947, Some aspects to the determination and distribution of zinc: Ann. Roy. Agricult. Coll. Sweden, v. 15, p. 1.

MacDonald, G. A., 1968, Composition and origin of Hawaiian lava: Geol. Soc. Am., v. 60, p. 1541-1596.

Melson, W. G., and Thompson, G., 1970, Layered basic complexes in oceanic crust, Romanche Fracture, Equatorial Atlantic Ocean: Science, v. 168, p. 817-820.

Miyashiro, A., 1975, Volcanic rock series and tectonic setting: Annual Review of Earth and Planetary Sciences, v. 3, p. 251, 269.

Moorhouse, W. W., 1959, The study of rocks in thin section: Harper & Row, Publishers, New York, 514 p.

Naldrett, J., and Cabri, L. J., 1976, Ultramafic and related mafic rocks: their classification and genesis with special reference to the concentration of nickel sulfides and platinum-group elements: Econ. Geol., v. 71, p. 1131-1158.

Naldrett, A. J., Goodwin, A. M., Fisher, T. L., and Ridler, R. H., 1978, The sulfur content of Archean volcanic rocks and a comparison with ocean floor basalts: Can. Jour. Earth Sci., v. 15, n. 5, p. 715-728.

Naqvi, S. M., and Hussain, S. M., 1973, Relation between trace and major element composition of the Chitaldrug metabasalts, Mysore, India, and the Archean mantle: Chem. Geol., v. 11, p. 17-31.

Nesbitt, R. W., 1971, Skeletal crystal forms in the ultramafic rocks of the Yilgarn block, western Australia; evidence for an Archean ultramafic liquid: Geol. Soc. Australia Spec. Pub., v. 3, p. 331-347.

Nesbitt, R. W., and Sun, S., 1976, Geochemistry of Archean spinifex-textured peridotites and magnesian and low magnesian tholeiites: Earth Planet. Sci. Let., v. 31, p. 433-453.

Nisbet, E. G., Bickle, M. J., Martin, A., 1977, The mafic and ultramafic lavas of the Belingwe greenstone belt, Rhodesia: Jour. Petrol., v. 18, pt. 4, p. 521-566.

Osborn, E. F., 1959, Role of oxygen pressure in the crystallization and differentiation of basaltic magma: Am. Jour. Sci., v. 257, p. 609-647.

_____, 1962, Reaction series for subalkaline igneous rocks based on different oxygen pressure conditions: Am. Mineral., v. 47, ns. 3 and 4, p. 211-226.

Payne, C. W. C., 1978, Petrography, geochemistry and structure of the Timmins area, Ontario: Unpublished M. Sc. thesis, Brock University.

Pearce, J. A., and Cann, J. R., 1971, Ophiolite origin investigated by discriminant analysis using Ti, Zr, and Y: Earth Planet. Sci. Let., v. 19, p. 290-349.

_____, 1973, Tectonic setting of basic volcanic rocks determined using trace element analyses: Earth Planet. Sci. Let., v. 19, p. 290-300.

Pyke, D. R., 1971, McArthur Township, District of Timiskaming: Ont. Dept. Mines and Northern Affairs. prelim. Map p. 631, Geol. Ser., scale 1 inch to 1/4 mile.

_____, 1972, Bartlett Township, District of Timiskaming: Ont. Dept. Mines and Northern Affairs. prelim. Map p. 745, Geol. Ser., scale 1 inch to 1/4 mile.

_____, 1973, Peterlong Lake area, Districts of Timiskaming and Sudbury: Ont. Div. Mines, GR104, 31 p. Accompanied by Map 2253 scale 1 inch to 1/2 mile.

_____, 1974, Timmins area, Districts of Timiskaming and Cochrane: Ont. Div., Mines, Prelim. Map p. 941, Geol. Ser., scale 1 inch to 1 mile.

_____, 1975, On the relationship of gold mineralization and ultra-mafic rocks in Timmins area: Ont. Dept. Mines, Miscellaneous Paper 62.

_____, 1978, Geology of the Peterlong Lake area, District of Timiskaming and Sudbury: Ont. Geol. Sur., Rept. 171.

Pyke, D. R., Naldrett, A. J., and Eckstrand, O. R., 1973, Ultramafic lavas in Munro Township, Ont.: Bull. Geol. Soc. Am., v. 84, p. 55-68.

Rankama, K. and Sahama, T. G., 1968, Geochemistry: University of Chicago Press, Chicago, 912 p.

Seki, Y., Oki, Y., Matsuda, T., Mikami, K., and Okumura, K., 1969, The metamorphism in the Tanzawa Mountains, central Japan: Jour. Japan Assoc. Min. Pet. Econ. Geol., v. 61, n. 1, p. 1-24.

Siever, R., 1972, Silica and silicate in weathering. in: Handbook of geo-chemistry, editors: Wedepohl, K. H., Correns, C. W., Shaw, D. M., Zemann, J.: Springer-Verlag, New York. p. 14-G-1.

Smith, R. E., 1968, Redistribution of major elements in the alteration of some basic lavas during burial metamorphism: Jour. Petrol., v. 9, pt. 2, p. 191-219.

Spence, C. D., and de Rosen-Spence, A. F., 1975, The place of sulfide miner-alization in the volcanic sequence at Noranda: Econ. Geol., v. 70, p. 90-101.

Stanton, R. L., 1972, Ore petrology: McGraw-Hill, New York, 713 p.

Sun, S. S., and Nesbitt, R. W., 1977, Chemical heterogenity of the Archean mantle, composition of the earth and mantle evolution: Earth Planet. Sci. Let., v. 35, p. 429-448.

_____, 1978, Petrogenesis of Archean ultramafic and basic volcanics: evidence from rare earth elements: Contrib. Mineral. Petrol., v. 65, p. 301-325.

Turner, F. J., 1968, Metamorphic petrology, mineralogical and field aspects: McGraw-Hill, Toronto, 403 p.

Viljoen, M. J., and Viljoen, R. D., 1969, The geology and geochemistry of the lower ultramafic unit of the Onverwacht Group and a proposed new class of igneous rock: Geol. Soc. South Africa Spec. Pub., v. 2, p. 55-85.

Vogt, J. H. L., 1931, On the average composition of the Earth's crust, with particular reference to the contents of phosphoric and titanic acid: Skrifter Norske Videnskaps-Akad. Oslo, I. Mat.-naturv. Klasse, n. 7.

Watkins, N. D., Gunn, B. M., and Coy-yll, R., 1970, Major and trace element variations during the initial cooling of an Icelandic lava: Am. Jour. Sci., v. 268, p. 21-49.

Wedepohl, K. H., Correns, C. W., Shaw, D. M., Turekian, K. K., and Zeman, J., 1969, Handbook of Geochemistry: Springer-Verlag, New York, v. 2, pt. 1.

_____,
1970, Handbook of Geochemistry: Springer-Verlag, New York, v. 2, pt. 2.

_____,
1972, Handbook of Geochemistry: Springer-Verlag, New York, v. 2, pt. 3.

_____,
1974, Handbook of Geochemistry: Springer-Verlag, New York, v. 2, pt. 4.

Williams, D. A. C., 1972, Archean ultramafic, mafic and associated rocks, Mt. Monger, Western Australia: Geol. Soc. Australia Jour., v. 19, p. 163-188.

Winkler, H. G. F., 1974, Petrogenesis of metamorphic rocks: Springer-Verlag, New York, 320 p.

APPENDICES

SAMPLE NO.	14	16	17	13	19	224	226	228	230	232
MAJOR OXIDES (Wt %)										
SIO2	46.67	41.28	44.40	51.49	42.45	41.62	42.95	42.38	43.82	42.54
AL2O3	8.72	3.53	7.06	8.56	5.41	6.59	6.85	8.35	7.81	8.56
FE2O3	9.83	6.62	12.34	9.48	9.85	10.19	11.04	11.36	11.32	11.59
MGO	22.70	18.45	16.62	19.05	30.70	22.96	22.64	23.59	23.27	22.24
CAO	8.02	12.53	12.34	7.33	5.41	5.92	5.74	5.83	6.61	6.65
NA2O	ND	0.43	0.63	0.46	0.50	0.33	0.59	ND	ND	0.17
K2O	0.04	0.04	0.12	0.06	0.02	0.04	0.11	0.02	0.02	0.04
TIO2	0.41	0.22	0.36	0.58	0.43	0.33	0.36	0.52	0.49	0.42
MNO	0.07	0.22	0.12	0.02	0.15	0.07	0.06	ND	ND	ND
P2O5	0.04	0.03	0.16	0.01	0.01	0.05	0.09	0.04	0.07	0.03
LOI	5.37	9.32	4.90	1.85	6.70	11.35	7.41	7.10	6.46	5.99
TOTAL	101.88	99.19	99.89	98.95	101.63	99.45	97.84	99.19	99.81	99.24
TRACE ELEMENTS (PPM)										
BA	50.3		72.5	124.2		28.6	77.6		38.1	47.7
CO	6.3		ND	ND		5.9	9.3		8.0	20.3
CU	3.3		10.5	23.9		18.6	3.7		3.5	77.0
NI	1197.5		254.0	976.0		1408.9	1546.4		1303.7	1267.0
RB	ND		0.3	ND		ND	9.6		0.7	ND
SR	26.4		850.0	1315.0		56.0	1288.0		47.0	54.0
GA	ND		64.3	34.7		33.4	11.7		5.3	23.0
Y	5.0		1.1	5.5		1.1	0.2		7.5	3.5
ZN	63.4		40.9	29.2		59.0	56.2		35.2	54.1
ZR	40.8		25.1	25.6		22.5	21.4		22.5	21.7
NORMATIVE MINERALS										
Q	0.00	U	0.00	1.04	0.00	0.00	0.00	0.00	0.00	0.00
OR	0.24	N	0.71	0.35	0.12	0.24	0.65	0.12	0.12	0.24
AB	0.00	D	5.33	3.89	4.23	2.79	4.99	0.00	0.00	1.44
AN	23.69	E	18.53	21.11	12.45	15.38	15.71	22.72	21.24	22.47
NE	0.00	R	0.00	0.00	0.00	0.00	0.00	0.00	0.00	0.00
C	0.00		0.00	0.00	0.00	0.00	0.00	0.00	0.00	0.00
OPX	12.67	S	34.11	12.42	11.50	10.20	9.83	4.77	8.95	7.96
CPX	37.51	A	5.79	56.24	10.36	25.31	26.06	31.22	33.47	30.59
OL	20.63	T	28.72	0.00	54.54	30.58	31.44	31.29	27.68	28.56
MT	2.77	U	2.70	3.02	2.80	2.65	2.70	2.93	2.89	2.89
IL	0.78	R	0.68	1.10	0.82	0.63	0.63	0.99	0.93	0.93
HM	0.01	A	0.00	0.01	0.01	0.00	0.00	0.01	0.01	0.01
AP	0.10	T	0.24	0.02	0.02	0.10	0.19	0.10	0.14	0.19
		Z								
		D								
GRID REFERENCE	733375	733374	733377	733374	734372	733372	733372	730370	731370	731368

FeO* Total Fe as FeO
ND Not detected
Appendix I. Geochemical analyses and CIPW normative calculations of the Donut Lake Formation.

SAMPLE NO.	264	266	268
MAJOR OXIDES (Wt.%)			
SIO2	41.62	41.21	40.95
AL2O3	6.01	5.85	6.30
FEO*	10.32	9.79	9.53
MGO	26.23	26.37	27.32
CAO	4.99	10.89	5.25
NA2O	0.43	0.15	ND
K2O	0.04	0.02	0.03
TIO2	0.38	0.33	0.31
MNO	ND	0.03	0.02
P2O5	0.03	0.02	0.05
LOI	8.14	6.69	12.82
TOTAL	98.19	101.35	102.58
TRACE ELEMENTS (PPM)			
BA	0.4		7.8
CR	10.4		17.2
CU	3.2		5.6
NI	1654.4		1501.0
RB	ND		1.8
S	111.0		26.6
SR	ND		28.9
Y	2.9		1.7
ZN	47.8		56.4
ZR	19.5		20.8
NORMATIVE MINERALS			
Q	0.00	U	0.00
OR	0.24	N	0.18
AB	3.54	D	0.00
AN	14.35	E	17.10
NE	0.00	R	0.00
C	0.00		0.00
OPX	8.16	S	6.87
OLX	21.42	A	23.68
CC	40.63	T	40.41
MT	2.73	U	2.62
IL	0.72	R	0.59
PY	0.00	A	0.00
AP	0.07	T	0.12
		E	
		D	
GRID REFERENCE	730374	731373	734357

FeO*   Total Fe as FeO

ND   Not detected

Appendix I (continued).   Geochemical analyses and CIPW normative calculations of the Donut Lake Formation.

SAMPLE NO.	32	34	36	38	39	40	41	42	43	91
MAJOR OXIDES (wt.%)										
SIO2	43.88	41.88	53.04	49.05	50.98	54.51	47.07	47.71	50.65	49.15
AL2O3	12.12	14.47	13.42	14.12	13.89	14.25	16.22	15.53	16.90	13.02
FEO*	25.19	16.12	9.55	10.96	14.23	9.56	11.52	10.12	10.06	16.63
MGO	3.08	5.63	3.01	4.35	5.08	3.92	7.96	4.21	5.60	3.19
CAO	9.22	15.74	6.30	17.11	8.32	8.93	11.84	17.43	8.66	6.55
NA2O	ND	0.17	5.20	0.26	2.58	3.29	1.58	0.05	4.76	6.15
K2O	0.43	0.27	0.06	0.05	0.53	0.64	0.50	0.05	0.19	0.05
TIO2	2.40	0.88	2.78	0.90	1.27	1.29	0.65	0.84	0.86	1.72
MGO	ND	0.22	ND	0.03	ND	ND	0.09	0.03	0.03	0.31
P2O5	0.59	0.09	0.74	0.06	0.08	0.17	0.08	0.10	0.06	0.27
LOI	1.12	3.62	3.61	3.18	3.25	3.07	3.21	3.18	1.55	8.55
TOTAL	98.03	99.09	99.71	100.07	100.21	99.63	100.72	99.25	99.31	100.22
TRACE ELEMENTS (PPM)										
BA	195.3	49.2	65.2	84.2	145.0	297.3	215.8	45.5	99.7	103.7
CE	ND	ND	32.6	ND	ND	6.1	2.3	ND	ND	ND
CU	27.2	ND	0.4	37.0	85.0	73.2	82.8	ND	ND	11.8
NI	3.1	91.1	47.0	72.5	70.0	77.1	255.0	89.7	39.7	20.2
RB	5.2	3.1	ND	ND	3.9	15.3	17.6	2.7	ND	2.1
S	1155.0	51.5	668.9	48.8	965.0	13.0	20.0	285.0	ND	410.0
SR	43.0	727.6	76.7	25.2	126.9	169.6	146.4	145.7	175.4	197.6
Y	13.2	10.7	21.3	9.8	11.6	15.3	6.2	7.9	4.1	12.8
ZN	109.3	72.9	51.1	90.7	82.5	65.4	64.2	45.4	47.9	97.6
ZR	48.5	112.2	127.3	36.3	65.3	73.3	46.5	52.7	60.2	95.7
NORMATIVE MINERALS										
Q	3.95	0.00	7.27	7.00	2.34	6.99	0.00	5.40	0.00	17.78
OR	2.54	1.80	0.35	0.30	3.13	3.79	2.95	0.30	1.06	0.30
AB	0.00	1.44	43.99	2.20	21.83	27.83	13.37	0.42	36.48	1.27
AN	31.79	37.91	13.09	37.20	24.74	22.22	35.68	41.99	24.21	32.22
NE	0.00	0.00	0.00	0.00	0.00	0.00	0.00	0.00	2.05	0.00
C	0.00	0.00	0.00	0.00	0.00	0.00	0.00	0.00	0.00	0.91
CPX	8.79	33.53	11.14	39.80	13.52	17.57	18.65	36.82	15.27	0.00
OPX	42.18	1.96	11.35	7.53	27.58	14.10	11.92	7.32	0.00	33.51
OL	0.00	15.94	0.00	0.00	0.00	0.00	12.51	0.00	15.85	0.00
MT	5.65	3.45	6.21	3.48	4.02	4.05	3.12	3.39	3.42	4.67
IL	4.57	1.67	5.29	1.71	2.42	2.45	1.24	1.60	1.64	3.27
RU	0.03	0.01	0.03	0.01	0.02	0.02	0.01	0.01	0.01	0.02
AP	1.41	0.22	1.77	0.14	0.19	0.41	0.19	0.24	0.14	0.65
GRID REFERENCE	750383	749336	748386	751393	753407	753406	753405	751412	753416	803372

FeO*   Total Fe as FeO

ND   Not detected

Appendix I. Geochemical analyses and CIPW normative calculations of the Redstone Formation.

SAMPLE NO.	189	191	192	199	201	203	209	211	213	221
MAJOR OXIDES (wt.%)										
SIO2	47.92	47.28	49.59	50.20	50.33	45.24	52.47	48.84	46.94	49.07
AL2O3	14.31	12.46	14.69	14.19	15.74	16.68	13.49	13.59	14.06	14.72
FEO*	16.09	19.42	12.74	11.89	10.10	12.80	14.11	16.05	16.68	7.52
MGO	6.65	5.85	7.05	8.07	8.44	5.00	4.55	5.91	7.17	6.01
CAO	9.03	9.19	10.09	8.58	7.52	17.04	11.12	12.01	9.70	9.94
NA2O	2.98	0.00	1.53	3.02	2.14	0.97	1.03	0.49	0.00	1.20
K2O	0.40	0.18	0.49	0.68	1.00	0.09	0.36	0.33	0.25	0.65
TIO2	1.22	2.15	0.90	0.77	0.38	0.96	1.35	1.38	1.30	0.98
MNO	0.10	0.77	0.19	0.20	0.06	0.13	0.00	0.02	0.67	0.15
P2O5	0.03	0.15	0.09	0.13	0.06	0.09	0.09	0.11	0.12	0.07
LOI	1.46	0.47	1.24	2.04	3.53	1.55	1.11	1.12	1.00	1.23
TOTAL	100.24	97.92	98.65	99.77	99.44	100.55	99.69	99.86	97.89	95.53
TRACE ELEMENTS (PPM)										
BA	91.1	133.9	200.2	173.8	158.9	66.9	154.8	115.6	64.3	134.7
CE	ND	ND	ND	ND	14.5	ND	ND	ND	ND	ND
CU	32.5	10.6	38.2	60.0	26.9	17.4	ND	114.8	ND	3.4
NI	61.7	30.7	108.9	161.0	136.6	98.7	48.7	42.2	74.8	93.2
RB	5.5	3.6	13.6	15.8	26.1	1.4	3.6	4.2	1.3	14.9
S	420.0	579.2	79.0	111.0	12.0	380.0	20.0	1145.0	32.0	77.5
SR	115.2	44.0	70.5	128.3	115.2	162.9	83.9	41.7	45.2	117.4
Y	10.8	7.4	9.0	9.1	8.9	7.7	12.4	9.9	13.0	12.5
ZN	77.7	32.2	70.4	75.9	61.7	53.4	79.4	103.7	153.5	77.2
ZR	58.9	39.5	49.6	52.8	41.7	58.1	56.8	53.1	52.6	51.0
NORMATIVE MINERALS										
Q	0.00	7.76	1.45	0.00	0.00	0.00	10.09	4.58	5.03	2.45
OR	2.36	1.06	2.90	4.02	5.91	0.53	2.13	1.95	1.45	3.84
AB	25.21	0.00	13.37	25.55	18.10	6.87	8.71	4.15	0.00	10.15
AN	24.43	33.45	31.53	23.14	30.38	40.88	31.11	33.90	37.41	32.82
NE	0.00	0.00	0.00	0.00	0.00	0.72	0.00	0.00	0.00	0.00
C	0.00	0.00	0.00	0.00	0.00	0.00	0.00	0.00	0.00	0.00
CPX	16.66	9.47	14.94	15.37	5.38	36.29	19.88	21.08	8.17	13.50
OPX	5.31	38.89	30.07	14.17	32.86	0.00	22.65	28.95	39.95	31.20
OL	20.97	0.00	0.00	12.52	1.38	10.51	0.00	0.00	0.00	0.00
MT	3.94	5.29	3.48	3.29	2.73	3.57	4.13	4.16	4.06	5.80
IL	2.32	4.09	1.71	1.46	0.72	1.03	2.57	2.63	2.47	1.86
RU	0.02	0.03	0.01	0.01	0.00	0.01	0.02	0.02	0.02	0.01
AP	0.19	0.36	0.22	0.31	0.14	0.22	0.22	0.26	0.29	0.17
GRID REFERENCE	742410	764411	748413	746416	744413	736416	768389	769388	768387	751393

FeO*   Total Fe as FeO
ND   Not detected
Appendix I (continued).   Geochemical analyses and CIPW normative calculations of the Redstone Formation.

SAMPLE NO.	20	21	25	26	27	28	45	53	92	164
MAJOR OXIDES (WT.%)										
SIO2	59.40	65.70	55.98	62.81	62.39	60.96	57.66	48.72	51.35	57.25
AL2O3	13.33	14.44	12.90	14.35	12.92	14.37	14.00	17.35	14.83	15.47
FEO*	6.95	5.36	9.91	7.23	6.69	6.02	8.75	16.55	12.69	9.56
MGO	3.33	2.25	2.50	2.81	6.60	2.61	5.32	2.76	1.33	2.71
CAO	4.84	3.37	7.13	3.39	3.20	6.02	3.82	4.48	10.06	6.56
NA2O	2.06	3.89	2.77	3.52	2.61	2.13	5.81	2.24	ND	1.92
K2O	0.88	1.26	0.49	0.93	0.35	1.10	0.29	0.72	0.93	0.92
TIO2	0.55	0.57	0.48	0.53	0.43	0.62	0.67	0.65	0.53	0.65
MNO	0.11	0.05	0.11	0.03	0.77	0.03	0.14	0.02	0.23	0.14
P2O5	0.11	0.15	0.16	0.17	0.12	0.14	0.20	0.19	0.19	0.30
LOI	6.43	4.54	7.41	4.52	4.25	4.96	1.68	4.07	11.18	3.30
TOTAL	98.06	101.57	99.64	100.31	100.33	98.96	98.34	97.75	100.92	98.77
TRACE ELEMENTS (PPM)										
BA	173.9	238.8	46.9	144.4	129.3	525.7	133.0	100.6	120.6	691.0
CE	2.6	29.5	30.5	89.4	94.1	95.9	40.2	ND	ND	61.2
CU	12.8	27.2	17.4	54.4	40.3	9.8	5.0	4.5	9.8	37.6
NI	273.1	234.8	109.8	78.4	335.4	82.9	156.6	17.4	6.1	117.1
RB	32.4	43.5	6.1	33.4	13.2	32.3	2.6	14.2	20.6	26.5
S	47.5	3.0	47.5	21.0	283.0	51.5	1.0	1.0	22.0	2400.0
SR	160.8	223.5	75.3	144.9	134.4	218.2	192.2	56.5	110.5	854.5
Y	9.3	6.7	0.8	9.8	6.7	9.0	7.4	7.6	8.4	10.0
ZN	86.3	62.1	81.8	84.0	99.1	60.4	58.2	112.3	53.7	124.5
ZR	113.6	137.4	113.2	142.9	85.5	127.7	121.2	89.2	99.7	186.3
NORMATIVE MINERALS										
Q	24.38	24.89	15.37	22.91	24.96	24.75	2.60	7.23	15.53	25.46
OR	5.20	7.45	2.90	5.50	2.07	6.50	1.71	4.26	5.50	5.32
AB	17.43	32.82	23.43	29.78	22.03	18.02	49.15	18.95	0.00	16.24
AN	23.29	15.74	21.31	15.71	15.09	26.39	11.26	20.99	29.52	30.50
NE	0.00	0.00	0.00	0.00	0.00	0.00	0.00	0.00	3.00	0.00
C	0.45	0.92	0.00	1.79	2.71	0.00	0.00	5.19	0.00	0.11
OPX	0.00	0.00	11.16	0.00	0.00	2.14	5.30	0.00	16.61	0.10
CPX	16.50	12.80	15.80	17.76	16.44	13.71	23.80	34.41	15.98	21.45
OL	0.00	0.00	0.00	0.00	0.00	0.00	0.00	0.00	0.00	0.00
MT	2.97	3.00	2.87	2.94	2.30	3.07	3.15	3.12	2.94	3.12
IL	1.05	1.08	0.91	1.01	0.82	1.18	1.27	1.24	1.01	1.24
HM	0.01	0.01	0.01	0.01	0.01	0.01	0.01	0.01	0.01	0.01
AP	0.26	0.36	0.38	0.41	0.29	0.34	0.43	0.46	0.46	0.72
GRID REFERENCE	778403	778402	784404	784404	787412	783388	751427	750430	804373	805394

FeO*   Total Fe as FeO
ND   Not detected

Appendix I (continued).   Geochemical analyses and CIPW normative calculations of the Boomerang Formation.

SAMPLE NO.	115	116	117	171	175	176	180	194
MAJOR OXIDES (Wt.%)								
SIO2	65.42	60.50	54.41	68.63	57.58	56.06	49.96	60.99
AL2O3	16.42	14.76	12.42	14.13	12.35	13.07	12.50	14.87
FEO*	4.39	5.03	10.55	6.24	5.52	7.70	12.22	8.52
MGO	1.12	3.84	2.92	1.02	2.19	3.46	4.46	3.57
CAO	0.81	3.38	6.08	0.29	9.40	7.78	8.65	1.83
NA2O	8.75	4.85	1.85	1.36	4.11	2.44	1.46	4.59
K2O	0.46	0.08	0.80	2.67	0.77	0.79	0.10	0.68
TIO2	0.52	0.57	0.60	0.34	0.88	0.68	0.58	0.76
MNO	0.22	0.16	0.07	0.05	0.55	0.23	0.15	0.11
P2O5	0.15	0.12	0.16	0.13	0.17	0.12	0.14	0.18
LOI	1.65	4.58	8.01	2.66	9.55	8.41	10.00	3.33
TOTAL	99.91	98.87	97.87	97.72	100.07	100.74	100.22	99.23
TRACE ELEMENTS (PPM)								
BA	106.7	46.3	175.4	506.7	219.2	250.2	60.6	167.8
CE	93.0	115.6	110.0	128.3	105.0	94.9	99.5	136.3
CU	15.8	293.8	100.9	40.9	225.6	131.1	271.3	113.5
NI	15.3	5.1	10.4	ND	8.5	6.9	8.0	10.7
RB	15.0	11.0	39.0	82.5	ND	ND	34.8	14.0
S	12.0	70.5	117.4	54.8	52.7	74.2	92.3	58.8
SR	304.7	142.6	23.7	254.5	3.8	8.4	21.0	97.2
Y	4.3	179.7	87.2	ND	51.1	140.2	206.5	94.1
ZN	47.0	3.9	13.2	66.5	25.0	24.6	ND	14.3
ZR	148.3	48.2	7.2	41.8	46.6	53.7	ND	40.5
NORMATIVE MINERALS								
Q	7.27	15.53	16.76	44.46	8.77	15.53	10.49	17.42
OR	2.72	0.47	4.73	15.78	4.55	4.67	0.59	4.02
AB	74.02	41.03	15.65	11.51	34.77	20.64	12.35	38.83
AN	3.04	15.99	25.94	0.59	12.97	22.37	27.25	7.20
NE	0.00	0.00	0.00	0.00	0.00	0.00	0.00	6.00
C	0.41	0.83	0.00	0.78	0.00	0.00	0.00	3.68
CPX	0.00	0.00	2.71	0.00	24.39	12.93	12.47	0.00
OPX	8.33	17.99	22.55	11.92	0.00	13.40	24.59	21.06
OL	0.00	0.00	0.00	0.00	0.00	0.00	0.00	0.00
MT	2.93	3.00	3.04	2.67	3.45	3.16	3.02	3.28
IL	0.99	1.08	1.14	0.65	1.67	1.29	1.10	1.45
RU	0.01	0.01	0.01	0.00	0.01	0.01	0.01	0.01
AP	0.36	0.29	0.38	0.31	0.41	0.29	0.34	0.43
GRID REFERENCE	805390	805372	805372	812359	794358	795355	396352	737433

FeO*   Total Fe as FeO

ND   Not detected

Appendix I (continued).   Geochemical analyses and CIPW normative calculations of the Boomerang Formation.

SAMPLE NO.	62	64	66	69	120	124	129	138	140	1-5
MAJOR OXIDES (wt.%)										
SiO2	41.38	41.03	41.67	43.85	46.97	41.46	41.84	39.39	42.09	45.63
AL2O3	5.70	4.75	6.33	8.01	3.43	6.79	5.48	8.28	5.52	6.65
FEO*	12.05	10.30	10.55	9.62	2.08	10.29	12.17	13.35	9.31	10.72
MGO	28.69	30.96	27.05	26.18	30.02	29.26	27.31	14.30	28.02	24.91
CAO	4.27	3.93	6.22	6.24	7.77	5.76	5.08	7.06	3.68	2.57
NA2O	ND	0.01	0.39	ND	0.57	ND	ND	0.37	0.25	ND
K2O	0.01	0.01	0.04	0.02	0.02	0.12	0.02	0.04	0.02	0.02
TIO2	0.45	0.42	0.39	0.51	0.16	0.32	0.35	0.43	0.34	0.47
MNO	0.47	0.07	0.09	0.05	ND	0.09	ND	ND	0.03	ND
P2O5	0.02	0.01	0.03	0.01	ND	0.07	0.06	0.04	0.03	0.05
LOI	8.93	10.10	7.52	6.73	7.48	7.27	5.90	11.45	3.54	5.92
TOTAL	101.98	101.59	100.22	101.22	98.49	100.93	98.21	100.22	97.83	99.94
TRACE ELEMENTS (PPM)										
BA		ND	29.9	9.1	ND	3.5	46.9	39.3	13.0	ND
CE		53.2	9.5	22.1	38.4	12.7	ND	5.0	31.4	22.8
CU		27.0	23.3	37.5	330.7	9.3	5.0	2.5	7.2	11.9
NI		1688.0	1429.5	1270.7	1350.9	1509.5	1615.7	912.5	1661.2	1641.0
RB		ND	ND	ND	ND	1.9	ND	ND	2.1	ND
S		301.0	300.0	119.0	32.0	371.0	81.5	11.0	15.0	275.0
SR		3.6	10.8	10.5	4.6	6.8	10.4	47.2	32.6	22.4
Y		2.0	0.2	ND	3.8	0.5	ND	4.6	0.3	3.0
ZN		59.8	55.3	53.7	55.0	64.0	48.9	68.3	67.2	60.3
ZR		21.9	21.5	23.9	40.2	22.6	17.8	26.7	23.7	22.1
NORMATIVE MINERALS										
Q	0.00	0.00	0.00	0.00	0.00	0.00	0.00	0.00	0.00	0.00
OR	0.06	0.06	0.24	0.12	0.06	0.71	0.12	0.24	0.06	0.12
AB	0.00	0.08	3.30	0.00	4.82	0.00	0.00	7.36	2.11	0.00
AN	13.52	12.88	15.40	21.79	6.77	18.17	14.89	18.56	15.88	12.42
NE	0.00	0.00	0.00	0.00	0.00	0.00	0.00	0.00	0.00	0.00
C	0.00	0.00	0.00	0.00	0.00	0.00	0.00	0.00	0.00	2.07
CPX	4.43	5.22	12.19	7.26	24.88	5.46	7.95	13.12	3.33	0.00
OPX	24.53	22.29	12.60	29.58	25.34	17.81	25.32	5.31	31.10	62.38
OL	46.28	49.21	47.30	33.81	28.15	49.34	42.41	42.42	37.19	12.13
MT	2.83	2.78	2.74	2.91	2.41	2.64	2.68	2.80	2.67	2.86
IL	0.86	0.85	0.74	0.97	0.30	0.61	0.67	0.61	0.65	0.89
RU	0.01	0.01	0.00	0.01	0.00	0.00	0.01	0.00	0.00	0.01
AP	0.05	0.02	0.07	0.02	0.00	0.17	0.14	0.10	0.07	0.12
GRID REFERENCE	799413	799414	300415	798417	829403	833400	628399	836384	836385	83338-

FeO* Total Fe as FeO
ND Not detected
Appendix I (continued). Geochemical analyses and CIPW normative calculations of the Donut Lake Formation.

SAMPLE NO.	153	C₂ 247	SF 243	S 249	C₁ 250	C₁ 252	S 253	SF 254	SF 255	S 256
MAJOR OXIDES (wt.%)										
SIO2	37.43	41.89	44.67	41.36	43.38	45.04	41.10	39.83	41.35	44.01
AL2O3	3.42	5.69	6.90	12.10	11.54	6.59	11.88	3.65	4.01	5.61
FEO*	7.81	14.41	10.65	14.72	12.49	7.28	13.55	8.70	8.54	11.73
MGO	30.74	24.30	25.56	17.82	19.27	26.73	18.75	28.43	30.09	22.73
CAO	3.15	4.86	7.39	6.55	6.51	7.35	6.37	3.14	2.45	5.50
NA2O	0.31	0.06	0.56	0.93	0.78	0.67	1.57	0.25	0.55	0.03
K2O	0.04	0.01	0.04	0.02	0.02	0.03	0.02	0.02	0.02	0.02
TIO2	0.16	0.46	0.34	0.72	0.64	0.35	0.66	0.26	0.30	0.46
MNO	0.10	0.11	0.03	ND	0.11	0.11	ND	0.04	0.09	ND
P2O5	0.04	ND	0.01	0.01	ND	0.02	ND	0.03	0.01	ND
LOI	15.45	7.19	5.75	5.27	5.26	5.94	5.73	13.41	12.01	7.76
TOTAL	98.65	98.98	101.90	99.50	100.00	100.11	99.63	97.76	99.82	97.84
TRACE ELEMENTS (PPM)										
BA	5.7	35.7	31.3	45.4	9.2	13.2	13.6	ND	ND	17.5
CE	31.9	0.8	ND	ND	ND	22.8	ND	33.3	23.3	ND
CU	1.8	7.0	29.3	2.4	10.3	47.1	4.2	6.5	3.9	47.2
NI	2121.9	1448.0	1268.7	753.6	983.7	1366.7	857.0	2003.0	1946.1	1445.3
RB	ND	ND	ND	ND	ND	ND	1.5	ND	ND	3.1
S	500.0	305.0	310.0	19.0	43.2	103.0	18.0	181.0	140.0	1750.0
SR	84.0	1.7	14.8	17.3	22.8	10.7	8.2	80.7	84.7	21.7
Y	1.3	ND	0.8	3.2	3.5	5.5	6.6	0.6	ND	5.6
ZN	52.4	49.2	36.7	88.4	54.2	41.6	57.0	62.3	57.9	49.6
ZR	30.5	12.0	13.2	26.3	28.1	19.6	19.2	27.9	22.6	18.1
NORMATIVE MINERALS										
Q	0.00	0.00	0.00	0.00	0.00	0.00	0.00	0.00	0.00	0.00
CR	0.24	0.06	0.24	0.12	0.12	0.13	0.12	0.12	0.12	0.11
AB	2.62	0.51	4.74	7.87	6.60	5.67	13.18	2.11	4.65	0.25
AN	7.82	15.22	16.19	28.77	27.92	14.88	25.35	8.77	8.41	15.11
NE	0.00	0.00	0.00	0.00	0.00	0.00	0.00	0.00	0.00	0.00
C	0.00	0.00	0.00	0.00	0.00	0.00	0.00	0.00	0.00	0.00
CPX	5.99	7.17	16.29	2.98	3.54	17.02	5.09	5.25	2.92	9.16
OPX	13.32	30.32	17.80	12.83	22.84	17.39	0.00	27.75	26.21	32.64
OL	51.98	36.67	38.34	39.28	31.45	36.52	47.95	38.45	44.01	20.45
MT	2.41	2.94	2.67	3.22	3.10	2.68	3.13	2.551	2.61	2.84
IL	0.30	0.88	0.65	1.37	1.22	0.67	1.26	0.49	0.57	0.88
RU	0.00	0.01	0.00	0.01	0.01	0.00	0.01	0.00	0.00	0.01
AP	0.10	0.00	0.02	0.02	0.00	0.05	0.00	0.07	0.02	0.00
GRID REFERENCE	827386	799416	799416	799416	799416	799416	799416	827386	827386	827386

FeO* Total Fe as FeO   C₁ Upper chilled margin   S Spinifex zone
ND Not detected   C₂ Lower chilled margin   SF Spinifex-free zone

Appendix I (continued). Geochemical analyses and CIPW normative calculations of the spinifex-textured flows within the Goose Lake Formation (with the exception of 153).

SAMPLE NO.	C_2 258	SF 259	S 260	C_1 262
MAJOR OXIDES (Wt.%)				
SIO2	40.75	41.30	43.41	40.46
AL2O3	8.99	3.86	9.47	9.69
FEO*	14.45	11.01	12.38	16.60
MGO	21.73	30.61	20.03	21.12
CAO	5.67	4.20	6.56	5.60
NA2O	0.11	0.49	0.50	0.22
K2O	0.01	0.02	0.02	0.01
TIO2	0.57	0.34	0.57	0.59
MNO	0.11	0.04	0.01	ND
P2O5	ND	ND	ND	ND
LOI	5.80	9.48	6.25	7.06
TOTAL	99.19	100.35	99.20	101.35
TRACE ELEMENTS (PPM)				
BA	16.5	51.0	9.1	0.8
CE	17.1	17.1	ND	7.2
CU	8.2	10.6	77.0	82.6
NI	1133.5	1821.8	984.6	1073.7
RB	ND	ND	0.3	ND
S	36.2	560.0	29.0	26.5
SR	15.3	19.3	22.1	6.3
Y	3.3	3.8	5.1	0.7
ZN	52.3	35.1	69.5	58.6
ZR	18.5	11.7	20.7	16.3
NORMATIVE MINERALS				
Q	0.00	0.00	0.00	0.00
OR	0.06	0.12	0.12	0.06
AB	0.93	4.15	4.23	1.86
AN	24.00	8.27	23.53	25.41
NE	0.00	0.00	0.00	0.00
C	0.00	0.00	0.00	0.00
CPX	3.34	10.02	7.28	1.92
OPX	24.29	13.27	28.14	19.43
OL	37.66	54.55	27.65	43.55
MT	3.00	2.67	3.00	3.03
IL	1.08	0.65	1.08	1.12
RU	0.01	0.00	0.01	0.01
AP	0.00	0.00	0.00	0.00
GRID REFERENCE	831398	831398	831398	831398

FeO*   Total Fe as FeO
ND   Not detected

C_1 Upper chilled margin   S   Spinifex zone
C_2 Lower chilled margin   SF   Spinifex-free zone

Appendix I (continued).   Geochemical analyses and CIPW normative calculations of the spinifex-textured flows within the Goose Lake Formation.

SAMPLE NO.	72	73	77	79	81	82	83	157	158	159
MAJOR OXIDES (Wt.%)										
SIO2	50.52	51.43	51.59	52.56	49.65	51.07	51.14	58.08	52.34	49.01
AL2O3	13.10	14.83	15.50	14.79	14.75	14.04	15.48	14.94	14.34	11.90
FEO*	11.74	10.01	10.02	11.15	11.52	9.80	11.02	6.50	8.82	11.27
MGO	9.38	8.44	10.69	6.94	7.94	6.61	7.52	2.03	8.62	7.50
CAO	12.83	8.36	7.10	9.44	10.96	12.66	10.75	3.48	6.48	9.60
NA2O	0.80	2.75	1.02	ND	0.46	1.59	1.11	5.00	0.70	3.32
K2O	0.40	1.05	0.65	0.73	0.50	0.19	0.08	2.19	0.84	0.57
TIO2	0.63	0.62	0.68	0.81	0.82	0.73	0.93	0.62	0.58	0.72
MNO	0.05	0.04	0.39	0.52	0.12	0.02	0.06	0.17	0.09	0.12
P2O5	0.05	0.09	0.01	0.14	0.13	0.12	0.06	0.17	0.11	0.20
LOI	1.20	2.02	1.96	3.20	2.98	2.06	3.18	4.25	4.88	4.90
TOTAL	100.70	99.64	98.61	100.28	99.83	98.89	101.33	97.43	97.80	99.11
TRACE ELEMENTS (PPM)										
BA	115.6	538.7	632.3	224.4	209.9	99.8	28.4		182.8	109.1
CE	ND	10.9	ND	5.8	ND	2.4	ND		27.1	11.0
CU	ND	14.8	18.4	42.7	ND	8.9	103.5		34.2	12.8
NI	358.5	131.6	1099.4	140.3	121.6	107.1	116.8		335.4	104.7
RB	7.9	27.7	17.4	17.1	15.0	2.0	1.1		21.5	12.1
S	41.8	48.3	11.9	27.5	14.0	332.0	135.8		36.0	1100.0
SR	95.8	414.6	176.8	220.1	170.7	83.6	80.7		206.3	343.5
Y	3.6	9.1	3.8	8.1	11.9	10.4	11.1		8.2	12.4
ZN	39.7	51.2	55.4	60.2	72.2	61.2	72.6		78.2	99.8
ZR	37.2	78.1	46.5	72.7	66.5	55.6	52.1		98.4	95.1
NORMATIVE MINERALS										
Q	1.45	0.00	5.46	13.41	5.60	4.44	6.15	7.38	12.48	0.00
OR	2.36	6.21	3.84	4.31	2.95	1.11	0.47	12.94	4.96	3.37
AB	6.77	23.26	8.63	0.00	3.89	13.45	9.39	42.30	5.92	28.09
AN	30.96	25.01	33.05	38.19	36.69	30.60	37.01	11.85	31.43	15.88
NE	0.00	0.00	0.00	0.00	0.00	0.00	0.00	0.00	0.00	0.00
C	0.00	0.00	0.00	0.00	0.00	0.00	0.00	0.00	0.76	0.00
CPX	26.65	13.04	1.72	6.41	13.91	25.98	13.16	3.65	0.00	25.20
OPX	29.05	20.96	41.28	31.35	30.80	18.61	28.95	12.38	34.99	4.48
OL	0.00	6.79	0.00	0.00	0.00	0.00	0.00	0.00	0.00	14.30
MT	3.09	3.66	3.16	3.35	3.36	3.23	3.52	3.07	3.02	3.22
IL	1.20	1.18	1.29	1.54	1.56	1.39	1.77	1.18	1.10	1.37
RU	0.01	0.01	0.01	0.01	0.01	0.01	0.01	0.01	0.01	0.01
AP	0.12	0.22	0.02	0.34	0.31	0.29	0.14	0.41	0.26	0.48
GRID REFERENCE	800419	799419	798419	802404	802403	802403	803401	828382	828382	826384

FeO* Total Fe as FeO
ND Not detected
Appendix I (continued). Geochmical analyses and CIPW normative calculations of the Schumacher Formation.

SAMPLE NO.	23	29	37	57	36	87	95	132	160	169
MAJOR OXIDES (wt.%)										
SIO2	48.58	50.01	49.42	49.53	50.74	47.05	47.08	49.67	50.64	47.27
AL2O3	15.06	15.26	14.60	16.20	14.14	12.79	14.35	14.45	14.04	14.90
FEO*	13.89	11.33	14.95	13.81	15.63	17.43	13.63	14.56	14.72	13.86
MGO	5.20	6.86	6.68	5.57	6.22	6.77	6.59	5.87	6.49	5.60
CAO	10.56	11.62	9.13	10.27	9.68	8.75	11.28	9.97	10.20	6.65
NA2O	0.93	ND	3.17	ND	ND	2.15	0.91	ND	ND	3.20
K2O	0.17	0.59	0.19	0.32	0.34	0.29	0.27	0.44	0.35	0.09
TIO2	0.99	0.77	1.04	1.11	1.27	1.30	1.11	1.31	1.12	0.94
MNO	0.23	0.02	0.32	0.23	ND	ND	0.32	0.16	0.01	0.02
P2O5	0.06	0.04	0.14	0.13	0.11	0.10	0.11	0.11	0.11	0.09
LOI	2.96	2.18	1.20	2.56	2.27	2.28	2.55	1.76	2.30	6.87
TOTAL	99.63	98.68	100.84	99.73	100.40	98.93	98.20	98.31	99.98	97.79
TRACE ELEMENTS (PPM)										
BA	97.3	241.0	96.9	101.5	69.0	59.2	127.9	85.8	57.1	90 E
CE	ND	ND	ND	ND	ND	ND	ND	ND	ND	ND
CU	134.9	39.6	123.3	104.2	127.2	90.8	54.1	120.3	130.5	22.5
NI	56.9	163.3	85.8	48.9	69.2	67.0	89.5	86.6	65.6	70.6
RB	4.7	20.3	ND	3.8	6.4	ND	41.	6.7	1.4	1.5
S	83.0	23.0	1800.0	535.0	4360.0	514.0	60.0	1420.0	2180.0	11.0
SR	98.3	184.5	71.7	93.0	78.4	88.7	198.1	69.1	93.8	54.2
Y	10.6	8.4	8.1	6.4	7.0	12.4	12.9	7.1	9.9	6.5
ZN	95.0	65.4	90.4	69.7	87.7	85.3	57.7	55.5	65.7	75.1
ZR	49.1	54.6	42.9	49.3	52.0	56.9	60.6	42.4	54.5	46.4
NORMATIVE MINERALS										
Q	4.25	8.48	0.00	10.11	10.77	0.00	2.02	10.34	10.33	0.00
OR	1.00	3.49	1.12	1.89	2.01	1.71	1.60	2.60	2.07	0.53
AB	7.87	0.00	26.82	0.00	0.00	18.19	7.70	0.00	0.00	37.07
AN	36.40	39.88	25.04	43.24	37.56	24.38	34.26	38.14	37.26	29.02
NE	0.00	0.00	0.00	0.00	0.00	0.00	0.00	0.00	0.00	0.00
C	0.00	0.00	0.00	0.00	0.00	0.00	0.00	0.00	0.00	0.00
CPX	13.09	14.53	16.23	5.77	8.20	15.49	17.55	8.92	10.59	5.35
OPX	30.72	27.55	10.95	32.36	35.69	22.05	28.72	32.40	32.88	11.82
OL	0.00	0.00	15.75	0.00	0.00	10.90	3.78	0.00	0.00	15.02
MT	3.61	3.29	3.68	3.78	4.02	4.06	3.78	4.07	3.80	2.54
IL	1.88	1.46	1.98	2.11	2.42	2.47	2.11	2.49	2.13	1.79
RU	0.01	0.01	0.01	0.01	0.02	0.02	0.01	0.02	0.01	0.01
AP	0.14	0.10	0.34	0.31	0.26	0.24	0.26	0.25	0.26	0.22
GRID REFERENCE	788405	788388	754391	764591	801403	802404	807381	833397	825380	812360

FeO*   Total Fe as FeO
ND   Not detected
Appendix I (continued).   Geochemical analyses and CIPW normative calculations of the Gabbroic Sills.

131

SAMPLE NO.	186	206
MAJOR OXIDES (Wt. %)		
SIO2	68.14	50.30
AL2O3	15.51	14.33
FEO*	2.48	13.43
MGO	1.43	8.25
CAO	2.69	10.45
NA2O	6.82	2.32
K2O	3.28	0.25
TIO2	0.32	0.91
MNO	0.19	0.24
P2O5	0.24	0.11
LOI	1.09	1.37
TOTAL	102.19	101.96
TRACE ELEMENTS (PPM)		
BA		62.2
CE		ND
CU		47.4
NI		69.1
RB		1.4
S		146.0
SR		93.5
Y		3.0
ZN		68.3
ZR		51.7
NORMATIVE MINERALS		
Q	9.66	0.00
OR	19.38	1.48
AB	57.73	19.63
AN	2.01	27.94
NE	0.00	0.00
C	0.00	0.00
CPX	8.01	19.25
OPX	2.18	20.16
OL	0.00	8.88
MT	2.64	3.49
IL	0.61	1.73
RU	0.00	0.01
AP	0.58	0.26
GRID REFERENCE	744441	755427

FeO*   Total Fe as FeO
ND   Not detected
Appendix I (continued).   Geochemical analyses and CIPW normative calculations of the Gabbroic Sills.

SAMPLE NO.	2	13	54	214	216	219	233	244	245
MAJOR OXIDES (Wt.%)									
SIO2	55.65	56.28	64.14	67.97	50.24	53.50	58.14	51.83	50.59
AL2O3	14.29	15.13	15.05	14.95	14.68	13.26	16.03	14.69	15.29
FEO*	9.08	7.78	5.52	1.36	3.35	9.24	7.02	9.38	9.10
MGO	5.09	5.65	1.74	ND	7.63	10.14	1.52	6.96	7.10
CAO	5.63	5.84	4.30	1.90	8.56	8.10	6.16	11.42	7.51
NA2O	3.24	2.83	3.29	8.15	5.38	2.93	4.50	2.91	3.47
K2O	0.25	1.28	1.68	1.94	0.83	0.50	1.38	0.61	1.35
TIO2	0.85	0.73	0.63	0.22	0.35	0.93	1.05	0.85	0.83
MNO	0.05	0.11	ND	0.05	0.22	0.03	0.13	0.12	ND
P2O5	0.17	0.18	0.13	0.13	0.13	0.09	0.27	0.18	0.18
LOI	2.90	2.48	1.77	2.53	2.76	2.76	1.17	1.85	2.54
TOTAL	97.20	98.29	98.24	99.70	99.13	100.84	97.42	100.80	98.05
TRACE ELEMENTS (PPM)									
BA			333.9			181.4			311.8
CE			83.2			20.8			6.5
CU			10.4			15.8			32.7
NI			48.2			314.0			230.3
RB			56.9			24.4			44.0
S			50.7			175.0			103.6
SR			249.4			154.8			231.6
Y			22.7			6.1			12.1
ZN			61.9			71.1			86.8
ZR			221.9			64.1			55.5
NORMATIVE MINERALS									
Q	11.33	10.03	23.81	12.88	0.00	1.37	9.85	0.00	0.00
OR	1.48	7.56	9.93	11.46	4.91	5.50	8.16	3.60	8.16
AB	27.41	23.94	27.83	66.07	28.37	19.37	38.07	24.62	29.36
AN	23.70	24.79	20.48	0.00	13.45	23.15	19.59	25.21	22.06
NE	0.00	0.00	0.00	0.00	9.28	0.00	0.00	0.00	0.00
C	0.00	0.00	0.00	0.00	0.00	0.00	0.00	0.00	0.00
CPX	2.59	2.48	0.00	4.43	23.09	13.41	7.86	24.92	11.52
OPX	24.64	24.10	11.65	0.00	0.00	33.24	8.84	13.19	9.94
OL	0.00	0.00	0.00	0.00	15.30	0.00	0.00	4.26	11.46
MT	3.41	3.23	3.09	1.23	2.68	2.90	3.70	3.41	3.38
IL	1.62	1.39	1.20	0.42	0.67	0.95	2.00	1.62	1.58
RU	0.01	0.01	0.01	0.00	0.00	0.01	0.01	0.01	0.01
AP	0.41	0.43	0.31	0.31	0.31	0.22	0.65	0.43	0.43
GRID REFERENCE	696453	734375	752381	769385	765386	769983	753378	697447	698447

FeO* Total Fe as FeO
ND Not detected
Appendix I (continued). Geochemical analyses and CIPW normative calculations of the Peterlong Lake Complex.

SAMPLE NO.	51	74	75	195	204
MAJOR OXIDES (Wt.%)					
SIO2	67.29	66.25	66.47	67.18	66.58
AL2O3	15.37	15.71	15.33	15.57	14.38
FEO*	2.34	2.85	1.74	2.08	1.60
MGO	0.98	ND	ND	0.85	0.77
CAO	3.02	2.11	2.74	1.89	1.86
NA2O	4.80	7.18	8.02	6.57	8.75
K2O	2.85	3.79	2.31	2.75	1.99
TIO2	0.27	0.33	0.22	0.30	0.24
MNO	0.08	0.01	0.14	0.07	ND
P2O5	0.10	0.14	0.05	0.17	0.11
LOI	1.32	1.27	1.07	1.40	1.44
TOTAL	98.42	98.64	98.10	98.83	97.68
TRACE ELEMENTS (PPM)					
BA	795.6	882.6			732.3
CR	80.5	102.3			156.8
CU	8.6	34.9			5.9
NI	11.6	23.7			9.4
RB	65.0	151.7			52.0
S	46.5	18.3			49.3
SR	1151.3	772.8			1044.9
Y	12.9	27.8			8.9
ZN	102.5	46.2			46.5
ZR	240.8	234.0			225.0
NORMATIVE MINERALS					
Q	20.24	6.60	7.70	13.51	
OR	16.84	22.40	13.65	16.25	
AB	20.61	59.68	65.97	55.58	
AN	11.97	0.00	0.00	4.86	
NE	0.00	0.00	0.00	0.00	
C	0.00	0.00	0.00	0.00	
CPX	1.96	6.48	3.59	2.81	
OPX	3.86	0.00	0.00	2.57	
OL	0.00	0.00	0.00	0.00	
MT	2.57	2.19	1.66	2.61	
IL	0.51	0.63	0.42	0.57	
RU	0.00	0.00	0.00	0.00	
AP	0.24	0.34	0.14	0.41	
GRID REFERENCE	753452	798423	798422	741427	751456

FeO* Total Fe as FeO
ND Not detected
Appendix I (continued). Geochemical analyses and CIPW normative calculations of the Adams Pluton.

134

SAMPLE NO.	113	148	151	165	237	242
MAJOR OXIDES (wt.%)						
SIO2	55.09	56.57	59.24	74.39	60.97	63.87
AL2O3	13.81	17.08	14.10	12.99	15.08	16.50
FEO*	7.69	8.39	7.26	0.97	6.21	4.44
MGO	8.23	1.29	1.54	0.37	3.02	2.18
CAO	6.08	2.17	2.85	1.18	2.67	4.33
NA2O	2.37	8.58	7.21	6.59	5.33	5.26
K2O	0.99	0.15	0.82	1.41	1.15	0.55
TIO2	0.54	0.99	0.96	0.06	0.69	0.53
MNO	0.19	ND	ND	0.08	0.13	ND
P2O5	0.12	0.17	0.27	0.04	0.20	0.17
LOI	3.28	3.90	3.43	1.88	2.57	1.73
TOTAL	99.39	99.29	97.68	98.29	99.24	99.37
TRACE ELEMENTS (PPM)						
BA	220.0	118.2		661.7	189.0	
CO	27.9	170.9		163.1	44.6	
CU	28.8	165.5		34.4	65.0	
NI	302.7	24.8		ND	69.3	
RB	26.9	23.0		53.3	38.2	
S	63.4	3100.0		265.8	257.5	
SR	227.2	264.8		220.2	228.1	
Y	9.3	10.1		10.9	13.5	
ZN	71.8	10.8		ND	108.2	
ZR	108.9	232.5		141.1	157.5	
NORMATIVE MINERALS						
Q	8.40	0.00	3.99	27.88	8.65	17.35
OR	5.85	0.39	4.85	8.33	6.90	2.07
AB	20.05	69.36	60.99	56.60	49.32	44.50
AN	24.11	7.64	3.68	1.25	11.57	20.37
NE	0.00	1.75	0.00	0.00	0.00	0.00
C	0.00	0.00	0.00	0.00	0.00	0.00
CPX	4.29	1.74	7.43	2.74	0.31	11.02
OPX	30.07	0.00	9.75	0.00	17.11	0.00
OL	0.00	10.62	0.00	0.00	0.00	0.00
MT	2.90	3.61	3.57	2.26	3.18	2.94
IL	0.95	1.88	1.83	0.11	1.31	1.01
RU	0.01	0.01	0.01	0.01	0.01	0.01
AP	0.29	0.41	0.65	0.10	0.48	0.41
GRID REFERENCE	829288	829387	829386	824377	693457	693456

FeO*   Total Fe as FeO
ND   Not detected
Appendix I (continued).   Geochemical analyses and CIPW normative calculations of Quartz diorte sill (118), trondhjemite (148, 151), quartz feldspar porphyry (165), and Timiskaming sedimentary rock (237-242).

135

SAMPLE NO.	12	33	52	97	144	147	185	231
MAJOR OXIDES (wt.%)								
SIO2	50.88	51.31	39.71	46.96	33.90	47.95	53.37	49.47
AL2O3	15.33	16.68	10.81	14.33	8.11	12.86	14.69	15.72
FEO*	14.44	13.59	14.76	15.76	9.00	9.34	12.70	13.77
MGO	4.72	3.91	6.09	7.35	12.49	12.40	6.44	5.85
CAO	10.44	9.71	11.76	9.16	10.46	8.64	4.06	10.94
NA2O	1.02	ND	0.90	1.01	1.30	0.89	0.49	ND
K2O	0.34	1.60	1.09	0.24	0.65	1.09	1.59	0.32
TIO2	1.42	1.39	5.23	1.15	0.92	0.41	0.92	1.33
MNO	0.10	0.45	0.44	0.14	0.02	0.19	0.08	0.05
P2O5	0.11	0.24	3.17	0.09	0.61	0.05	0.07	0.19
LOI	0.05	1.62	0.00	1.66	20.51	3.54	5.87	0.69
TOTAL	99.17	99.35	98.95	97.85	97.38	97.65	100.28	98.33
TRACE ELEMENTS (ppm)								
BA	19.7		738.1		430.6	133.8		86.6
CE	35.0		14.9		22.8	18.2		ND
CU	7.3		8.3		200.7	34.5		219.2
NI	1669.5		5.3		377.5	381.9		72.4
ZN	3.6		8.4		ND	24.8		11.3
S	119.4		428.2		1068.0	515.0		84.0
SR	27.3		370.4		317.9	100.8		113.5
Y	2.5		20.9		13.4	7.2		21.2
ZR	61.1		78.9		93.0	45.4		86.3
ZN	17.3		98.0		195.5	56.6		62.0
NORMATIVE MINERALS								
Q	7.85	15.76	0.00	0.91	0.00	0.00	17.32	9.57
OR	2.01	5.91	6.44	1.42	0.50	6.38	9.40	1.89
AB	8.63	0.00	7.61	8.54	3.61	7.53	4.15	0.00
AN	36.23	42.54	22.23	33.85	16.14	27.89	19.69	41.93
NE	0.00	0.00	0.00	0.00	4.00	0.00	0.00	0.00
C	0.00	0.00	0.00	0.00	0.00	0.00	4.95	0.00
DI	12.57	1.18	12.96	9.22	25.66	13.08	0.00	9.32
OPX	27.18	29.40	23.89	38.54	0.00	31.85	35.84	50.66
OL	0.00	0.00	5.13	0.00	22.93	5.65	0.00	0.00
MT	4.23	4.19	9.76	3.84	3.51	2.77	3.51	4.10
IL	2.70	2.64	9.95	2.19	1.75	0.76	1.73	2.53
RU	0.02	0.02	0.07	0.01	0.01	0.01	0.01	0.02
AP	0.26	0.53	7.60	0.22	1.46	0.12	0.17	0.46
GRID REFERENCE	736369	750384	753454	808382	834334	829986	779378	731370

FeO* Total Fe as FeO
ND   Not detected
Appendix I (continued). Geochemical analyses and CIPW normative calculations of the Diabase dykes.

APPENDIX II

GENERAL

The sampling of the major portion of the specimens took place in May and June 1977. Later during the field season, the spinifex-textured flows were sampled with the aid of a portable diamond drill. In all, 267 samples were selected for the study, mainly along two traverses across the area, and thin sections were made of 260 of these, (161 extrusives, 92 intrusives, and 7 sediments). The samples were taken so as to represent the composition of the rock immediately surrounding each sample point. The diamond drill core specimens measured about 2.5 cm in diameter and 7 to 10 cm in length and generally weighed 100 to 150 gms. The least weathered samples selected for chemical analysis were dried for about twelve hours in an oven heated to about $100^{o}C$. Afterward, the specimens were ground by a Jaw Crusher and a Roll Mill down to sand sizes. Later by use of a tungsten carbide shatter box, the samples were ground down to about 200 mesh. To avoid possible contamination of the drill cores by the diamond drill, the samples were sand-papered and washed by acetone and deionized water.

ANALYTICAL METHODS

The concentration of 20 elements were determined by x-ray fluorescense spectrometry using a Philips 1450/20 sequential automatic x-ray spectrometer. The following are the different parameters on XRF used for each determination.

MAJOR ELEMENT PARAMETERS

Element	Det.	Coll.	Crystal	$2\theta^{\circ}$ Pk	$2\theta^{\circ}$ Bkg	Count Time	LL	Window	kV	mA
Si	Flow	coarse	PET	109.42	108.70	4	250	500	50	45
Al	Flow	coarse	PET	145.48	144.37	10	200	800	50	45
Fe	Flow	fine	LiF200	57.52	56.50	4	150	750	30	45
Mg	Flow	coarse	TLAP	45.37	44.83	20	250	700	50	45
Ca	Flow	coarse	LiF200	113.35	114.85	2	50	600	50	45
Na	Flow	coarse	TLAP	55.27	55.05	20	300	400	50	45
K	Flow	coarse	LiF200	136.94	135.60	10	300	400	50	45
Ti	Flow	coarse	LiF200	86.30	85.20	10	250	700	50	45
Mn	Flow	fine	LiF200	56.65	56.84	20	150	750	60	45
P	Flow	coarse	GE	141.16	140.54	10	200	800	50	45

MINOR ELEMENT PARAMETERS

Element	Det.	Coll.	Crystal	$2\theta^{\circ}$ Pk	$2\theta^{\circ}$ Bkg	Count Time	LL	Window	kV	mA
Ba	Scint.	Fine	LiF200	11.02	11.50	20	250	500	50	45
Ce	Scint.	Fine	LiF200	10.22	9.22	40	250	500	50	45
Cu	Scint. + Flow	Coarse	LiF200	45.10	45.60	40	300	400	60	45
Ni	Scint. + Flow	Coarse	LiF200	48.78	48.00	40	250	500	60	45
Rb	Scint.	Fine	LiF200	26.30	26.57	20	300	400	50	45
S	Flow	Coarse	GE	109.20	110.79	20	200	800	50	45
Sr	Scint.	Fine	LiF200	25.12	24.75	20	250	500	50	45
Y	Scint.	Fine	LiF200	23.72	23.50	20	250	500	60	45
Zn	Scint. + Flow	Coarse	LiF200	41.90	41.20	40	300	400	60	45
Zr	Scint.	Fine	LiF200	22.48	22.95	20	300	400	50	45

SAMPLE PREPARATION

Major oxides were measured on fused glass discs and trace elements on pressed powder pellets.

Loss of ignition:

(1) One gram of powdered sample was placed into a pre-weighed porcelain crucible with the degree of accuracy of $\pm$ 0.0000 gm.

(2) The crucible was heated at 1100°C in a muffled furnace and held for 30 minutes.

(3) It was removed from the furnace and allowed to cool down to room temperature in a desicator.

(4) The crucible and sample were reweighed and the difference from the original weight (LOI) was calculated.

The difference in weight is due to loss of molecular water and all of the CO_2 and sulfur contents. In three samples, weight gains of up to 0.5% were observed. They are assumed to be the result of the oxidation of ferrous iron (Fe^{+2}) to ferric iron (Fe^{+3}). The maximum amount of LOI was 20%.

Preparation of the glass disc:

(1) 1 gram of sample powder, 10 gms of flux (lithium tetraborate and lithium carbonate in 9 to 1 ratio) plus weighed amount of flux equivalent to LOI were mechanically mixed.

(2) The mixture was fused at 1100°C in non-wetting platinum crucible. The fused material is swirled several times during 30 minutes of the fusion to ensure homogenity and complete dissolution of the sample.

(3) The molten glass is then poured into a platinum mold which was heated on a bunsen burner with a high flame.

(4) After 1 minute the flame was turned off to allow the disc to cool

fast. The disc would pop out within a minute and is then ready
to analyse.

Preparation of the powder pellet:

15.00 gms of the powdered rock were pressed into a pellet with
the aid of a mechanical press under 1.6 ton/cm^2 pressure. As a
binding agent two x-ray mix tablets (1.00 gm) were ground and
mixed with sample powder.

Standard samples:

The following 11 U.S.G.S. Powders (Flanagan, 1969) and 2 mixed
powders were used as reference standards.

DTS - 1	Dunite
PCC - 1	Peridotite
BHVO	Basalt
BCR - 1	Basalt
QLO - 1	Quartz latite, alkaline
GSP - 1	Granodiorite
G - 2	Granite
RGM - 1	Rhyolite
STM - 1	Kyanite schist
SDC - 1	Biotite - muscovite schist
SCO - 1	Cody shale
PPB	(3.5 gms PCC - 1, 4 gms BCR - 1)
P - B	(1 gm PCC - 1, 1 gm BHVO)

The minimum of three and nine closely spaced standards surrounding
the unknown sample were used respectively for major and trace element
comparisons. The analytical results of the U.S.G.S. standards in
a graph form are presented in the following page.

XRF counts/sec. on USGS standard rocks

U.S.G.S. Standard Rocks Precision Tests

tcps= total counts per second

ppm= parts per million
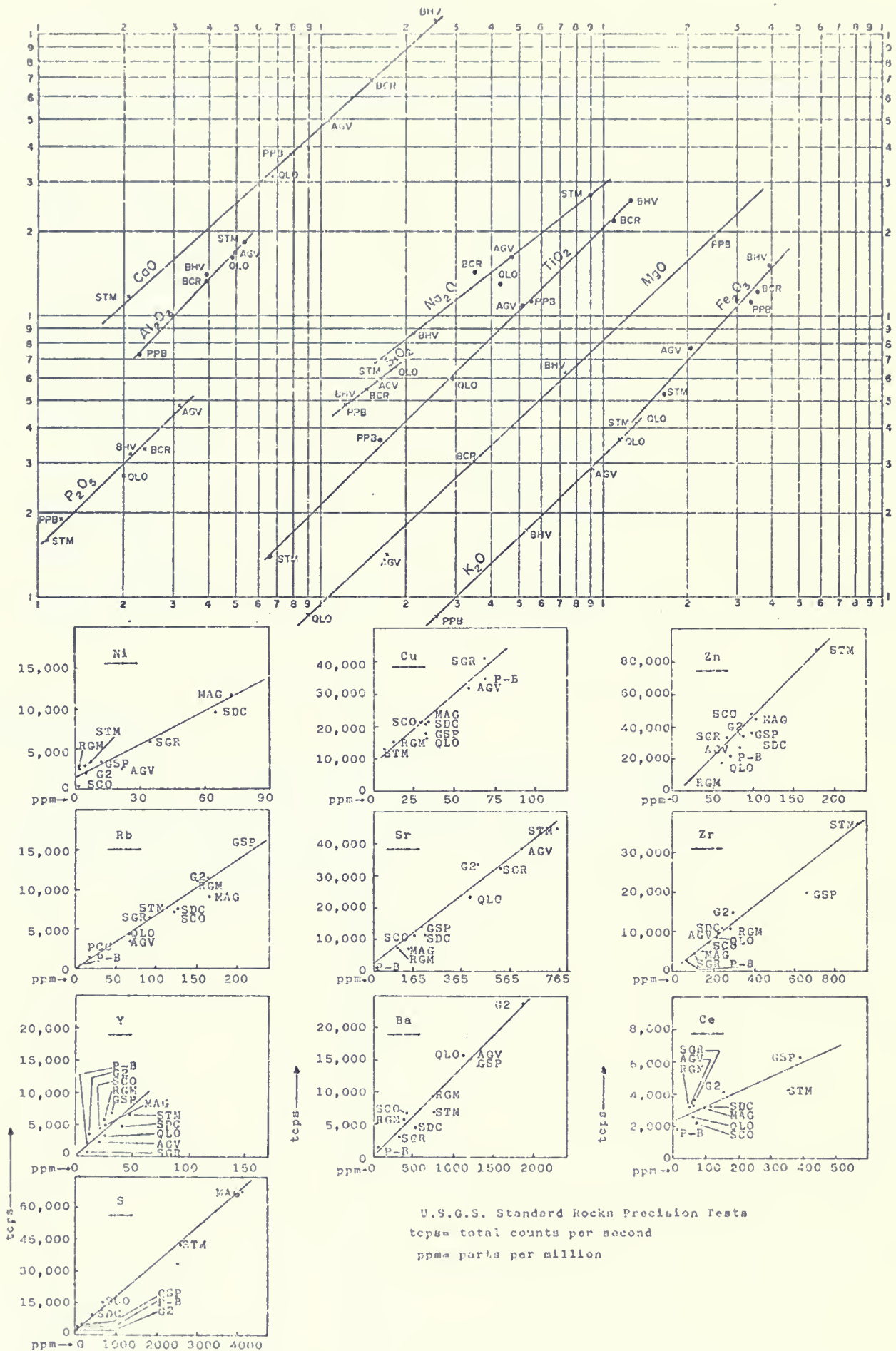
The precision limits of major oxides and trace elements are presented below:

(wt.%)	(ppm)
SiO_2 = ± 1.0	Ba = ± 129.73
Al_2O_3 = ± 1.0	Ce = ± 54.56
FeO* = ± 0.2	Cu = ± 8.66
MgO = ± 0.05	Ni = ± 10.79
CaO = ± 0.2	Rb = ± 18.40
Na_2O = ± 0.3	S =
K_2O = ± 0.05	Sr = ± 50.12
TiO_2 = ± 0.1	Y = ± 9.33
MnO = ± 0.05	Zn = ± 14.39
P_2O_5 = ± 0.05	Zr = ± 47.76

DATA TREATMENT

Raw data (i.e. counts and time) were recorded on a tape by a data cassette and fed into the computer for drift correction and least squares analysis of U.S.G.S. standard rocks.